Erika Tinoco Guimarães

Parametrical Studies of the
Behavior of Aerial Lime Mortars

November, 2014

Universidade do Minho
Escola de Engenharia

Erika Tinoco Guimarães

Parametrical Studies of the
Behavior of Aerial Lime Mortars

MSc Dissertation
Integrated Masters in Civil Engineering

Supervised by:
Miguel Ângelo Dias Azenha

DECLARAÇÃO

Nome:

Erika Tinoco Guimarães

Endereço eletrónico: a73479@alunos,uminho.pt   Telefone: 912473422_

Número do Bilhete de Identidade: 15703061

Título da dissertação:

Parametrical Studies of the Behavour of Aerial Lime Mortars

Orientador(es):

Miguel Ângelo Dias Azenha

Ano de conclusão: 2013/2014

Designação do Mestrado:

Mestrado Integrado em Engenharia Civil

Nos exemplares das teses de doutoramento ou de mestrado ou de outros trabalhos entregues para prestação de provas públicas nas universidades ou outros estabelecimentos de ensino, e dos quais é obrigatoriamente enviado um exemplar para depósito legal na Biblioteca Nacional e, pelo menos outro para a biblioteca da universidade respetiva, deve constar uma das seguintes declarações:

1. É AUTORIZADA A REPRODUÇÃO INTEGRAL DESTA DISSERTAÇÃO APENAS PARA EFEITOS DE INVESTIGAÇÃO, MEDIANTE DECLARAÇÃO ESCRITA DO INTERESSADO, QUE A TAL SE COMPROMETE;

2. É AUTORIZADA A REPRODUÇÃO PARCIAL DESTA DISSERTAÇÃO (indicar, caso tal seja necessário, nº máximo de páginas, ilustrações, gráficos, etc.), APENAS PARA EFEITOS DE INVESTIGAÇÃO, MEDIANTE DECLARAÇÃO ESCRITA DO INTERESSADO, QUE A TAL SE COMPROMETE;

3. DE ACORDO COM A LEGISLAÇÃO EM VIGOR, NÃO É PERMITIDA A REPRODUÇÃO DE QUALQUER PARTE DESTA TESE/TRABALHO

Universidade do Minho, ___/___/_____

Assinatura:

RESUMO

A cal aérea foi muito utilizada como ligante de argamassas antes do surgimento do cimento Portland, sendo usualmente encontrada em construções históricas. O interesse contemporâneo em cal aérea tem sido aumentado dentro dos campos de reabilitação estrutural e restauro devido a sua compatibilidade com materiais antigos.

O processo químico através do qual dá-se o endurecimento da cal é conhecido por carbonatação. De modo a compreender a influência das condições ambientais na carbonatação, o presente trabalho procede à continuidade de um estudo previamente realizado acerca do comportamento de argamassas de cal aérea em termos de validação de modelos de simulação multi-físicos e obtenção de parâmetros de modelação.

Através de modificação dos ambientes de exposição e comparação dos resultados obtidos, foram conduzidos estudos sistemáticos sobre o efeito de parâmetros como humidade relativa, concentração de dióxido de carbono e velocidade de conversão no desenvolvimento da carbonatação.

A carbonatação foi investigada por análises temo-gravimétricas e coloração de Fenolftaleína. Processos de secagem e transporte de água através do material foram avaliados através de monitoramento de perfis de humidade. Propriedades mecânicas também foram avaliadas e discutidas face a resultados de investigação química.

PALAVRAS-CHAVE

Argamassa de Cal Aérea, Carbonatação, Análises Termo-gravimétricas, Hot-Lime Mix,Humidade

ABSTRACT

Aerial lime has been largely used as binder in mortars before the emergence of Portland cement, being commonly found in historic constructions. The contemporary interest in aerial lime mortars has enlarged concerning the field of structural restoration, given its compatibility with traditional materials.

The process through which lime hardens is the carbonation reaction. Aiming to understand the influence of environmental conditions on carbonation, the current work extends a previously developed study on the behaviour of aerial lime mortars, in view backing multi-physics simulation models and obtaining modelling parameters.

Systematic studies on the effect of relative humidity, carbon dioxide concentration and carbonation rate throughout time were followed by modifying the environments of exposure of specimens and comparing the results.

Carbonation has been investigated using thermo gravimetric analysis and phenolphthalein staining. Additionally, drying and water transport mechanisms were assessed through humidity profiles monitoring. Mechanical properties have also been evaluated and discussed in view of chemical investigation results.

KEYWORDS

Aerial Lime Mortar, Carbonation, Thermo Gravimetric Analysis, Hot Lime Mix, Humidity

FIGURES INDEX

TABLE INDEX

1. INTRODUCTION

1.1 Brief description of aerial lime and historic applications in construction

Aerial lime is obtained from lime stones, a common type of sedimentary rock, composed of Calcium Carbonate – $CaCO_3$. When lime stones are calcinated, it is produced Carbon Oxide – CaO, known as quicklime, which is highly reactive and hygroscopic (Meneghini, 2014).

The addition of water produces hydrated (or slaked) lime, composed of Calcium Hydroxide. Aerial lime is a type of hydrated lime. Lime hardening process is given by carbonation. In this process, hydroxide reacts with atmospheric CO_2, producing calcium carbonate. Carbonation can be seen as an inverse process of aerial lime production, since it returns to the original calcite form.

Literature shows that carbonation is very slow and depends on parameters such as atmosphere exposing time (Van Balen & Van Gemert, Modelling lime mortar carbonation, 1994), variation of relative humidity throughout the material (Van Balen, Carbonation reaction of lime, kinetics at ambient temperature, 2005), environment temperature (Grandet, 1975; Van Balen & Van Gemert, Modelling lime mortar carbonation, 1994) and carbon dioxide diffusion inside the mass (Van Balen & Van Gemert, 1994). In the case of lime mortars, the porosity of the mixture (Lawrence R. , 2006), types of components and the adopted ratio (Thomson, 2002; Elert, 2002) are also relevant and should be considered. Furthermore, by hardening lime, carbonation increases the mechanics capacities of mortars.

Aerial lime mortars have been largely used as a structural and ornamental- material for at least the past 16 centuries before the emergence of the Portland cement (Coppola, n.d.). A significant portion of architectural heritage throughout Europe and Western Asia employs aerial lime mortars in their constitution (Lawrence R. , 2007).

Aerial lime was used by Romans as a construction material from the 3rd century B.C (Colombo & Festa, 2005). Lime stone-based substances were mixed with water, varied types of sands and other additives, such volcanic ashes – *Pozzolan* or rocks - C*aementa* to make many kinds of pastes. One of the best known is the so called *Opus Caementicium*, in which Pozzolan had a great importance as additive (Colombo & Festa 2005).

Throughout the Roman Empire, aerial lime mortars were amply employed in constructive elements and played a variable range of functions, from joining brick elements to filling empty spaces between masonry layers – multiple leaf walls (Ferretti & Bazant, 2006).

With the fall of antique civilizations and the beginning of the medieval wars, the traditional abilities and innovations were lost. Because of the lack of records, techniques and methods were progressively forgotten and fell into disuse. During the course of the middle ages, lime mortars quality became very poor, given the low quality of furnaces and scarcity of proper artefacts (Viollet-le-Duc, 1854).

From the 12th century, practices in lime started to be retaken thanks to translations of reminiscent books, such as Vitruvio's and Plinio's, increasing mortar's quality (Società Impianti calce, n.d.). During renaissance, Palladio had made some efforts towards the resumptions of lime production. His product, the *Calce nigra*, consisted of lime with hydraulic properties obtained from clay impurities (Società Impianti calce, n.d.). The growing interest in lime can be noted more fiercely in the modern ages. Given the advent of industrial revolution in Europe in the beginning of the 18th century, industrial production of hydraulic lime has started. In 1818, Vicat patented a type of hydraulic lime, made from calcination of limestone and clay. Other patents based on his mixture followed until the emergence of Portland cement in 1824 (Coppola, n.d.).

The use of aerial lime in constructions before the 20th century was very often particularly in the form of lime putty, a slurry paste obtained by the adding of excessive water. Nevertheless, industry invested in the development of products based in Portland cement, given its proven efficiency and superior mechanic properties in comparison with aerial lime (Lanas & Alvarez, 2003).

The contemporary interest in aerial lime concerns the fields of structural restoration and conservation of historic heritage. Recent cases of restoration acknowledged deterioration in ancient masonry elements given by contact with cement mortars. Damages were caused mainly by incompatibility between these materials, once cementitious mortars were proven excessively hard to work with porous and weaker historic bricks (Lawrence R. , 2006). In addition, Portland cement promotes corrosion of ancient materials, given its alkaline character (Cultrone, Sebastián, & Ortegas Huertas, 2005).

On the contrary of Portland cement, lime is advised to operate with traditional materials. Besides of preventing corrosive effects, lime mortars are capable of resisting some degree of movement in masonry (Cultrone, Sebastián, & Ortegas Huertas, 2005). Furthermore, the slow characteristic of the carbonation is beneficial because it gives the mortar the ability to retain plasticity for long time and thus accommodate structural movements (Lawrence R. , 2006).

2

Beyond mentioned abilities, aerial lime mortars can also be used to eliminate unwanted water contents by absorbing humidity. It can be used as sacrifice material, being replaced when saturated. An additional advantage reflects in potentially lower costs of restoration, given lime's commercial prices (Lanas & Alvarez, 2003).

1.2   Scope and motivation

In views of the strong presence of aerial lime in historic constructions, mainly in mortars, as well as its renovating importance in structural restoration, recent interests in the study of the properties and behaviour of this material are perceived.

Although significant advances regarding chemical and physical characterization of lime were achieved (Lawrence R. , 2006; Veiga, Fragata, Velosa, & Magalhães, 2010; Van Balen & Van Gemert, 1994; Baronio, Binda, & Saisi, 2000; Lanas & Alvarez, 2003), it is still noticed a lack of accurate information concerning the reactions that occur within, as well as precise establishments of experimental parameters. It is thereby remarkable the need to deepen the existing knowledge on the subject.

Given the remarkable lack of understanding phenomena, models and parameters towards modelling in this important field of aerial lime mortar behaviour, a research gap is thereby identified.

1.3   Objectives

The purpose of this work is to understand in which way the values of relative humidity, carbon dioxide concentration and carbonation rate interact and influence aerial lime mortar specimen´s hardening process.

In pursuit of such objectives, experimental procedures developed and validated in a previous research work are adopted (Meneghini, 2014). Based on models proposed in the literature, ratios and mixtures, and the referred experimental procedures, systematic studies on the effects of the above mentioned variables throughout carbonation are made by modifying the environments of exposure of specimens and comparing the obtained testing results.

1.4   Description of the work

The current work is divided in six chapters: I-Introduction; II-Aerial Lime; III-Approaches and experiments in aerial lime mortars; IV-Experimental program; V-Main results and discussion; VI-Conclusions.

The present introduction intends to demonstrate a contextualization of the proposed theme, the scope and motivation of the work, as well as its objectives and description of content.

The second chapter refers to an opening descriptive part on the relevant phenomenology associated to aerial lime phenomenology, giving with insights about the processes of carbonation, humidity and carbon dioxide diffusion and the related factors, as well as some numerical models related to the mentioned process. In the same chapter, some considerations are made concerning lime mortars' mixture, components and main properties.

The third chapter follows a review on previous experimental works focused in aerial lime mortars, regarding the mixture design, casting procedures, curing conditions and the observation of specific properties in experimental tests.

The fourth chapter pertain to the experimental campaign developed in the scope of this work, in which are addressed the procedures that where followed concerning the casting method and curing process, and also the execution of the tests.

The fifth chapter describes the main results of all the performed tests and also conclusions regarding comparisons between the results.

In the last chapter the main conclusions of this work are acknowledged, and also some proposals for further work are forwarded.

2. AERIAL LIME

2.1 Definition of aerial lime and its forms

Lime is an inorganic compound obtained by artificial modifications of a natural mineral crystal found in nature in the form of lime stones, commonly known as calcite. The main reaction in the process of production of lime is called calcination and consists in burning the calcite to obtain calcium oxide, also called quick lime.

Quick lime is highly reactive and hygroscopic and, when mixed with water provides calcium hydroxide, known as hydrated or slacked lime. Different slaking conditions determine the form and properties of the final product. When lime is hydrated with the precise amount of water needed, it adopts the form of a fine, white powder, whereas when an excess of water is put into the process, the product is a slurry paste called lime putty, which has different properties and applications.

Hydrated lime that originates from calcinated lime with significant amounts of argillaceous impurities, such as silica and alumina, is referred to as natural hydraulic lime for it has the capacity of setting under water, in a reaction called hydrolysis. On the contrary, when lime stones containing up to 5% of impurities are used to make lime (Coutinho, 2002), the product is known as non-hydraulic lime - commonly referred to as air or aerial lime. The reason for this denomination is that aerial lime, unlike hydraulic lime, will not set under water. Instead, it is set by the carbonation process, which requires exposure to atmospheric carbon dioxide. This causes a much slower set and the lime remains softer and more breathable (Lime Stuff Ltd.).

As previously mentioned, the subject of study of this work is mortars which have aerial lime as major component. In this matter, the present subchapter focuses on the definition of this compound and the main forms of classifying it.

2.1.1 Types of lime

Aerial limes are mostly composed of calcium oxides or hydroxides, but their composition may include other elements, such as clay, that are usually termed as impurities. In terms of impurity content, aerial lime can be classified as fat or thin. Fat limes are originated from light-colored calcites, containing no less than 99% of $CaCO_3$, and have this designation because of their fluid consistency and workability. Thin limes come from grayish lime stones,

which have clay and other impurities contents between 1 to 5 %, and are not as workable and soft as the previous ones. Both thin and fat limes have the same setting reaction, though.

Despite the impurity content, which may vary largely for the same lime impurity classification (fat/thin), there are two main types of aerial lime, classified according to the chemical composition: calcium lime and dolomitic lime (neither of them contains hydraulic or pozzolanic component).

Calcium lime, CL, is the kind of lime in which the main chemical element that forms the compound is calcium in the form of calcium oxide and/or calcium hydroxide. Additionally to the strong presence of calcium, dolomitic lime, DL, also shows significant amounts of magnesium in the composition of oxides and hydroxides. This type of lime exhibits good workability characteristics, such as high plasticity and water retention. For such reasons, it has been largely used in contemporary construction.

The present work reserves the study of the behaviour of calcium lime exclusively. According to BS EN 459-2 (2010) calcium lime are classified in respect to calcium and/or magnesium oxide contents, as Table 1 reports.

Table 1: Chemical requirements of calcium lime given as characteristic values (BS EN 459-2: 2010)

Type of calcium lime	Values given as mass fraction in percent				
	CaO + MgO	MgO[a]	CO_2[b]	SO_3	Available lime[c]
CL 90	≥ 90	≤ 5	≤ 4	≤ 2	≥ 80
CL 80	≥ 80	≤ 5	≤ 7	≤ 2	≥ 65
CL 70	≥ 70	≤ 5	≤ 12	≤ 2	≥ 55

The values for CaO + MgO, MgO, CO_2 and SO_3 are applicable to all forms of calcium lime. For quicklime these values correspond to the finished product; for all other forms of lime (hydrated lime, lime putty and milk of lime) the values are based on the product after subtraction of its free water and bound water content.

The values for available lime (calcium oxide for quicklime, calcium hydroxide for hydrated lime) refer to the product when tested in accordance with EN 459-2.

[a] MgO content up to 7 % is permitted if the soundness test in accordance with EN 459-2 is passed.

[b] A higher content of CO_2 is permitted, if all other chemical requirements in Table 2 are satisfied and the test frequency satisfies the requirements in Table 7.

[c] Higher values of available lime may be requested.

2.1.2 Lime cycle

Although lime stones are commonly considered the origin of lime due the fact that they are the main source of this substance in nature, it is important to notice that there are other forms of calcium compounds, which differ by the type of chemical process which the material have been submitted to. The sequence of transformations that affect lime is called lime cycle, and a simplified representation of it can be seen in Figure 1.

Aerial Lime
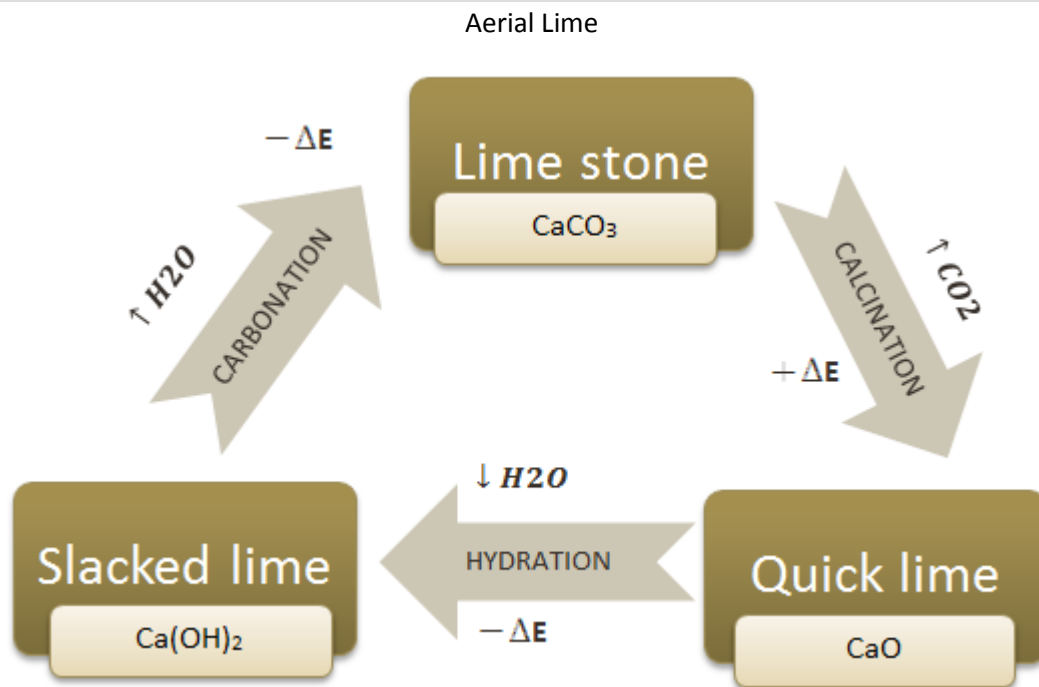
Figure 1: Simplified lime cycle

In the following paragraphs each stage of the cycle and modifying reactions are explained.

Limestone and Calcination

Calcium carbonate, or calcite, exists in nature under the form of mineralogical formations known as lime stones. According to Boynton (1984) and Holmes (1997), lime stones can have different crystal forms and compositions, and these are the main factors that affect the quality and properties of the lime.

Two main groups of lime stones are classified according to their origin: organic and inorganic. Organic lime stone occurs in nature from the accumulation of shells, corals and fossils layer in the oceans, seas and lakes. Inorganic lime stones are formed by chemical reactions with precipitation of calcium carbonate ions (Boynton, 1984).

The chemical composition of lime stones is altered by a process called calcination, a thermal decomposition of calcite where carbon dioxide is released in gaseous form, as follows equation 1.

$$CaCO_3 + \Delta E \longrightarrow CaO + CO_2 \qquad (1)$$

Calcination of calcium carbonate $CaCO_3$ is a highly endothermic reaction, and it requires 178 kJ/mol of heat input. The reaction only takes place when the temperature is above the dissociation temperature of the carbonates in limestone or lime mud, typically between 780°C and 1340°C (Moffat & Wimsley, 2006), and has to be maintained in that range until the end of the process.

Traditional lime kilns reach temperatures of 900°C. Higher calcination temperatures, around the order of 1400ºC, produce a dark-coloured product, often called burned lime due its low quality. According to Hassibi (2009), burned limes' lower quality is related to lower porosities, of about 8-12%, which makes the lime less reactive and thus less efficient in further chemical processes.

On the other hand, soft-burned limes, calcined at low temperature, are more porous because carbon dioxide's outflow occurs more slowly. Soft-burned pebbles have up to 54% in porosity and thus greater chemical reactivity. When this lime is exposed to wetting, water penetrates the cracks and fills the cavities quickly, providing a fast hydration (Hassibi, 2009).

The size of the stone also influences the process. Smaller stones react much faster and due to a greater surface for heat transference, while larger stones require more time, and often higher temperatures (Elert, 2002).

The dissociation of the calcium carbonate proceeds gradually from the outer surface of the particle inward, leaving a porous layer of calcium oxide as a product (Moffat & Wimsley, 2006). Thus, the calcination zone advances as a front towards the centre of the piece and leaves behind a calcined outer zone.

The reactivity of lime is not only determined by chemical purity of the parent limestone and the calcination temperature, but it is also affected by physical properties of the limestone, such as surface, porosity, pore size distribution and crystalline size (Elert, 2002). The optimum calcination parameters vary for the different types of limestone, and they are influenced by chemical and textural characteristics of the starting material.

Quicklime and Hydration

The product of calcination is a solid product called quicklime, having a characteristic white colour and is highly reactive to water.

Quick lime is available under the form of lumps, with 10 to even 20 cm in diameter, or in the form of powder (BS EN 459-2, 2010). ASTM standard C51 classifies lime according to the size of the cluster, as explained in Table 2.

Table 2: ASTM 51 Classification of quicklime (ASTM C51 -11, n.d.)

Denomination	Classifying Parameter
Large lumps	Diameter ≤ 8 in. (20,32 cm)
Crushed / pebble lime	2,5 in. (6.35 cm) ≤ diameter ≤ 0.25 in. (0.64 cm)

Aerial Lime

Ground lime	Diameter ≤ 0.25 in. (0.64 cm)
Pulverized lime	Maximum grain size passes through 0.033 in. (8.4 mm) sieve
Pelletized lime / briquettes	Grain average dimension : 1 in. (2.5 cm)

Quick lime can be added to water to produce calcium hydroxide, according to a reaction described as hydration − or slacking, represented in equation 2. Hydration of lime is an exothermic process that causes a volumetric expansion of the mass and generates around 273 kcal of heat per kilogram of lime.

$$CaO + H_2O \rightarrow Ca(OH)_2 + \Delta E \qquad (2)$$
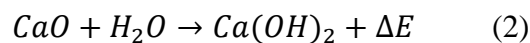
Hydrated lime, also referred as slacked lime, is an aerial lime mainly in the hydroxide form produced by the controlled slaking of quicklime (Meneghini, 2014). The hydration can be made in two forms: aspersion or immersion. Aspersion consists in the slacking of the lime with the exact amount of water needed to the hydration reaction, and produces hydroxide under the form of a powdery, fine substance. Immersion on the other hand, corresponds to a hydration with excessive water, conducted by the drowning of lime blocks, and takes to a product covered by a layer of water, ensuring the complete hydration of calcium oxide. The result of an immersive hydration can be presented in the form of putty, or, in other cases of lime milk.

Lime milk is presented in a liquid stage, and consists of a white-coloured suspension of calcium hydroxide particles in water. It is not used in mortars or other cementitious materials. Instead, it was usually applied as coating on architectonical surfaces in order to change their original pigmentation and for this reason can be considered a primitive form of paint.

Lime putties water content varies from 30 to 40% (Boynton, 1984), and this amount is relative to free water, in addition to the chemically combined water (Elert, 2002). Usually the minimum time of maturation for lime putties is 3 months. In fact, this is a permeable product, presenting very low porosity and carbonation rates.

Slacked Lime and Carbonation

Carbonation is the name of the process responsible for the last transformation described in the lime cycle presented in Figure 1, corresponding to the conversion of the calcium hydroxide present in slacked lime back into the calcium carbonate compound found in lime stones. For

this reason, as it was previously mentioned, it can be considered the inverse process of calcination and hydration combined.

This reaction acts exclusively in calcium hydrate, regardless of the form that this compound is found – putty or powder, and other types of substances that may be mixed together with it (sand, pozzolans, and other aggregates and additives), and is the main responsible of the stiffness process of lime-based materials.

Because of carbonation's great influence in aerial lime mortars, a further sub-section of the present chapter is reserved to characterize it properly and describe the main parameters that govern its development.

2.2 The carbonation process in aerial lime corresponding mortars

2.2.1 Carbonation and aerial lime

As previously stated, carbonation is the process through which the $Ca(OH)_2$ present in slaked lime reacts with atmospheric CO_2 to form calcium carbonate, or calcite, which is stronger and less soluble then calcium hydroxide, or portlandite. (Meneghini, 2014). Although this phenomenon is more strongly observed in lime concrete and plasters, it is one of the main reactions that acts in aerial lime mortars. In fact, in exception for an initial loss of free water during the drying process at early ages, the hardening of lime mortars is given mainly due carbonation (Callebaut, 2000; Ngoma, 2009) .

In order to provide a proper conservation and achieve a longer durability of lime- based materials, it is critical to understand correctly the parameters that influence carbonation and the circumstances in which the reaction occurs, as well as its behaviour given determinate conditions.

Aiming to give a theoretical basement to the developed study, the present section of the chapter intends to describe the main characteristics and parameters of the carbonation process, such as the stages of the reaction, factors that influence it and a brief presentation of some proposed models for coupling carbonation, humidity and carbon dioxide diffusion.

2.2.2 Stages of carbonation

According to Lawrence (2006), from a wide perspective, there are five principal stages involved in the carbonation process, described below.

A. Diffusion of carbon dioxide through the pores of the mortar

This is a natural process that occurs when the mortar is exposed to the atmosphere. In sealed specimens, the diffusion of CO_2 is prevented from occurring, and thus the reaction is limited.

B. Dissolution of carbon dioxide in pore water

CO_2 dissolves in water into H^-, HCO_3^{--} and CO_3^- ions. The combination of these ions leads to the formation of carbonic acid, according to equations 3 and 4.

$$2(CO_2 + H_2O) \rightarrow 2H^- + HCO_3^- + CO_3^- \quad (3)$$
$$3H^- + HCO_3^- + CO_3^- \rightarrow 2\,H_2CO_3 \quad (4)$$
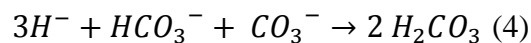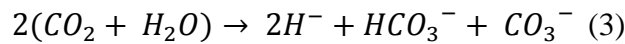
C. Dissolution of calcium hydroxine in pore water

The dissolution of portlandite molecules in the pore water originates Ca^{++} and $(OH)^-$ ions, as follows equation 5.

$$Ca(OH)_2 \rightarrow Ca^{++} + 2(OH)^- \qquad (5)$$
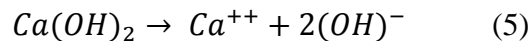
D. Solution reaction between portlandite and carbonic acid

Carbonic acid and calcium hydroxide react in the form of dissolved ions. The resulting Ca^{++} ions are combined with the CO_3^- ions, thus forming calcium carbonate. The simplified representation of this reaction is given by equation 6.

$$Ca(OH)_2 + H_2CO_3 \rightarrow CaCO_3 + 2H_2O \qquad (6)$$
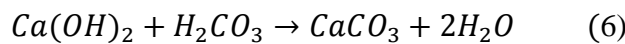
E. Precipitation of solid calcium carbonate

The reaction of precipitation of $CaCO_3$ is exothermic, releasing energy of about 74 KJ/mol. This may slightly contribute to evaporation of water from the pores. With the reduction of pore water, the medium where the reaction occurs is impaired, thus decreasing the rate of carbonation (Lawrence R. , 2006).

These five mentioned stages keep occurring repeatedly, either until all the available calcium hydroxide is converted into calcium carbonate or the capillary water has evaporated due to the heat generated by the late stage reaction.

The process also may be slowed by a reduction of carbon dioxide diffusion due the presence of a carbonated layer, which can make the surrounding substrate become "impermeable" to gaseous compounds.

Another possibility for the delay of the process is eventual excessive increase of moisture content, which also leads to a very slow diffusion of carbon dioxide.

2.2.3   Factors that influence carbonation

Diffusion of carbon dioxide through the porous structure

Carbon dioxide diffusion is strictly related to the amount of water in the mortar. The diffusion of carbon dioxide diffusion through porous lime mortar depends on the width of the pore structure of the mortar, depending thus on the water content of the mixture. The basic controlling parameters of carbon dioxide diffusion are: pore diameter, pore size distribution, pore water content and relative humidity.

According to Van Balen (2005) the diffusion of gases in aqueous medium occurs approximately 10000 times lower than in air; for this reason, it cannot be considered that the transfer of carbon dioxide inwards the mortar takes place in water. Also, the diffusive flux of within the mortar is related to concentration field, going from regions of high concentration to regions of low concentration, with a magnitude that is proportional to the concentration gradient (spatial derivative).

Based on Fick's laws, Van Balen (Cizler, Van Balen, & Gemert, n.d.) proposed an expression to describe the rate of gas transfer, following reported as a function of the water content through the diffusivity term, described in equation 7.

$$N_e = -D_e \frac{dC_a}{dx} \qquad \begin{cases} Ne = \text{ effective rate of gas transfer} \\ De = \text{effective diffusion coefficient} \\ Ca = \text{carbon dioxide concentration} \\ \quad x = depth\ of\ carbonation \end{cases} \qquad (7)$$

The diffusion coefficient has been defined from Van Balen & Van Gemert (1994) for lime mortars as a function of water content shown in a graph in Figure 2
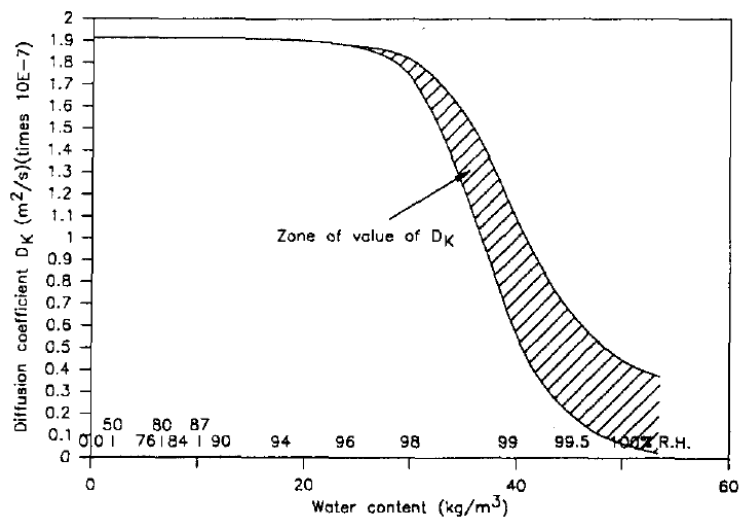
Figure 2: Diffusion coefficient for CO2 (Van Blen & Van Gemert, 1994)

According to Meneghini (2014), the capillary water corresponds to the amount of water at which the water transport in form of vapour can take place and the critical water corresponds to the maximum adsorption on the pore surface before extensive capillary condensation occurs.

From the graph it is possible to note that the diffusion coefficient tends to 0 for higher water contents. Basically this means that while water transport cannot occur in vapour phase, the presence of high condensed water contents act as hindrance for the carbon dioxide diffusion (Meneghini, 2014).

With respect to the concentration of carbon dioxide in the surrounding environment, Moorehead (1986) states that increasing values would lead to an increasing amount of calcite, so that in a saturated CO_2 atmosphere, the heat generated during reaction would be such that a premature drying would take place, occasioning the halting of the carbonation process.

Experiments made firstly by Van Balen (2005) and later by Shin (2009) show contrary results, though. Both authors state that it is actually the availability of moisture which guides the process and that carbonation proceeds at a rate that is independent of the carbon dioxide concentration, thus being considered a zeroth order reaction in regard to this reactant.

Solubility of gases and calcium compounds within the mass

The solubility of carbon dioxide and lime are influenced by temperature, being the optimum speed of dissolution related to temperatures of about $20^{o}C$ (Van Balen & Van Gemert, 1994).

Although Lawrence (2006) assumed that all the calcium hydroxide present in the composition of a mortar is available to react, the dissolution of this substance is faster than that of carbon dioxide and depends on the size of particles. For that reason, as long as carbonation is not ceased, a maximum content of hydroxide will be available at the pores surface (Elert, 2002; Van Balen & Van Gemert, 1994).

Also, the solubility of the calcium hydroxide is known to be greater than that of calcium carbonate. Thus, when an amount of water reaches the carbonation front during the occurrence of the reaction, a carbonate region separated from the aqueous solution is formed by the precipitate compound. According to Van Balen (2005), this carbonate deposit that is formed around the uncarbonated area prevents further penetration of outside carbon dioxide.

Water content and transport

Solid materials can contain water in two different forms: non-evaporable and evaporable, or free water. Non-evaporable water is present in stoichiometric quantities as part of the crystalline structures of the chemical compounds. Free water, in the other hand, corresponds to the amount available to evaporate because it is not chemically bound to a compound.

Among this, water can exist in both liquid and gaseous phases and it can be classified as: *adsorbed water,* when retained by the solid surface; *absorbed water,* when it is condensed and held in capillary structure of colloidal solids; and *occlusion or capillary water,* when it is occluded in the microscopic cavities of crystalline solids.

In aerial lime mortars, water plays two main roles. Firstly, it is the main agent in the production of calcium hydroxide by hydration of calcium oxide, process in which it is combined with calcium ions to form the hydroxide compound. Water is also a product of carbonation, and its formation modifies the global water content of the mixture, altering its properties.

Aside from the above mentioned states, possible excess of adsorbed water, given by hydration or mortar mixing processes, influences the pore structure of hardened mortar, thus the diffusivity of gases through the material (Arandigoyen, 2005; Lawrence R. , 2006).

During an initial drying process, the transport of free water happens in two phases. The first one corresponds to capillary water transport. According to Van Balen& Van Germet (1994), in this phase it is considered that carbonation does not occur, since "*there is not enough openness of the pore structure to allow carbon dioxide diffusion*". In this stage of drying, water is displaced to the surface through the capillary structure, and in this process, only the very outer surface can start to carbonate. Once it is reached the capillary water content, the second phase begins, corresponding to the water transport in form of vapour diffusion.

However, carbon dioxide diffusion does not begin until it is reached a critical water content present on the pore's surface. For lime mortars without specified characteristics, Van Balen (2005) estimates the value of 53,4 kg/m^3 as a critical water content that can start the diffusion.

On the other hand, environments with very low relative humidity (RH) hold carbonation back, for it has been observed that in environments with less than 8% RH the reaction between calcium hydroxide and carbon dioxide did not occur, since they both have to dissolve in water to react (Cultrone, Sebastián, & Ortegas Huertas, 2005).

Porosity

Porosity is a factor that influences carbonation as far is influenced by it, and is also a parameter that determines the strength and resistance of a mortar. In contrast with hydraulic mortars and concrete, Lanas & Alvarez (2003) report that aerial lime mortars specimens with higher pores' openness and quantity showed highest strength. The authors suggest that this phenomenon is given by a greater accessibility to carbon dioxide from atmosphere, resulting in greater carbonation rates.

The pore size distribution conditions the gaseous permeability. A large water:lime ratio conducts to more open porosity, but an adding of excessive portion of water leads to shrinkage cracks and weakens the mortar (Arandigoyen, 2005).

The course of carbonation affects the mortar's porosity as well, because as the precipitation of calcium carbonate promotes its attachment to the aggregates or the portlandite crystals surface, the volume of the pores is thereby altered. According to Lawrence (2006), the referred process tends to increase the amount of smaller pores (with up to $0,1 \ \mu m$ diameter), while slightly reduce the quantity of bigger pores.

Elapsed time

Time is related to carbonation trough the diffusion of carbon dioxide. In fact, the front of carbonation can be expressed as function of time by means of a factor k (that can be determined in experimental methods) and a constant e, according to equation 8 (Van Balen & Van Gemert, 1994).

$$x = e + k\sqrt{t} \qquad \begin{cases} x = carbonation \ front \\ \qquad t = time \end{cases} \qquad (8)$$

2.3   Aerial lime mortars

The most common form of employment of aerial lime in ancient buildings is as binder in cement pastes, most of all mortars. Aerial lime mortars usage move from holding masonry units to filling ancient concrete, as in multiple leaf walls (Ferretti & Bazant, 2006). Mortar was also employed as a complement in external resistance and internal lateral forces. In fact, one of its primary functions the load distribution throughout the structure (Gimbert, 2008).

Aerial lime mortars take long to harden and according to Lourenço (2004), are usually weaker than masonry units. This material is mainly made of lime, water, aggregates and, in some cases, additives. Different proportions of components leads to mortars with different

properties, as well as different types of grain size distribution and shape should be considered in this perspective (Lanas & Alvarez, 2003).

The present sub-section presents the main types of components practiced in contemporary recreations of ancient aerial lime mortars, as well as the acknowledged methods of mixing and also introduces the main properties of the studied material, characterized by the presentation of values found in literature. The main results are related to the type of binder, aggregates and ratio used in the mixture, listed by author. This information is summarized in Annex I.

2.3.1   Components

Types of binder

Lime of different forms can be used as binder in mortars. From putty to dry-hydrated powder, different authors have reportedly tried varied mixture design in the preparation of specimens of mortar for experimental purposes.

Teutonico (1993) and later Baronio (2000) developed their research based exclusively in mortars made from lime putty. In earlier works, it can be noticed a preference in the use of more plastic materials in the making process, perhaps due the fact that it was the most common form of binder used ancient times, or even due facilities in workability and casting characteristics. Works developed later use mostly dry hydrated lime. It is also the type of lime employed by a bigger number of researches. It can be observed, though, a growing tendency to testing mortars made by a larger variety of lime forms and ages.

Granulometry and types of aggregates

According to Elert (2002), aggregates are necessary to impart strength, hardness, and a certain degree of porosity to the mortar, that can later facilitate carbonation. The most used material is sand, of variable granulometry. Not rare, more than one type of inert is employed, usually differing in the grain size and format.

The chemical characteristics of aggregates, as well as its granulometry and particle shape, play an important role in the composition of a mortar's properties. Although there are not restrictive stablished standards in these terms, aggregates also influence the ratio used in the mix, for it can alter the performance of the binder.

According to Lanas & Alvarez (2003), calcitic aggregates made from limestone confer higher mechanical strengths in comparison with silicate sand. The same authors attested that

granulometry affects the mechanical properties by improving mechanical resistance particles smaller than 2 mm are utilised.

Concerning the grain shape, while silicate particles are mostly round-shaped, stone-derived powder are sharper and have greater specific surface that allows a tighter contrast between particles and offers larger grip areas (Lanas & Alvarez, 2003).

The existing norms recommend, for crushed stones fillers, a 30% maximum percentage of fines passing a 0.063 mm (BS EN 13139, 2002). The mentioned norm recommend for sand to fit an envelope with wider dimensions than those proposed in previous norms.

2.3.2   Mixing method

The mixing procedures of aerial lime mortar can vary greatly. The quicklime may be hydrated before mixed with aggregates or slacked along the process of execution of mortar. Regarding the second mentioned form of mixing, a traditional method of preparing mortar largely adopted in the literature the hot-lime mix method. In this mixing procedure, quicklime is slaked involving the addition of sand during the slaking procedure, thereby the slacking of the lime and the mixing of the mortar happen in the same time. Thus, the hot-lime mix shortens the production of mortar for it passes through the slacking step by combining it with the water addition, necessary to the making of mortar.

2.3.3   Main properties

Consistency

According to EN 1015-11 (1999), the flow value is the indicator of fresh mortars consistency and workability. The flow value is directly related to the density of the mortar, so that different flow values are recommended for each ranges of bulk density of fresh mortar, as shown in Table 3.

Table 3:Flow value according to the bulk density of fresh mortar (BS EN 1015-11, 1999).

Bulk density - ρ [kg/m3]	Flow value [mm]
$\rho > 1200$	175 ± 10
$1200 \geq \rho > 600$	160 ± 10
$600 \geq \rho > 300$	140 ± 10
$\rho \leq 300$	120 ± 10

Porosity

Porosity of mortars is influenced by the porosity of its contents, the amount of binder used and, the amount of water, at early ages, and later by the precipitation of calcium carbonate that alters of the pore structure (Meneghini, 2014).

For lime mortars, in contrary to cement mortars, it has been demonstrated that higher porosities leads to higher mechanical properties (Lanas & Alvarez, 2003), but it should be noted that the increase of lime content over the 2:1 lime:aggregate ratio can influence porosity in a way that may reduce strength (Lawrence R. , 2007).

The porosity of a material can be determined according to the measurement of its open porosity. This parameter corresponds to the ratio between the volume of open pores and apparent volume of the specimen (the latter made up of solid part + volume of voids), and the method to measure it is based on the principle of Archimedes.

The referred property is not reportedly normalized for aerial lime mortars in particular, however, literature results show typical values of open porosity that vary from 19% to 25% in aged hydrated lime mortars based on different forms of binder (Lanas & Alvarez, 2003). Particularly for early ages, open porosities of 23,5% to 32% are reported in lime putty mortars, and 26% to 29% in dry hydrated lime mortars (Baronio 2000, Cazalla 2000).

Compressive Strength

As it is known, the acting of carbonation leads to a progressive hardening process in aerial lime mortars, which is directly related to the improvement of mechanical properties of the material (Lawrence R. , 2006).

During lime mortar's hardening process, the compressive strength resistance has an initial growing stage due to drying, followed by a continuous increase given by carbonation reaction (Callebaut, 2000), as Figure 3 illustrates.
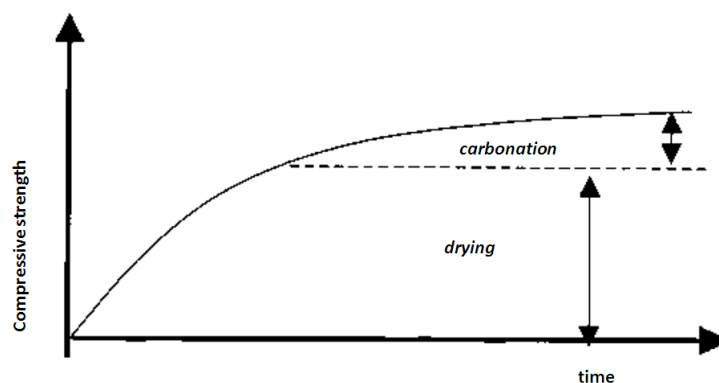
Figure 3:Evolution of compressive strengh resistance in lime mortars (Ngoma, 2009).

18

The final compressive strength values of aerial lime mortars do not exhibit mechanical properties with values comparable to hydraulic or cement mortars though, for they are remarkably weaker than these usual materials.

Cement mortars mixed in a 1:2 water/cement ratio, for instance, present from 47 to 61 MPa of compressive strength by the end of 28 days, according to Farkas and Kliege (1986). As examined by Stewart (2001), much older aerial lime mortar's resistances do not exceed a tenth of the cement lime average value. A comparison between the compressive strength of some types of mortar is shown in Figure 4 (Stewart, 2001).
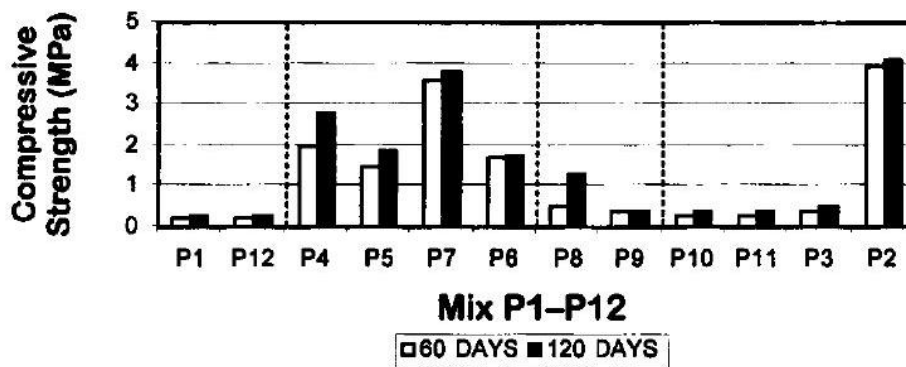
Figure 4:Comparison between mortar strengths. P1,P12 : aerial lime mortars; P4-P7: hydraulic lime mortars; P8,P9: hydraulic and air lime combined mortars;P10,P11,P3,P2: air lime mortars with additives. (Stewart, 2001)

2.3.4   Models for coupling carbonation, humidity and carbon dioxide diffusion

The behaviour of aerial lime mortar during its life is determined by chemical and physical interdependent processes. Therefore, the separate modelling of these processes, such as carbonation, humidity diffusion, carbon dioxide diffusion, modification of the pore structure, without taking into account the entirety of the is highly limited and imprecise. In this matter, there have been proposed some multi physics models, with combined diffusion and reaction models, to describe aerial lime mortar. Two of the most well-known models are following described.

Van Balen and Van Gemert model

According to Van Balen & Van Gemert (1994), carbonation is described by the differential equation given in equation 9.

$$div\left(D_{eff}\Delta c\right) + \psi\frac{dc}{dt} + R(w,c) = 0 \qquad (9)$$

In this equation, the first term $div\left(D_{eff}\Delta c\right)$ considers the diffusion of CO_2 through the pores, and is a function of the carbon dioxide diffusivity - D_{eff} and its concentration - c. The second

$\psi \frac{dc}{dt}$ acknowledges the change of c over time – t given by its penetration inside the voids of the mass. The last one, the sink term $R(w, c)$, expresses the dependence on c and water content - w.

The sink term, in isothermal conditions, can be expressed as follows equation 10, considering the specific surface of lime mortar pore system as 3,953 m^2/m^3 and the estimated amount of water with a thickness of five molecular layers.

$$R = 0,7062[CO_2]\alpha(RH)\beta([Ca(OH)]_2) \quad (10)$$

In the presented equation, α(RH) is the term that takes into account the effect of relative humidity and β([Ca(OH)$_2$) is the ratio of the pore surface for the amount of remaining lime over the initial pore surface.

For the presented model, some assumptions have to be made, namely:

- In an elementary volume of dimensions dx, dy, dz, the carbonation reactions consumes R moles of gas per unit of time and unit of mortar volume;
- Likewise, in an elementary volume, R moles of calcium hydroxide are converted into carbonate;
- Lime, water and carbon dioxide available in the mortar are concentrated ate the pores surface.

Ferretti and Bažant model

The study of Ferretti and Bažant was focused on ancient masonry towers and, especially, on failure cases of towers with no or imperceptible warning signals. In particular, the results from the numerical simulation confirmed that the time-scale of the diffusion-reaction processes is compatible with the age at which some towers had problems. (Meneghini, 2014).

For modelling the interaction between water transport, carbon dioxide diffusion and carbonation in lime mortars, Ferretti and Bažant took as base a model for low strength cement, by Saetta, Schrefler and Vitaliani. Given the few number of tests developed in lime mortars that could lead to the calibration of parameters, the authors assumed, as an approximation, the same values used to describe low strength concrete. In general terms, they have considered the simulation realistic, even if they suggest further researches on calibration of the parameters of the model.

In the presented model, the rate of carbonation is described according to equation 11.

$$\frac{\partial R}{\partial t} = \alpha_1 \times f_1(h) \times f_2(c) \times f_3(R) \times f_4(T) \quad (11)$$

In this equation, $f_1(h)$ is a function of relative humidity – h, governed as follows.

Aerial Lime

$$f_1(h) = \begin{cases} 0 & for \quad 0 \leq h < 0,5 \\ 2,5(h-0,5) & for \quad 0,5 \leq h < 0,9 \\ 1 & for \quad 0,9 \leq h < 1 \end{cases} \qquad (12)$$

Relative humidity is coupled with relative concentration of carbonate, considering the expelled water during carbonation, and can be described in terms of Fick's second law equation(equation 13).

$$\frac{\partial h}{\partial t} = \nabla(C\nabla h) + \frac{\partial h_s}{\partial t} + \alpha_2 \frac{\partial R}{\partial t} \qquad (13)$$

Where C is the diffusivity related to h, h_S is the self-desiccation term, α_2 is a constant that concerns the effect on pore humidity due to carbonation liberated moisture. C can be described through semi-empirical expressions that take into account the effect of humidity h, temperature T, the rate of carbonation R, the equivalent hydration time t_e and the diffusivity at 28 days and 296° K temperature - equation 14.

$$C = C_0 \times (h) \times F_2(T) \times F_3(t_e) \times F_4(R) \qquad (14)$$

$f_2(c)$ is the ratio of a given carbon dioxide concentration $-c$ by its maximum value, assumed the average concentration in air (0,0035%) – equation 15.

$$f_2(c) = \frac{c}{c_{max}} \qquad (15)$$

Carbon dioxide diffusion can also be described in terms of Fick's law by algebraically adding a term that considers the effect of carbonation - equation 16. D_C is the diffusivity of carbon dioxide in concrete (adapted for lime mortar), c is the concentration of carbon dioxide and R the relative concentration of carbonate.

$$\frac{\partial c}{\partial t} = \nabla(D_c\nabla c) - \alpha_3 \frac{\partial R}{\partial t} \qquad (16)$$

It is possible to give an expression – equation 17 of the diffusivity of carbon dioxide dependent to the same variables considered for humidity diffusion (humidity, temperature, equivalent hydration time, relative concentration of carbonate) and to the diffusivity at normal conditions for cement Portland concrete (28 days, 296 K temperature)- $D_{C,0.}$

$$D_c = D_{c,0}F_1(h)F_2(T)F_3(t_e)F_4(R) \qquad (17)$$

The third term $f_3(R)$ corresponds to the rate of carbonated material $- R$, as follows:

$$f_3(R) = 1 - R \qquad (18)$$

The rate R is the relative concentration of calcium carbonate, given by the ration between the given carbonate concentration and the maximum possible value (equation 19).

$$R = \frac{[CaCO_3]}{[CaCO_3]_{max}} \qquad (19)$$

The factor $\alpha_1 \times f_4(T)$ takes into account the kinetics of the chemical reaction, where T stands for temperature, and α_1 an constant.

3.   APPROACHES AND EXPERIMENTS IN AERIAL LIME MORTARS

3.1   General remarks

This chapter is focused on a dedicated review of existing experimental methodologies and protocols targeted for testing aerial lime mortars. This review comprises several issues, namely: mix design, casting and storing conditions of specimens and the main experimental tests performed to study the behaviour of the material in terms of specific properties.

It is remarked that a significant part of this literature review is based on a recent research work conducted at the University of Minho, which specifically focused on the establishment of feasible experimental protocols for aerial lime (Meneghini, 2014).

3.2   Mortar mixture design and preparation

Mortars are basically composed by binder, aggregates and water mixed in specific proportions. In some cases, additives may also be added, in order to improve certain characteristics, such as plasticity and curing time. In addition, the sequence/manner in which the ingredients are put together and mixed influence the behaviour of the mortar. The current section presents and describes the components and main parameters that influence the composition and characteristics of mortars.

3.2.1   Binder

Several types of aerial lime slacked in diverse manners and conditions, and even quicklime can be used as binder in mortars. In attempts to approach the tested mortar specimen's composition to mortars and pastes usually found in ancient buildings and cultural heritages from diverse European regions, authors have performed test in specimens made of diverse lime forms.

In fact, in early studies on aerial lime mortars it is remarkable a preference in lime putty, as it is the binder most commonly found in ancient mortar elements (Teutonico, 1993). However, later works give great importance to the use of hydrated lime as well, and some authors restrict dry hydrated lime powder in their mixings (Lanas & Alvarez, 2003; Moropoulou, 2005; Válek & Matas, 2010; Veiga, Fragata, Velosa, & Magalhães, 2010). Other publications work with more diverse ranges, reporting the appliance of both putties and dry hydrated lime (Baronio, Binda, & Saisi, 2000; Cazalla, 2000; Lawrence R. , 2006; Margalha, 2011; Van

Balen, 2005) or even quicklime, adopting the hydration of CaO within the mortars making procedure (Lawrence R. , 2006; Válek & Matas, 2010; Meneghini, 2014). Annex I reports in detail the binders mostly found in the literature research and does a comparison of results on tested properties among them.

Regarding the use of quicklime as binder, previous research programs report the use of quicklime in a micronized form, classified as CL90 Q according to BS EN 459-1 (BS EN 459-1, 2010; Meneghini, 2014). A characterization of CL90 Q is available on annex II.

Further information obtained from Thermo gravimetric analysis – TGA (also presented in annex II) reveal the presence of a certain amount of $Ca(OH)_2$ and $CaCO_3$. Hence, even if the precautions have been taken in order to prevent air contact, it has to be considered that inevitable hydration and carbonation have occurred and partially converted calcium oxide in hydrated lime and calcium carbonate, for quicklime can easily hydrate and carbonate in contact with the external environment, all the more in the micronized form (Meneghini, 2014).

3.2.2 Aggregates

The range of aggregate types used for aerial lime mortars is relatively wide. Some authors have worked with calcitic aggregates (Lanas & Alvarez, 2003) and bioclastic and oolitic lime stones (Lawrence R. , 2006). Nonetheless, most of the research works use siliceous sands (Baronio, Binda, & Saisi, 2000; Lawrence R. , 2006; Válek & Matas, 2010; Margalha, 2011; Meneghini, 2014; Lanas & Alvarez, 2003). In particular, Meneghini (2014) used to types of siliceous sand (fine and coarse sands), chemically characterized in annex III.

Regarding the granulometry of aggregates, although BS 1200 gives upper and lower limits, different for mortars made with crushed stone sand (0,06mm – 2mm), and BS EN 13139:2002 gives limits on the maximum grain size and on the percentage of fines with d<0,063mm), a properly defined standardized granulometry is not defined for lime mortar mixtures.

3.2.3 Mixture proportions

The composition of mortars varies greatly due to the wide possible types and quantities of aggregates, forms of binder and also additives that can be mixed.

Research has been developed varying proportions of raw materials in order to describe how the binder:aggregate ratio affects mortar properties (Meneghini, 2014). It is nonetheless remarked that traditional mixing usually comprises the volumetric proportion of 1:3 (limeaggregates) (Meneghini, 2014). It is further remarked that the description of mixing

ratios for aerial mortars is usually made in regard to volumetric proportions. Such situation is implied throughout this document, except when stated otherwise.

Teutonico (1993) used the ratios of 1:2,5 and 1:3. Baronio (2000) initially tried an unsuccessful ratio of 1:5, thus changing to 1:3. Lanas & Alvarez (2003) on the other hand, tried lower aggregate proportions (1:1, 1:2, 1:3 and 1:4), which did not presented casting issues. Moropoulou (2005) used 1:1,5 and 1:3. Lawrence (2006) repeated the three first ratios adopted by Lanas & Alvarez. Válek (2010) performed 1:0,9 and also 1:3 ratios. Margalha (2011) and Meneghini (2014) limited the studied mixes to the traditional ratio of 1:3. The criteria to adopt this value, despite being a well-known and practiced ratio, took into account the workability of the mortar, as well as the avoidance of cracking due shrinkage. For further information, the table presented in Annex I can be consulted.

3.2.4 Mixing method

A traditional method of preparing mortar largely adopted in the literature is the hot-lime mix (Meneghini, 2014). In this mixing procedure, quick lime is slaked involving the addition of sand during the slaking procedure, thereby the slacking of the lime and the mixing of the mortar happen in the same time.

Thus, the hot-lime mixing method shortens the production of mortar as the slacking step is combined with the mixing mortar of the mortar itself. The simplicity of the method provides more uniform physical fields, which can facilitate the isolation of physical phenomena. This characteristics is relevant for further numeric modelings and future back-analyses of the model.

It is important to regard that the hydration of the lime releases a significant amount of heat, which can cause the evaporation of part of the mixing water, thus reducing the quantity of available water. However, considering the claimed reactivity of lime (high) and the parts of water decided in the final mix, the amount of water should be enough to hydrate the lime and provide suitable plasticity to the mortar (Meneghini, 2014)

Some researches introduced alterations in the hot-lime mix traditional procedure. For instance, Válek (2010), added water gradually within 30 minutes breaks, while Margalha (2011) has subjected mortar up to 90 days of maturation before casting, adding water in the meanwhile to slake the lime.

3.3 Casting and curing procedures

The form in which the mortar is applied, as well as the shape of the molded element and the form it was cast also influence the properties behaviour of the mortar. In fact, samples taken from specimens made of the same material can exhibit different chemical characteristics according to the conditions in which have been conditioned inside the mould. It is also important to notice that the mould characteristics, such as shape, size and material may condition the storing and curing conditions, which influence the latter properties. This section details the major influences that concern the casting procedure and curing of aerial lime mortar specimens.

3.3.1 Specimen size

According to Lanas & Alvarez (2003), it is necessary to restrict lime mortar specimen sizes, conciliating the interests of the testing purpose and the potential shrinkage cracking problems. A simple normalized criterion to define the minimum thickness of a specimen is that the thickness should be at least 3 times and a half the nominal size of aggregate (BS EN 12390-3, 2002).

Deeper normalization regarding the dimensions of aerial lime specimens in particular is not reported, and not rare, adaptations are made from cimentitious materials. The size and shape of specimens vary accordingly to the designed testing's purposes. Literature shows the conforming of rectangular or cubic shaped specimens for assessing physical/mechanical properties: Teutonico (1993) molded specimens of 600x100x100 mm; Baronio (2000) casted three different sizes of specimens: 20x20x120 and 160x40x40 mm in an attempt to reproduce masonry joints and 70x70x70 mm to reproduce ancient concrete; Lanas & Alvarez (2003) repeated the 160x40x40 mm pattern; Lawrence (2006) tried a variation of 50x50x250 mm; Válek (2010) and Margalha (Margalha, 2011) adopted the same proportions as Lanas & Alvarez.

Concerning specific compressive strength testing, BS EN 1015-11 (1999) recommends previous flexural testing on 16x4x4 cm specimens and the reuse of broken parts for compressive test. Since Meneghini (2014) did not performed flexural tests, the author casted 5x5x5 cm cubic specimens in an attempt not to distance from the standard recommendations.

In the experimental campaign, Meneghini also made specimens for modulus of elasticity tests. Limitation related to cracking resulted in the adopted dimensions of 6 cm diameter by 12 cm height (Meneghini, 2014).

The referred author also performed chemical tests through thermo gravimetric analysis, introducing a reduced thickness specimen (3,7 cm diameter and 0,8 cm heigh) in order to minimize the influence of internal gradients (of moisture and/or carbonation) in the results.

3.3.2 Types of mold

Even though the European standards recommend the use of metal molds (BS EN 1015-11, 1999), the use of many other types of mold has been reported related to the casting conditions and testing purposes.

Teutonico (1993) adopted damped plywood molds in order to allow surplus water to be transported away more rapidly. Van Balen (2005) used brick molds and adapted blotting paper on the top and the bottom of the specimen to simulate the brick absorption on mortar joint. Lawrence (2006) adopted the plywood mold previously used by Teutonico, introducing a breathable membrane to facilitate demolding and avoid preventing the occurrence of moisture diffusion and carbonation from early ages. Meneghini (2014) adopted molds of varied material, according to the specifications of the samples in each performed test.

In the case of thin and small specimens designed for TGA analysis, Meneghini (2014) adapted a light steel ring structure that casted disc-shaped specimens, as illustrated in Figure 5.

Figure 5: Disc-shaped specimens for TGA analysis (Meneghini, 2014)

To perform humidity profile monitoring, the author used a plastic container with transparent surface in order to check possible cracking and its height, described in Figure 6. The mold had pre-embedded measuring sleeves as to allow insertion of humidity probes and thus infer moisture profiles. The sleeves are made of plastic tubes and introduced in holes made in the top of the container. The tubes have the mortar interface extremity covered in a Gore-Tex® membrane. The material's properties assert that relative humidity measurements can be compared with a direct-contact specimen measurement, for it is permeable to water vapor but does not allow the passage of liquids. The other end of the sleeve is capped with a rubber plug that seals completely the interface with outside air (Meneghini, 2014).

Figure 6:Vaisala sleeves and the mould apparatus for humidity profiles measurements (Meneghini, 2014)

The specimens used by the referred author for E-modulus determination were casted inside pieces of propylene tubes, as illustrated in Figure 7 (Meneghini, 2014). For the designed purposes, Prolypropylene is considered impermeable to vapor and liquids, and has stiffness properties that permit the maintaining of desired cylindrical shape. The mold is cut longitudinally to facilitate demolding. While molded, the tube's fragments are bound together by adhesive tape, wrapped around its external walls.
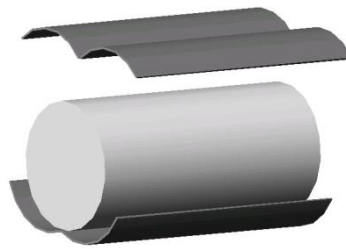
Figure 7:E modulus tests specimen and mould aparatus (Meneghini, 2014).

The specimens submitted to the compressive strength testing procedures have been casted inside a metal mold set, which conforms three cubic specimens. In Figure 8 is shown the mold filled with mortar, immediately after casting (Meneghini, 2014).

Figure 8:Compressive strnegth moulding apparatus (Meneghini, 2014).

3.3.3   Curing conditions

Concerning the curing conditions, different time and environmental conditions have been used in previous research works. Nonetheless, the average temperature of 20°C, reportedly related to optimum speed of carbon dioxide dissolution (Van Balen & Van Gemert, 1994), is maintained in all consulted works.

Regarding relative humidity conditions, the majority of authors stored mortar specimens at 60 ± 5% RH (Baronio, Binda, & Saisi, 2000; Lawrence R. , 2006; Válek & Matas, 2010; Meneghini, 2014), but some also introduced high moistures (of about 90%RH) in the curing process (Baronio, Binda, & Saisi, 2000; Lawrence R. , 2006). In particular, Baronio (2000) lowered the humidity gradually: for the first 24 hours, the author kept the mortar at high moisture, followed by 75%RH and then 60%RH from the third day of casting. Likewise, following BS EN 1015-11 (1999) recommendations, Lawrence (2006) maintained the mortar exposed to a 90%RH environment in the first 7 days and subsequently 60% until the testing date.

Meneghini (2014) stored the mortar specimens inside a climatic chamber with controlled conditions of 20°C and 60%RH during the whole ageing process, and attempted to let carbonation act from the first ages after casting. However, due molding apparatus difficulties, in the case of cylindrical specimens, mortar was not fully exposed since the very begging of curing period because specimens have been stored inside the mould for the first 3-4 days (Meneghini, 2014). This particularity may have prevented carbonation at early ages, and thus originated difficulty of analysis, for it was originally intended to preserve constant the boundary conditions throughout the curing period.

3.4   Testing of specific properties

In the seeking to a better understanding of the properties of aerial lime mortars, some experimental tests are recurrently found in the literature. The current section presents five experimental settings that are used to determine chemical and mechanical behaviors: thermo gravimetric analysis or TGA, carbonation front measurement, humidity profile monitoring, modulus of elasticity and compressive strength tests.

3.4.1   Thermo gravimetric analysis

The thermo gravimetric analysis - TGA is an experimental technique in which the mass of a sample is measured as a function of the induced temperature along the duration of the

experiment (controlled atmosphere, e.g. N_2). During testing, the TGA apparatus induces an increasing controlled temperature in the testing chamber, until the maximum desired temperature is reached. After that, the equipment begins the cooling of the system to the equilibrium with exterior temperature.

The results are given in terms of weight variation according to the imposed variation of temperature, and the interpretation relies on the analysis of weight decline according to related phenomena (e.g. thermal decomposition of compounds).

In a TGA analysis, the main important parameters to set are: the temperature range, which depends on the thermal breakdown temperature of the compound investigated; the atmosphere, as it can be reactive or inert, affecting reactions in the material during the experiment; the heating rate, that besides the accuracy of the analysis, plays a role in the curve heat flow [W/g] vs. temperature or time and is useful to identify if the thermic kind of reactions occurring at the respective temperatures. Table 4 reports parameters used by some authors which performed TGA analyses (Lawrence R. , 2006).

Table 4:TGA Analyses performed by different authors on lime and cement (Lawrence 2006)

Author(s)	Material	Temperature range	Heating rate	Atmosphere
Dheilly et al, 1998	Lime	20°C - 850°C	0.67°C min⁻¹	Dry O_2
Thomas et al, 1996	Cement	20°C - 900°C	10°C min⁻¹	?
Strydom et al, 1996	Lime	20°C - 800°C	5°C min⁻¹	Dry N_2
Balcerowiak, 2000	Lime	20°C - 950°C	24°C min⁻¹	Dry Air
Ubbriaco & Tasselli, 1998	Lime	20°C - 950°C	?	Dry Air
Lanas & Alvarez, 2004	Lime	20°C - 1200°C	20°C min⁻¹	Dry Air
Valenti & Cioffi, 1985	Cement	20°C - 700°C	10°C min⁻¹	?
Stepkowska, 2005	Cement	20°C - 1000°C	1°C min⁻¹	Dry Air
Alvarez et al, 2000	Lime	20°C - 1100°C	10°C min⁻¹	Dry Air
Montoya et al, 2003	Lime	20°C - 1050°C	20°C min⁻¹	Dry Air
Bruno et al, 2004	Lime	20°C - 1000°C	5/10°C min⁻¹	Dry Air
Ingo et al, 2004	Lime	20°C - 1000°C	20°C min⁻¹	Dry Air
Riccardi et al, 1998	Lime	20°C - 1300°C	10°C min⁻¹	Dry Air
Moropoulou et al, 2004	Lime	20°C - 1000°C	10°C min⁻¹	Dry Air
Gualtieri et al, 2006	Lime	20°C - 1000°C	20°C min⁻¹	Dry N_2/Air
Maravelaki-Kalaitzak, 2005	Lime	20°C - 1000°C	10°C min⁻¹	Dry Air
Paama et al, 1998	Lime	20°C - 900°C	10°C min⁻¹	Dry N_2/Air
Bakolas et al, 1998	Lime	20°C - 1000°C	10°C min⁻¹	Dry N_2

The typical results of a thermo gravimetric analysis are represented in graphic interface in terms of mass loss versus temperature, as figure 9 illustrates. The given curve presents the evolution of the sample weight and the behavior of mass loss through the variation of temperature, showing main declines of weight in certain ranges of temperature. The curve's

aspect depends on properties of the tested material. When subjecting materials based on aerial lime to TGA equipment, the thermal breakdown calcium hydroxide and calcium carbonate can be observed through the analysis of the plotted curve, as it is illustrated in Figure 9, taken from Meneghini (2014).
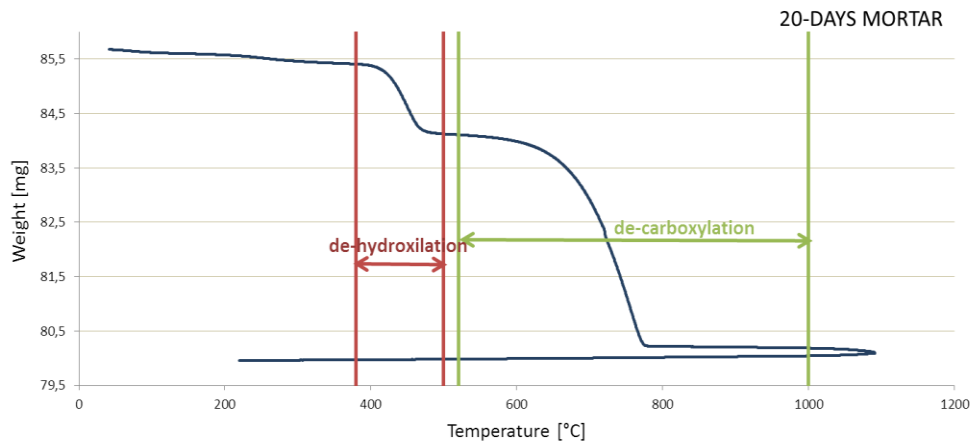
Figure 9:TGA curve of 20 days old mortar specimen showing the temperature ranges of the main phenomena related to mortars' compound analysis. (Meneghini, 2014)

The thermal breakdown of each compound is related to different phenomena presented in the graphic by two levels of weight drop, namely dehydroxylation and decarboxylation, respectively marked by red and green limits.

In the graphic it can be firstly observed a soft decline of mass, which is related to the evaporation of the free water content and thermal decomposition of other minor compounds of the mortar.

The second decline noted in the graphic is more abrupt, and shows the thermal decomposition of calcium hydroxide - Dehydroxylation. This phenomenon happens in a range of temperature about 350 – 500°C and describes the transformation of Calcium hydroxide into calcium oxide and water, as follows equation 20 (Lawrence R. , 2006). The measured variation of weight during dehydroxilation is assumed to be given due release of water. The hydroxide content is calculated indirectly, according to the supposed water variation.

$$Ca(OH)_2 \rightarrow CaO + H_2O \qquad (20)$$
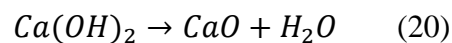
The last and greater decline observed in the graphic corresponds to Decarboxylation, which is the thermal decomposition of calcium carbonate in calcium oxide and carbon dioxide, as described in equation 21. This phenomenon occurs in a range of temperature about 600 – 1000°C. Theoretically the decomposition point is at 907°C, but in practice the reaction starts from a lower temperature, as it is not a punctual phenomenon (Lawrence R. , 2006). Likewise

dehydroxilation, the carbonate content is calculated indirectly, according to the measured variation of weight (which is assumed to be given due release of carbon dioxide).

$$CaCO_3 \rightarrow CaO + CO_2 \qquad (21)$$
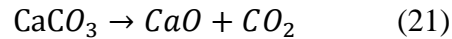
Dehydroxylation and Decarboxylation are the thermal decompositions of interest in investigating carbonation for the measured weight loss during these reactions represent respectively the drive-off of the chemically bound water as vapor and the carbon atom as carbon dioxide gas. To calculate the actual content of calcium hydroxide and calcium carbonate it is necessary to use stoichiometry in the conversion of the results obtained from TGA. The calculation is made taking into consideration that 1 mol of calcium carbonate or calcium hydroxide decomposes. Table 5 shows the molar masses of the related compounds.

Table 5:Molar masses of the compounds present in decarboxylation and dehydroxylation

Compound	Molar mass [mg/mol]
Ca(OH)2	74
CaCO3	100
CO2	44
H2O	18

Therefore, to obtain the estimated mass of hydroxide, the calculation is made according to the proportion using the molar masses of the dehydroxyaltion reaction, as reported in equation 22.

$$\frac{1mg \; weight \; loss}{Ca(OH)_2 mass} = \frac{18}{74} \rightarrow Ca(OH)_2 \; mass = 4,11 \times weight \; loss \qquad (22)$$

The same logic is applied to calculate the real mass of carbonate, replacing the molar masses of the compounds present in decarboxylation, as shows equation 23.

$$\frac{1mg \; weight \; loss}{CaCO_3 mass} = \frac{44}{100} \rightarrow CaCO_3 \; mass = 2,27 \times weight \; loss \qquad (23)$$

There are no reported standards regarding procedures for measuring carbonation in aerial lime using TGA. According to Meneghini (2014), the methods currently in use vary from the mostsimple TG/dTG in static air atmosphere to highly sophisticated TG/DTA analysis in different atmospheres.

Literature results shows higher rates of carbonate conversion from ages of 3 to 20 days, date from which the carbonation rates are considered to be stabilized (Meneghini, 2014). However, carbonation rates are not reported to reach 100% conversion degree, even for advanced ages (180 days) (Van Balen, 2005).

3.4.2   Carbonation front measurement

A recurrent form to investigate the amount of carbonated material on a specific sample of aged mortar concerns the search for areas with greater basicity, once the presence of unreacted lime can be inferred from the presence of calcium hydroxide (alkali that induces high pH value). The use of phenolphthalein as indicator in such concern is widespread in the context of aerial lime mortars (Lawrence R. , 2006).

The chemical formula of phenolphthalein is $C_{20}H_{14}O_4$. Phenolphthalein solutions change from a clear, transparent appearance to a magenta color when in contact with alkaline mediums. According to the pH scale, used to characterize the acidity of basicity of aqueous mediums, a substance can be considered alkaline or basic from pH greater than and acid when it has a pH less than 7, as can be seen in Figure 10.

As Lawrence (2006) states, the changing of color of phenolphthalein solutions is a gradual phenomenon that starts when the substance is stained in mediums with a pH range from pH 8,3 to pH 10. As Calcium hydroxide is a strong alkali, with an average pH varying from 10 to 12,4, phenolphthalein staining can be considered a reliable indicator of the presence of this substance, as Figure 10 demonstrates.
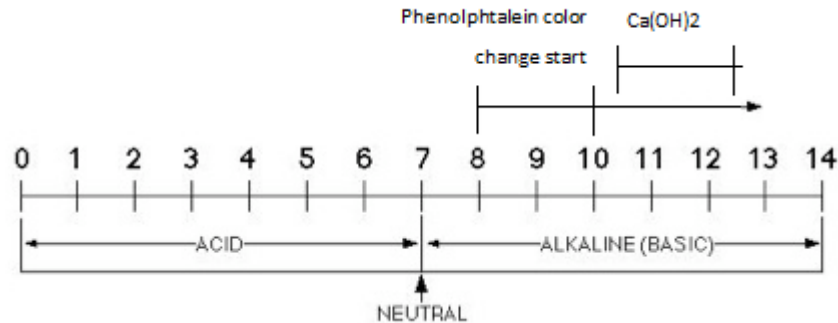
Figure 10:pH scale classification. Calcium hydroxide average pH and Phenolphthalein changing colour start ranges.

Although the changing of color would occur when phenolphthalein gets in contact with any alkaline medium, regardless of the alkali that it contains, it is reasonable to assume that, in the case of a lime-based mortar, the alkaline character indicated by the staining would be due the presence of calcium hydroxide. This statement can be strongly justified by chemical analysis of the lime and aggregates used in the mixing of the mortar, for instance.

Because of the fact that it is a very simple method and provides reliable results, phenolphthalein staining is a recurrent procedure found in literature to investigate the content of hydroxide in specimens, as well as the carbonation behaviour (Lawrence R. , 2006; Ngoma, 2009).However, it cannot be assumed that unstained material is fully carbonated. In

fact, comparisons made between staining results and carbonation percentage given by TGA demonstrated that unstained mortars can contain 40% to 50% of uncarbonated material content (Lawrence et al. 2006).

Although literature results agree to report a progressive evolution of the carbonation front towards inner regions of specimens, authors describe advancing rates of different orders. Square specimens, subjected to varied curing conditions and stained at different ages revealed advances from 10-17 mm at 120 days (Teutonico, 1993) to 100 mm at 21 days (Vestrynge, Schueremans, & Germert, 2010).

Meneghini (2014) stained phenolphthalein on the fresh-cut surface of 60 mm diameter cylindrical specimens at different ages, and found a maximum carbonation depth of 24,2% at 36 days. The aspects of stained specimens are illustrated in Figure 11.

Figure 11:Horizontal section of stained specimens at 4,7,14 and 36 days of age, respectively. (Meneghini, 2014)

The mentioned author also compared the results from specimens of different sizes and reports a significant scale effect, as the smaller specimens presented the higher carbonation depth (Meneghini, 2014).

3.4.3   Humidity profiles monitoring

The attempt of observing the behaviour of the moisture within a specimen of mortar is motivated by the investigation of the evolution of the drying process of the material. Such type of study has only been deployed by Meneghini (2014), who was particularly interested in studying 1D moisture flows in specimens, as to simplify the analysis of results and even the corresponding numerical simulation.

The measurements took place in a specimen with only one surface exposed. Meneghini (2014) also casted another type of specimen that was kept completely sealed, in a way that moisture self-consumption in the absence of exchanges with the surrounding environment.

As Figure 12illustrates, measurements were made through the insertion of sensor's probes in sleeves designed for this purpose. The sleeves' internal diameter permits a fast operation in inserting it, avoiding the environmental exposition. They also are water and vapor proof, and are capped with a plug that prevents the penetration of outside moisture. The extremity of the

sleeve that is kept in contact with the mortar is covered with a vapor-permeable membrane made of Gore-Tex®. Previous experiences that adopted the same procedure on concrete report that measurements of relative humidity made through the Gore-Tex® membrane or directly in contact with the specimen are equivalent (Granja, Azenha, de Sousa, Faria, & Barros, 2014).
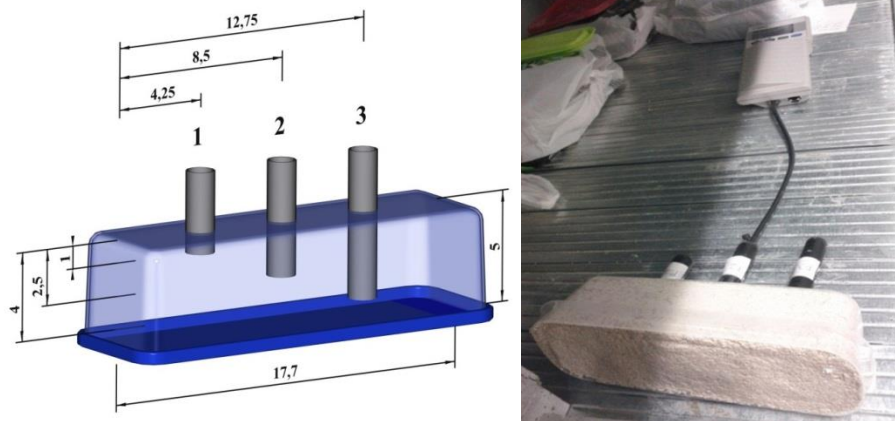
Figure 12: Representation of the mould and the depths of measurement and picture of the measuring apparatus (Meneghini, 2014)

The relative humidity has been measured at the depths of 1 cm, 2,5cm and 4 cm (measured from the exposed surface), and measurements have been collected for 40 days on the isolated and one-surface exposed specimens, as it can be observed in figure 12. Both specimens have been stored at 20ºC and 60%RH.

As Figure 13demonstrates, it was verified a significant decrease of the moisture. The one-face exposed specimen presented a variation from values close to the saturation, on early ages, to values considerably close to the chamber's conditions, of around 60% RH, by the end of 40 days. Even though the depth of measurement suggests a possible interference on the rate of variation of the moisture, the final value is common in the three depths. On the other hand, the sealed specimen did not show such a wide variation of measurement, stabilizing at 90%RH at the end of the monitoring period.

Testing of specific properties
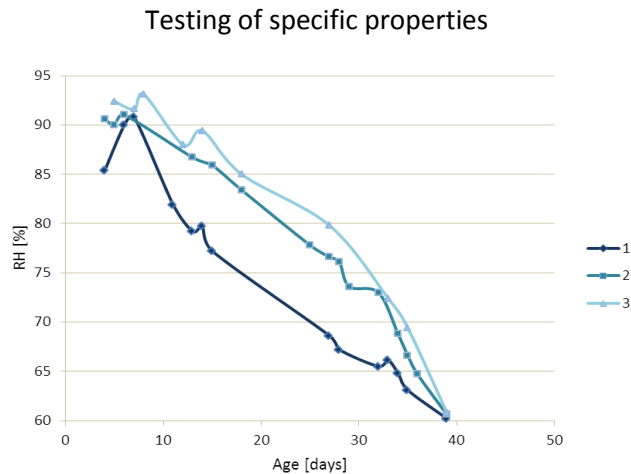
Figure 13: RH vs Time in 3 points of measurement (Meneghini, 2014).

3.4.4   Modulus of elasticity

The modulus of elasticity, also called Young's modulus, is a mechanical parameter that provides stiffness measure of a solid material. Two main forms of measuring this parameter are commonly employed in concrete researches, classified as dynamic or static testing techniques.

Literature presents some measurements regarding the dynamic modulus of elasticity on mortar through the resonance frequency method. This procedure consists on applying longitudinal resonance frequencies on a cylinder specimen. The elastic material constants is determined based on a three-dimensional vibration analysis using the Rayleigh-Ritz method (Kolluru et al. 2000).

Dynamic modulus results on aerial lime mortar vary from 0,11 GPa (Baronio, Binda, & Saisi, 2000) to 2,97 GPa (Margalha, 2011) at 28 days from casting. Older test ages (90 days) reveal the rise of the average modulus to the order of 4 – 4,6 GPa (Margalha, 2011; Veiga, Fragata, Velosa, & Magalhães, 2010). From Margalha's results, it can be observed an increase of about 50% in 62 days.

Static modulus measurements are made through the appliance of load cycles by hydraulic press. Figure 14 shows the testing apparatus. This technique is employed for a wide range of materials, and has already been used in University of Minho on soils reinforced with lime mortar (de Magalhães, 2013). The specimens are submitted to a pre-load of 100N, after which three cycles of uniaxial load with amplitude of 200 N are conducted. The testing procedure includes measuring the imposed displacements through three external sensors (Linear Variable Differential Transformers – LVDT) placed around the specimen perimeter. Aiming to minimize experimental errors, the first cycle of load is discarded and only the results of LVDTs in compression are considered.

Figure 14: Setting of experimental testing apparatus on specimen.

The result is given by the relation between strain and stress parameters. The strain is calculated by dividing the displacement read by each transformer by the length of measurement (which corresponds to the distance between the steel rings). The average strain is calculated by the media of the displacements measured by the LVDTs. The internal force applied is divided by the area of the average transversal section to calculate the tension. The modulus of elasticity is given by the first derivative of the tension vs strain curve.

As Meneghini (2014) acknowledged, the static modulus results vary according to the specimen's density. The author stated that specimens with higher densities reached higher values, whilst this trend is not very well defined and the data may show certain degree of scattering. Furthermore, the growing trend tends to be reduced at about 20 days, for specimens with higher density (Meneghini, 2014).

Disregarding the deviation of density of specimens, the average modulus from 35 to 38 days reaches 3,35 GPa. The author's results are illustrated in Figure 15.

Testing of specific properties
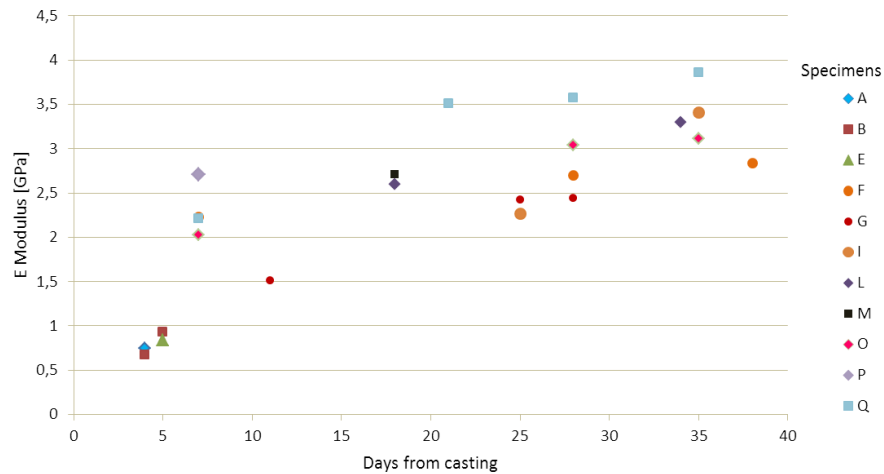
Figure 15: E-modulus vs. Time (Meneghini, 2014).

3.4.5   Compressive strength

The compressive strength corresponds to the capacity of a material to bear loads, according to a tendency to reduce its size and alter its original shape and structure (Callister Jr, 2007). This parameter can be measured by plotting the stress caused by the appliance of a constantly increasing force against the specific deformation suffered by the material.

Solid materials behave differently when submitted to compressive stress: some fracture at a maximum compression value, others deform irreversibly. By definition, the ultimate compressive strength of a material is given by the value of the compressive uniaxial stress that causes the failure or an irreversible, or non-plastic, deformation on the material (Judice & Perlingeiro, 2005).

The compressive strength is usually obtained experimentally by means of a compressive test, performed in a hydraulic press, illustrated in Figure 16. The equipment submits the specimen to a uniaxial compression load, resulting in a shortening and lateral spread of the material. During the compression test, the applied force and the respective displacements are measured proportionally, as the load increases.

Figure 16: hydraulic press apparatus for compressive test (Meneghini, 2014).

Literature results shows compressive strength at 28 days varying from 0,45 MPa in dry hydrated lime mortars (Baronio, Binda, & Saisi, 2000) to 1,6 MPa in mortars mixed according to the hot lime mix method (Válek & Matas, 2010). Regarding researches that followed exclusively the hot lime mix method, compressive strength values at 28 days are varied, reaching since 0,5 MPa (Meneghini, 2014) to 1,6 MPa (Válek & Matas, 2010).

Concerning prolonged exposure to different humidity values (365 days), Baronio (2000) reports higher strength of mortars submitted to 90%RH environments (2,19 to 2,24 MPa) in comparison to equivalent specimens stored at 60%RH (0,89 to 1,73 MPa).

4.   EXPERIMENTAL PROGRAM

4.1   Overview and strategies

The current chapter corresponds to the second task of the work methodology defined in 1.3 and is related to the development of the experimental program. The present research aims to extend the work of Meneghini (2014) which was mainly focused in developing and validating experimental methods to study aerial lime. For such reason, the same mortar mix, components and proportions were adopted in the present work. This study extends the previous one by directly focusing on the study of parameters related to the carbonation process.

The methodology adopted in the experimental program concerns two main objectives. The first one comprehends the investigation of the influence of environmental conditions on carbonation. The second is related to understanding the diffusive processes that act within the material.

The first main objective comprehends observing the separate coupling of carbonation with humidity and content of carbon dioxide available in the environment. For understanding the influence of external humidity, two environmental conditions are considered. The first one corresponds to a condition of 60% RH at 20ºC. This environment reproduces the conditions of storage used by Meneghini (2014), and is used as reference. For this reason it is referred to as standard environment, or chamber. The second environment concerns the exposure to humidity close to saturation. For this purpose, a wet chamber was used, that keeps atmospheric moistures of about 90%RH at 20ºC. The concentration of carbon dioxide is similar in both standard and wet chambers, of about 500 parts per million (or 0,05%).

To investigate the influence of the carbon dioxide available content on carbonation, a third environment is proposed. The third environment takes place in a chamber that keeps 4% of concentration of carbon dioxide. The high CO_2 concentration chamber conditions in terms of temperature and humidity are close to the reference ones (20ºC and 55%RH).

 Concerning sampling, it is intended to assess as directly as possible the effects of environmental conditions on the material. Aiming to reproduce a situation with minimized internal gradients, reduced thickness specimens casted inside thin metal rings, assuming the shape of discs with 40 mm of diameter and 10 mm of thickness. This value represents a thickness in which internal humidity gradients are minimized, while still being representative of the mortar mix.

Discs specimens are designed to provide samples to thermal gravimetric analysis. The samples are collected from the specimen's surface with a proper tool. The objective is to observe the evolution of carbonation for the specimens stored at the different environments. From previous works, it is acknowledged that carbonation rates are more significant until the first 20 days from casting (Meneghini, 2014). For this reason six ages of tests are prevised, focusing on early ages: 1, 4, 7, 14, 21 and 28 days from casting.

Still concerning the relation between carbonation and humidity, it is intended to evaluate the effect of humidity on mechanical behaviour of mortars, deepening specific subjects, as the elasticity modulus and compressive strength. To promote the comparability of results, dimensions of specimens and testing ages adopted in previous work are maintained.

The second main objective is related to understanding the rates of carbonation through the depth of mortar and observing water transport mechanisms. This objective concerns specimens stored at the same environmental conditions, so that only the use of the standard chamber is prevised.

To understand how the carbonation occurs throughout the depth of the material, it is proposed the performance of thermo gravimetric analysis in specimens of significant thickness (cylinders of 60 mm diameter and 120 mm height). Samplings are made from a transversal section at three different regions: the centre of the section (l=0), halfway through the radius distance (l=15mm), and as close as possible to the surface (l=30mm). To provide comparing results, testing ages similar to the ones performed for disc specimens are prevised. However, to evaluate later carbonation behaviour, it is also prevised the analysis at an older age (from 60 to 80 days from casting).

In order to observe the evolution of carbonation front on mortars, it is proposed the staining of specimens with phenolphthalein solution, a recurrent method to investigate the presence of hydroxide and carbonate.

To understand the water mechanism transport and also complement the results of carbonation at different depths, it is proposed to continuously observe and measure the variation of humidity inside mortar specimens. The testing duration consorts the TGA testing ages for cylindrical specimens. The test follows the procedure developed by Meneghini (2014), described in 3.4.4. To describe different humidity profiles, two measuring sleeves are casted inside the specimen at different depths, related to the sampling depths of TGA analysis: one sleeve reaches the center of the specimen (d= 30 mm) while the other is kept as close as possible to the periphery (d =10 mm). A sealed specimen, prevented from external influence,

is also prevised. The purpose of this specimen is to act as a standard result in comparison with the exposed specimen, and also observe if a self- consumption of water occurs.

Table 6 diagrams the described testing methodology by summarizing the quantity of specimens, testing ages, types of tests and environments encompassed in each objective.

Table 6: Summary of testing methodology

Test	Specimen shape	Diameter or side	Thickness or height	Environment of exposure	Test ages (days)	Specimen per environment	Amount of Specimens
TGA	Disc	40 mm	10 mm	.wet chamber .standard chamber . high CO2 concentration chamber	. 1 . 4 . 7 . 14 . 21 . 28	2	6
TGA	cylinder	60 mm	120 mm	.standard chamber	. 1 . 7 . 14 . 69	5	5
Humidity Profile	cylinder	60 mm	120 mm	. standard chamber . standard chamber (sealed)	Continuous	2	2
Elasticity Modulus	cylinder	60 mm	120 mm	. wet chamber . standard chamber	. 8 . 15 . 22	3	6
Compressive strenght	Cube	50 mm	50 mm	. wet chamber . standard chamber	. 28	3	6
	TOTAL			3	Up to 70	-	24

Beyond the described methodology, the experimental program includes an isolated analysis on the behaviour of lime itself. This testing has the objective of evaluating the behaviour of quicklime through time disregarding the interaction with the aggregates. For such purpose, a sample of lime mixed exclusively with water is submitted to an adiabatic environment, with stable conditions of temperature and humidity. The test intends to monitor the mass variations of the paste sample along a period of 25 days, and attempt to infer the reasons for such variation.

4.2   Mixture proportions and preparation

It has been settled a mixture that consists of quicklime, water and two types of siliceous aggregates, which differ in particle size (coarse and fine sand) in the ratio of *1: 1,3 : 3* parts in volume, respectively (Meneghini, 2014). The components characteristics are described in the following subsections.

4.2.1   Binder: Quicklime

Following the hot lime mix method, the binder used is quicklime – CaO. The quicklime employed is classified as CL90Q (which means that a content of more than 80% in weight of CaO is expected) and provided by the company Lusical.

Aiming to attest the chemical composing also investigate and attest the content of each compound, an X-ray fluorescence spectroscopy has been performed. The apparatus used to perform the analysis is Philips X'Unique II WDXRF. The result of this analysis is given in Table 7.

Table 7: Chemical characterization of CL90

compound name	conc. (%)	absolute error
Al2O3	0.097	0.007
CaO	97.2	0.3
Cr2O3	0.0209	0.002
CuO	0.0131	0.001
Fe2O3	0.112	0.006
MgO	1.05	0.01
MnO	0.0165	0.002
NiO	0.0111	0.001
SO3	1.32	0.01
SiO2	0.124	0.008
SrO	0.0328	0.001

As it can be seen, the content of calcium hydroxide is higher than 80%, complying the claimed classification. It is also important to notice that the presence of Magnesium Oxide is considerably lower than the calcium oxide (1.05% against 97.20%, respectively) and for this reason the influence of this compound in further results may be discarded.

Still concerning chemical analysis performed in the binder, a thermo gravimetric analysis (TA Instruments SDT simultaneous DSC-TGA) was conducted. The tested sample consists of quicklime mixed exclusively with water, right after the instant of mixing. The purpose of this

experiment is to investigate the initial amount of calcium hydroxide available for carbonation, as well as understand the initial content of carbonate and oxide. The results are listed in Table 8.

Table 8: Hydroxide and carbonate initial contents for lime and water paste

Initial weight of sample after mass stabilization	Measure TGA (Dehydroxylation)	Ca(OH)2 weight	Initial content of calcium hydroxide
	11.4165 mg	46.9 mg	69.14%
67.8813 mg	Measure TGA (Decarboxylation)	CaCO3 weight	Initial content of calcium carbonate
	3.851 mg	8.8 mg	12.89%

From the obtained results, it can be concluded that the hydration process does not convert the whole amount of available quicklime into hydroxide at once, thus a remaining amount of oxide is present. The experiment also shows a significant presence of carbonate. This can be a product of a possible carbonation reaction that might have occurred in the quicklime, since it has high reactivity, all the more in the micronized form, and the storing conditions do not prevent a total sealing from the atmospheric moisture.

4.2.2 Aggregates

Two types of siliceous sand are applied as aggregates in the mortar: coarse and fine sands. The aggregates have been analyzed by the X-ray fluorescence technique, in order to describe the composition of the material. The analysis revealed a predominant concentration of SiO_2 in both sands, although other types of compounds were also found. The chemical composition of the aggregates is described in Annex III.

 In order to eliminate dross as well as any particles that may react with the lime, the sands were washed and dried previously to their application. The washing procedure was performed for at least 2 hours, in order to proper remove all the impurity of the material. The sand was then placed inside stoves, settled at approximately 100ºC, for at least 24 hours. After this period, the material was stored properly inside plastic containers, covered with a suitable top, to prevent major contact with environment humidity.

In order to estimate the water content of the aggregates, a representative sample was weighted and put inside the stove for a 24 hour period. After that, it was weighted again, and the mass values are compared. Table 9 indicates the weight values (the content of water is considered

the variation of weight). As it can be seen, the water content of both aggregates is less than 1% in mass, thus its influence on the properties of the mortar can be considered negligible.

Table 9: Water content of the aggregates after drying

sand	initial weight	weight after 24 hours	weight variation	water content
fine	700.0 g	698.5 g	1.5 g	0.21%
coarse	700.0 g	699.2 g	0.8 g	0.11%

A granulometry analysis previously performed on both fine and coarse sands show that a smaller size of a specimen tested had a thickness of about 8 mm (Meneghini, 2014). To attend the basic requirement for representativity of having a thickness at least 3 times the aggregate size, the sand used for preparing mortar has to be sieved in order to have a maximum dimension of 2 mm.

4.2.3   Mixing method

The procedure of mixing follows the previously mentioned hot lime mix method and defined proportion. In the ratio adjustment, it has been considered the limitations of shrinkage cracking in larger specimens and also standard requirements regarding flow table established by BS EN 1015-11 (1999).

Before being added to the mixing recipient, each ingredient is separately weighted. It is important to notice that because quicklime is highly reactive, it should not be the first ingredient to be added. Also, because hydration starts very quickly when lime is put in contact with water, this must be added to the mixture at last, in order to prevent a rather homogeneous hydrated lime mortar. A high heterogeneity can influence the carbonation process, as well as the mechanic behavior of the mortar.

The mixer used in this procedure is a mortar mixer model Würk with a 3 liters capacity bowl that operated with a planetary speed of 40 r. p.m. and beater speed of 100 RPM, showed in Figure 17.

Figure 17: Mixer used in the mixture design

4.3 Moulding and curing processes

After the mixture is done, it is ready to be casted into mortar specimens. The fresh mortar is applied in the moulds as soon as the equipment is stopped, and the material is directly collected from the mixer bowl.

To guarantee the homogeneity of the casted material, it is important to ensure that the specimens have densities as close as possible. For this reason, based on the volume of the moulds, it is calculated the necessary weight required to reach a stablished density value. The density adopted for fresh mortar specimens is 2000 ± 100 kg/m^3.

Concerning the specimens' nomenclature, the names are given considering the type of test designed, the environment of exposure and the number of order of each specimen. Table 10 and Table 11 specify and explain the adopted nomenclature.

Table 10: Nomenclature of specimens regarding the type of tests conducted

nomeclature	Designed test	Specimen shape
1D	TGA - 1 depth sampling	disc
3D	TGA - 3 depths sampling	cylinder
EM	modulus of elasticity	cylinder

Moulding and curing processes

CP	compressive strenght	cube
HP	humidity profile	cylinder with sensor sleeves

Table 11: Nomenclature of specimens regarding the environments of exposure

nomeclature	chamber	temperature	RH	[CO2]
T20_H60	standard	20ºC	60%	0.05%
T20_H90	wet	20ºC	90%	0.05%
CO2_5%	CO2 high concentration	20ºC	55%	5%

The following paragraphs describe the curing and moulding conditions specified for each type of specimen.

4.3.1   Disc specimens

The casted specimens must have a thickness dimension small enough that permits to disregard the influence of depth and ensure uniformity of conditions, but also large enough to provide a representative behaviour.

To attend the mentioned purpose, the specimens have been casted in a thin ring made of light steel, as Figure 18 shows. The disc mould has an internal diameter of 40 mm and approximately 10 mm of thickness. After the casting procedure is complete, the specimens are immediately taken to chambers of specific storing conditions. Each chamber stored 2 of disc-shaped specimens. The specimens were kept sideways, allowing a uniform drying. To avoid spreading of fresh material, the steel ring is not removed. For this reason, periphery surface exposures are disregarded. The specimens are kept in these conditions through the whole experimental campaign duration.

Figure 18: Disc specimens stored in the standard and wet chambers, respectively

4.3.2 Cylindrical specimens

Cylindrical specimens are employed in three different types of experimental tests. However, the mould characteristics and the casting procedure followed in the cast of all of them is strictly the same.

Concerning the moulds, it was used a system of a plastic net wrapped inside a polypropylene tube. The tube has an internal diameter of 60 mm and 120 mm of height and cut longitudinally into two pieces to facilitate demolding. As Figure 19 shows, before casting the tube's pieces are bound together with adhesive tape. To ensure designed diameter and shape the net is stretched and positioned so that a full contact with the internal surface of the tube is verified. The bottom of the mould is sealed with a plastic membrane, to prevent spreading during the casting procedure.

Figure 19: Mould system used in the casting of cylindrical specimens

The molds used to cast the humidity profile monitoring specimens follow the net and tube system but present a particularity: the introduction of measuring sleeves in the lateral surface of the mold (Figure 20). The sleeves are plastic tubes covered in a GoreTex® membrane at one extremity and capped with a rubber plug at the other.
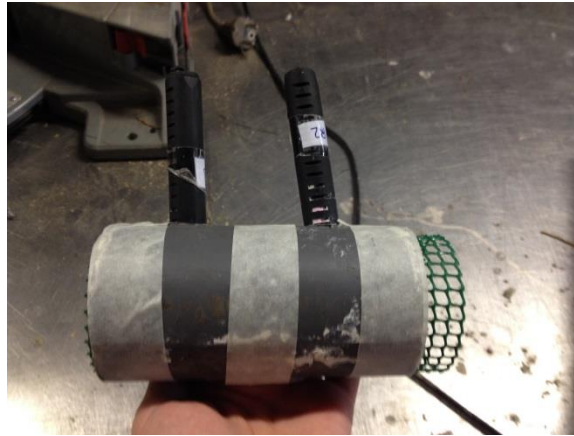
Figure 20: Humidity profile specimen mold

The sleeves are inserted inside the mold in two different depths: the bottom sleeve has the internal extremity placed in the center of the transversal section, while the top sleeve is placed as close as possible to the mold's internal wall (Figure 21). This settlement is made in order to compare moisture in different depths of the mortar.
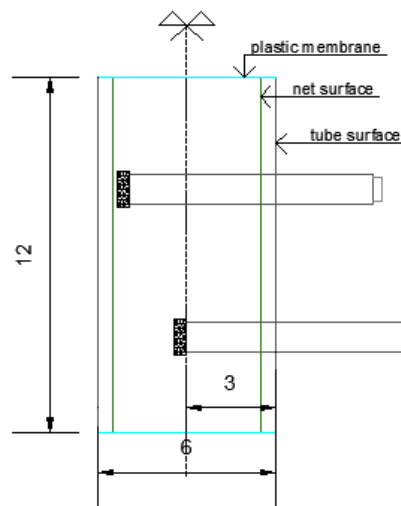

Figure 21: Scheme of sleeves positions inside the mold. Dimensions expressed in centimeters

The mold is vertically placed on a plane surface and gradually filled with fresh mortar. The material is progressively compacted against the mold's walls. During this process, the weight is continuously verified to reach the stablished value of fresh density.

After the casting is complete, the top of the mold is sealed with the same type of plastic membrane as the bottom. This procedure guarantees a total sealing of the specimen, keeping the mortar isolated from the external influences. The specimens are then moved to the designed chambers and kept in this condition for about 5 hours.

After that period, the specimens are partially demolded: the adhesive tape is removed, releasing the plastic tube pieces. The top and bottom plastic membranes are also removed.

The reason of this procedure is that keeping the mortar apart from the environmental conditions for longer periods would influence the drying process. Thus, a modification in the water transport mechanism would affect the latter properties of the material.

However, as fresh mortars have high water content, their consistency is too fluid to maintain the designed shape outside the mold. In an attempt to solve this problem, the specimens are kept wrapped in the plastic net, as Figure 22 shows. The net has a 5x5 mm overture. The overture is considered wide enough to allow a drying phase with minor alterations and closed enough so that the mortar cannot evade easily. Furthermore, the plastic which it is made off is sufficiently rigid to conserve the designed shape.

Figure 22: Cylindrical specimens after the tube removal, stored inside the standard chamber

To facilitate the latter numeric modelling of the carbonation field it is necessary to ensure a uniaxial symmetry condition concerning the water transport through the mortar. This situation is also appropriate to eliminate moisture gradients, which would infer differences water contents among the transversal sections of the specimen. To guarantee a significant homogeneous humidity within the mortar, the top and bottom surfaces were sealed by a paraffin layer right after the removal of the plastic membrane.

The net is removed after a 24 hour period. The specimens are then kept inside the chambers in the vertical position to maximize the surface of exposure to the environment's conditions, as Figure 23 demonstrates.

Figure 23: Demoulded cylindrical specimens storing position inside the standard chamber

Additional cylindrical specimens

During the development of the moisture measurements, the tightness of the mortar-sleeves interface was questioned. It was speculated that possible shrinkage cracks would have occurred and altered the measurements of relative humidity. For this reason a second specimen has been casted with the additional caution of applying a paraffin layer in the interface of the sleeves with the mortar, as indicated in Figure 24.

Figure 24: Detail of sleeve and mortar interface in specimen HP_T20H60_B

Later, it was questioned whether the horizontal positioning of the sleeves would be the most indicated, due difficulty in keeping the alignment of the sleeves during casting. Untidy sleeves positioning would infer experimental errors in the measurement of internal moisture. As Figure 25 indicates a third specimen was casted with the sleeves placed vertically.
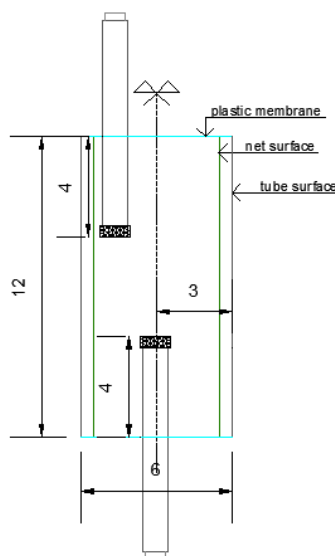

Figure 25: Scheme of sleeves positioned vertically inside the mold. Dimensions expressed in centimetres

The latter demolding process was conducted following the previously mentioned steps. As it can be seen in Figure 26, the paraffin layer applied in the top and bottom surfaces helps to seal the interface between the sleeves and the atmosphere.
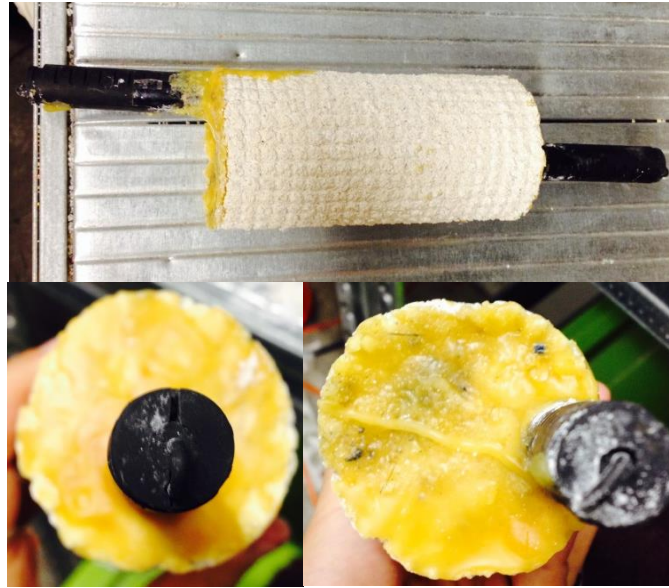
Figure 26: Specimen HP_T20H60_C after demoulding: longitudinal and transversal views.

4.3.3 Cubic specimens

The cubic specimens casted to perform the compressive strength test have the dimensions of 50x50x50mm. The mould sets used in the casting procedure are made of steel and cast three cubes each, as Figure 27 demonstrates. Two series of three specimens each are prevised: the first is destined to the standard chamber and the second to the wet chamber.

Figure 27: Mold sets used in the casting procedure and the demoulded cubic specimens

During the casting procedure, each steel mould is filled with fresh mortar and continuously weighted, in order to reach the targeted fresh density. Giving the mold set's settlement, the density of the specimens cannot be calculated individually.

About curing, it was followed the procedure recommended by BS EN 1015-11 (1999). After casting, the mould set is involved in a polyethylene bag, and sealed from external conditions for five days. After that, the bag is removed and the specimens have the top surface exposed to the chamber's atmosphere. Specimens are not yet demolded because the mortar is still to fluid. After two days, the mould set is removed and specimens are kept fully exposed to the chamber's environment until the designed age of testing.

4.4 Experimental setting

4.4.1 Thermo gravimetric analysis

General remarks

Thermo gravimetric analyses are conducted to investigate the rate of carbonation in the mortar according to the elapsed time since casting of specimens. The apparatus used to perform the tests is a TGA-DSC equipment model SDT 2960 V3.0F, which is capable to perform simultaneously thermo gravimetric analysis and differential scanning calorimetry, or DSC. DSC is a technique in which the difference in the amount of heat required to increase the temperature of a sample and reference is measured as a function of temperature. This parameter has secondary importance in the searched results, however it might be useful to determine with higher accuracy thermal decomposition of compounds.

The described apparatus is showed in Figure 28. The equipment subjects the tested sample to an inert Argon atmosphere and a variation of temperature from about 20°C to 1100°C, in heating rates that can be settled from 5°C/min to 30°C/min.

Figure 28: Apparatus general view and detail of sample's container

To analyse the influence of heating flow rates in the measurements, it was conducted a series of preliminary analyses using an existing aged aerial lime mortar specimen. Samples taken from the surface of the specimen were tested at the heating rates of 5°C/min, 7,5°C/min, 10°C/min, 15°C/min and 20°C/min. The results are shown in Figure 29.
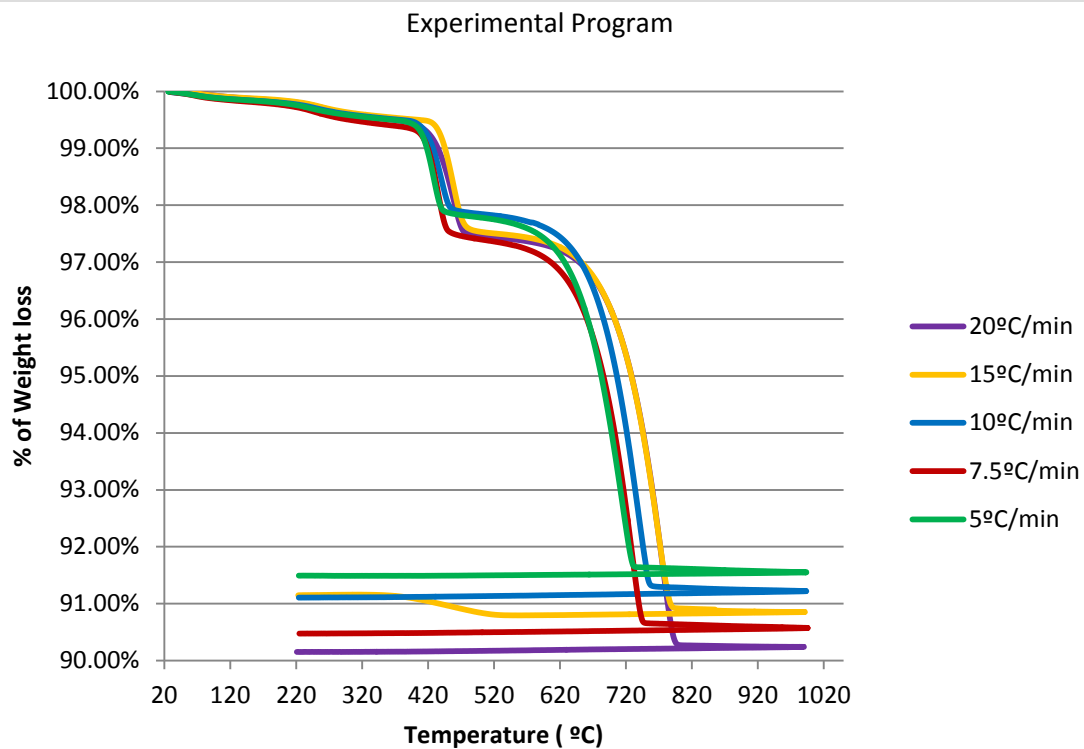
Experimental Program

Figure 29:TGA curve for different heating rates

The curves are plotted in terms of relative weight loss versus temperature. The curve's plotting are very similar up to 700-750ºC interval, especially considering the first weight drop, at about 420ºC. The aspect of the curves is considered sufficiently similar for the testing purposes. From this preliminary analysis, it can be concluded that the heat flow rate does not influence the final aspect of the TGA curve. Thus, higher heating rates can be applied without the interference of experimental errors.

In this matter, the adopted heating and cooling rates are respectively 25ºC/min and 30ºC/min. The samples are submitted from 20ºC to 1000ºC and then cooled down to the room temperature, of about 25-30ºC. A total of three analyses are performed at each testing age.

Disc specimens

Concerning the comparison between different exposure conditions, material has been collected from specimen's surfaces, always from the same side. It was used a steel tip and reaching about 3 mm of depth, thus sampling comprehends material up to 3mm depth, as Figure 30 demonstrates.

Figure 30: Collecting material and side used for sampling in disc

Cylindrical specimens

To study the carbonation rate throughout the depth of a specimen, thermo gravimetric analysis in samples taken from varied depths of a cylindrical specimen. For this purpose, as Figure 31 illustrates, material has been collected from three areas through the radius of a transversal section: P1 (l=30mm9, P2(l=15mm) and P3(l=0mm). The chosen section for sampling is located at an intermediary distance between the top and bottom of the specimen, at a 6 cm depth.
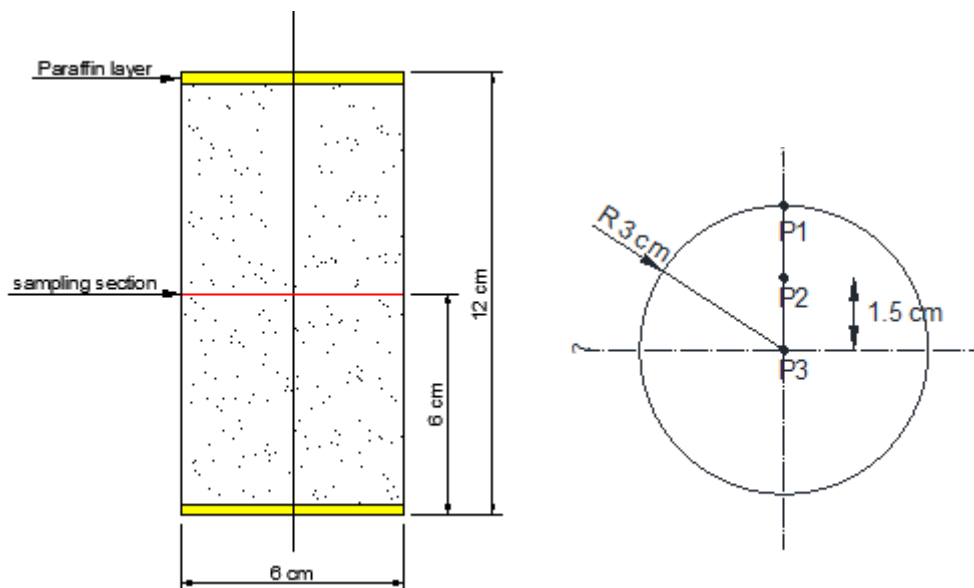

Figure 31: Adopted section and radial depths of sampling

For the purpose of this experiment, five specimens were casted, as it was intended to use one specimen per date of test. However, during the course of the experimental campaign, some of them showed excessively discrepant densities. In order to preserve the homogeneity of densities in a range up to 5% from the average, such specimens were discarded. Two specimens were eliminated, forcing the analyses from the 7th day to be performed in the same specimen.

Different depth of transversal section had to be adopted in the last two sampling procedures. Specimen 3D_T20H60_5 was sectioned in half (at 6 cm depth) for the testing age of 14 days. One piece was used in the sampling, while the other one had the sectioned side sealed with paraffin and kept stored for later analysis, as Figure 32 indicates. In the following age of test, the same procedure was conducted, and so the sampling occurred at the depth of 3 cm, considering the specimen's original height.

Figure 32: Specimen 3D_T20H60_5 after sectioning. The left piece is used in the 14 day testing, while the right one is saved for the next age of test.

4.4.2   Carbonation front measurement

The observation of carbonation rate and measuring of the carbonation front in aerial lime mortars is a complementary testing. The observations were conducted by the staining of phenolphthalein on the surface of the material at different ages from casting.

No specific specimens where casted for this analysis. Instead, specimens designed for other tests inside the scope of the experimental campaign where reutilised. In particular, cylindrical specimens showed more visible conditions for the observation of carbonation front. Unsuccessful attempts have also been made in the cubic specimens, cracked after the compressive strength test was performed. These where excessively damaged to properly observe the evolution of the carbonated regions.

After reaching the main purpose of which it was originally designed, the selected specimens where transversally sectioned and had the newly-cut side stained with phenolphthalein. Staining was made in inner sections because the external surface of the material was expected to be completely carbonated, not allowing adequate comparisons of the evolution of carbonation front.

In cylindrical specimens casted for TGA, the same transversal section employed in the sampling was used in the staining, as Figure 33 demonstrates. In reused humidity profiles it was adopted the depth in which the sleeves where placed.

Figure 33: Section adopted for staining of the reused TGA cylindrical specimens
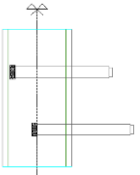
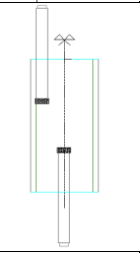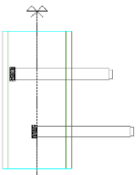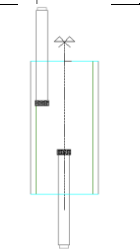## 4.4.3   Humidity profiles monitoring

This test has the purpose to observe and investigate how the water content varies through the different depths of the material, giving the conditions of exposure to the environment. The water content was measured in two points of different depths: one on the centre of the material and other placed as close as possible to the surface.

It was originally proposed the casting of two specimens, differing in exposing forms: while the first specimen had the moulding set removed, the second one remained completely sealed. However, due experimental difficulties, three other specimens where casted in order to

eliminate possible experimental errors in the collecting of the data. As Table 12indicates, the specimens differ in terms of sleeves orientation and exposure conditions.

Table 12: List of specimens casted for humidity profile measurements

Specimen name	Sleeve's position	Sleeve's horizontal dephts	Sleeve's vertical depths	Overview
HP_T20H60_A	Horizontal	30 and 60 mm	40 mm and 80 mm	
HP_T20H60_S	Vertical	30 and 60 mm	40 mm	
HP_T20H60_B	Horizontal	30 and 60 mm	40 mm and 80 mm	
HP_T20H60_C	Vertical	30 and 60 mm	40 mm	

The equipment used in the measurements is Vaisala HUMICAP® Humidity Indicator model HMI41 coupled with Vaisala HUMICAP® Humidity and Temperature Probes HMP45. Given a standard temperature of 20ºC, the measurement range of the probes in terms of relative humidity varies from 0 to 100%. The accuracy is ± 1% for moistures up to 90% and ± 3% RH for moistures higher than 90%. The temperature measurement range is from -40 to +100 °C, and readings show a precision of 1 decimal unit.

Figure 34 illustrates the measuring in course of two types of specimens. The measurement procedure consists of inserting the probe inside one specimen's sleeve, having the caution to prevent the influence of external air humidity with adhesive tape.

Figure 34: Measuring of humidity profiles in exposed and sealed specimens respectively.

The sensor is left in the same position for a period of about 90 minutes, so that moisture equilibrium can be settled in the interior of the sleeve. After this interval, the probe is altered to other position, following the described procedure. The measurements have been made for 20 days, exclusively on weekdays. The interval in the collecting of data is of about two days for the same type of specimen. However, longer distances between readings may have occurred due weekend's intervals.

4.4.4   Modulus of elasticity

The testing of the modulus of elasticity of mortar has the purpose of quantify the evolution of the mortar's stiffness. It is intended to analyse the parameter according to the relative humidity of the controlled storing environments.

As Figure 35 illustrates, the test is performed in a hydraulic press. The parameter is obtained from the appliance of uniaxial load cycles and the measuring of the respective displacements by LVDTs.

Figure 35: Experimental setting for the modulus of elasticity testing.

The testing has been conducted at the ages of 7, 15 and 22 days after casting. These values were adopted due similarity with the ages of testing of cylindrical specimens in the thermo gravimetric analysis.

For the specimens stored at the standard chamber (20ºC, 60%RH, [CO$_2$] = 500 PPM) it was applied a cyclical load with ramps of amplitude of 300N and a rate of 20N/second after a pre-load of 100 N. As Figure 36 shows, the testing of the specimens stored in the wet chamber (20ºC, 90%RH, [CO$_2$]= 500 PPM) did not resist solicitations of that order. For that reason, the cyclical load applied where reduced to the amplitude of 100N.

Figure 36: Damage in specimen EM_T20H90_1 on the first day of testing

4.4.5   Compressive strength

The investigation of the compressive strength is prevised to complement the characterization of the material in terms of mechanical behaviour. The results are compared according to the difference of relative humidity of the controlled storing environments.

The testing is composed of two series of three specimens. Each series corresponds to an environment of exposure, namely the standard and the wet chamber. The testing were made at 28 days from casting, as BS EN 1015-11 (1999) recommends.

The specimens are submitted to an increasing compression load at the rate of 50N/second, up to the failure of the material. The experimental setting and the failure patterns of the different types of specimen are illustrated in Figure 37.

Figure 37: Pattern of failure of specimens stored in the wet chamber (left) and standard chamber (right)

4.4.6   Lime paste testing

A mix of quicklime and water was prepared respecting the proportions used in the mortar mixture (1:1,3 lime:water).The sample was continuously monitored during a period of about 25 days. For the continuous measurement of the mass variation, the sample was placed within a thermo gravimetric device (SDT 2960 DSC TGA) and kept at 30ºC and 60%RH. The equipment's container prevents interference of outer conditions in the sample, so that the mentioned conditions are maintained throughout the testing duration.

There were two reasons for adopting and environmental temperature of 30ºC instead of the 20ºC that had been adopted in all other experiments at constant temperature: (i) the TGA does not have refrigerating capabilities and can only keep constant temperatures above room temperature (test performed in summer time with room temperatures above 20ºC); (ii) the

TGA has a high demand on behalf of its group of users, and by making a higher temperature experiment, the evolution of mass would definitely be faster than at a lower temperature.

Considering the environmental conditions of the experiment, it is expected to observe a significant increase of weight of the sample given by the hydration of lime and carbonation of the produced hydroxide. The first reaction occurs given the presence of added water, while the second happens also due the content of carbon dioxide present inside the equipment container. The expected increase of weight is given mainly by the production of $CaCO_3$ (equation 24), given that it has higher molar mass that the hydroxide (74 mg/mol for the hydroxide and 100 mg/mol for the carbonate).

$$Ca(OH)_2 \ + \ CO_2 \ \rightarrow CaCO_3 + H_2O \qquad (24)$$
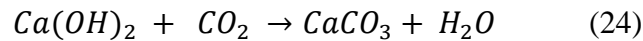
Based on stoichiometric proportions, the conversion of hydroxide into carbonate leads to an overall increase of 35% in weight (Lawrence R. , 2006). Thereby, from the experimental results it is expected increase of weight result consistent with the combined effects of the compound conversion and evaporation of water. In fact, given the high reactivity of quicklime and the exothermic characteristic of hydration, significant heat is released when lime is added to water. The released heat contributes to the loss of water due evaporation.

5. MAIN RESULTS AND DISCUSSION

5.1 Thermo gravimetric analyses

5.1.1 General remarks

An initial remark is given in regard to the necessary calculations that allowed estimating the percentages of CaO, Ca(OH)2 and CaCO3 on each tested sample. The calculations considered the division of the weight of the specific compound by the initial weight of the sample, as follows equation 25. The remaining amount of mass, which does not figure neither as hydroxide nor carbonate was considered to be composed of unhydrated calcium oxide.

$$\% \, CaCO3 = \frac{CaCO3 \; weight \; (mg)}{sample \; initial \; weight \; (mg)}$$

$$\% \, Ca(OH)2 = \frac{Ca(OH)2 \; weight \; (mg)}{sample \; initial \; weight \; (mg)} \quad (25)$$

Concerning the quantification of carbonation evolution, Ferreti and Bazant (2006), Lawrence (2006)and later Meneghini (2014) adopted the relative concentration of carbonate – R parameter, expressed as the division of the amount of carbonate by the total amount of carbonate and hydroxide (which is considered the potentially carbonating material), as follows equation 26.

$$R = \frac{CaCO_3}{Ca(OH)_2 + CaCO_3} \quad (26)$$

5.1.2 Disc specimens

The evolution of compounds contents according to the environment of exposure of the sampled specimens are reported from figure 39. Further sampling data is reported in annex IV. The correspondent TGA curves at each testing age are presented in Annex V.

Specimens stored at the Standard Chamber

Figure 38 illustrates the evolution of the percentage of the relevant compounds for samples collected from the disc specimens stored at the standard conditions (20ºC, 60%RH and CO_2 concentration of 500ppm).
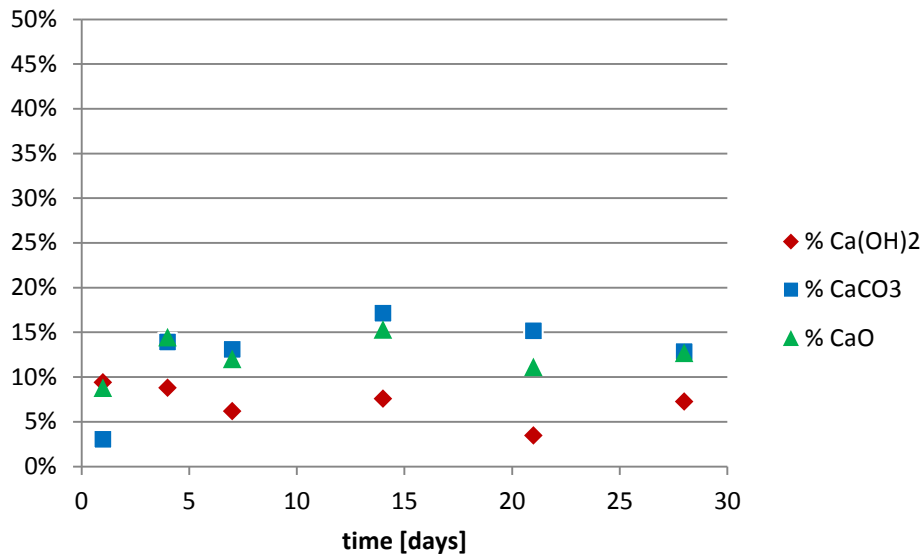
Thermo gravimetric analyses

Figure 38: Compounds' evolution in samples taken from disc specimens stored at the standard chamber

The graphic indicates an increasing content carbonate along time, concomitantly with decreasing hydroxide content, suggesting the production of the former and the consumption of the latter. The carbonation appears to reach its maximum value at 14 days. It is however recognized that some scattering is noted on the data. Nonetheless, the aforementioned tendencies are observable with ease.

Meneghini (2014) also reports a global decreasing tendency for the hydroxide content, but observes higher intensity of scattering, suggesting local increases (Figure 39). Meneghini explains this phenomenon by a possible late hydration of the quicklime. In her results, an initial unexpected increase of $Ca(OH)_2$ is described, suggesting partial effects of late hydration of the calcium oxide. It is also speculated that such alteration would be given by a significant presence of magnesium oxide in quicklime. This hypothesis can be however discarded in the current analysis due the chemical composition of quicklime.
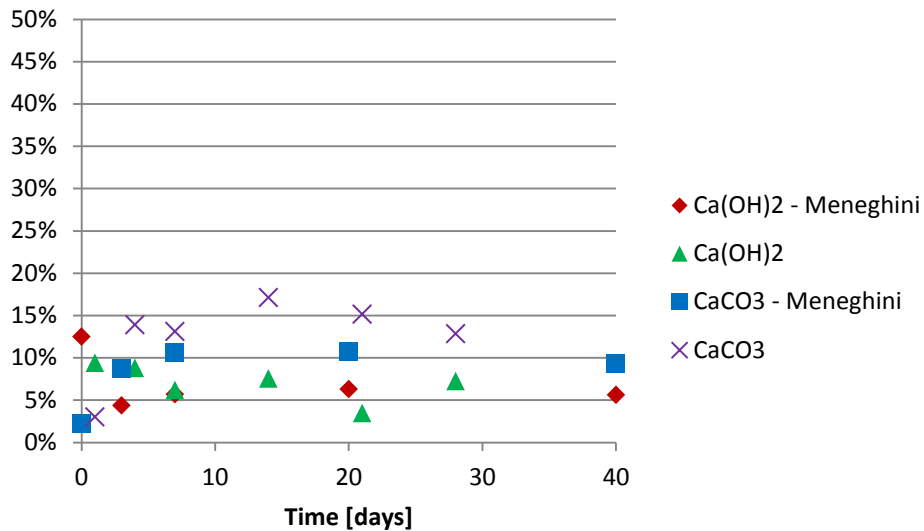
Main Results and Discussion

Figure 39: Comparison with Meneghini's average results for disc specimens stored in the standard chamber

Meneghini (2014) performed TGA analysis on disc specimens stored at the same conditions reproduced in the standard chamber. A comparison with the author's results is illustrated in Figure 40. The overall behaviour is significantly similar for both works, and it can be seen a general tendency of growth of carbonate while a remarkable decrease of hydroxide content.

In Figure 40 the comparison of relative concentration of carbonate between the current work and Meneghini's results is shown. From the results of the current work it is visible that the carbonation reaction rate is higher in the first ages, up to 14 days, tending to decrease from this age on, reaching a nearly stabilized value (some scatter is observed, though). This behaviour is compatible with Meneghini's results. Aside from a local outlier on the current work (21st day), both results are significantly similar, regarding an initial accelerated growth followed by a remarkable stagnation.
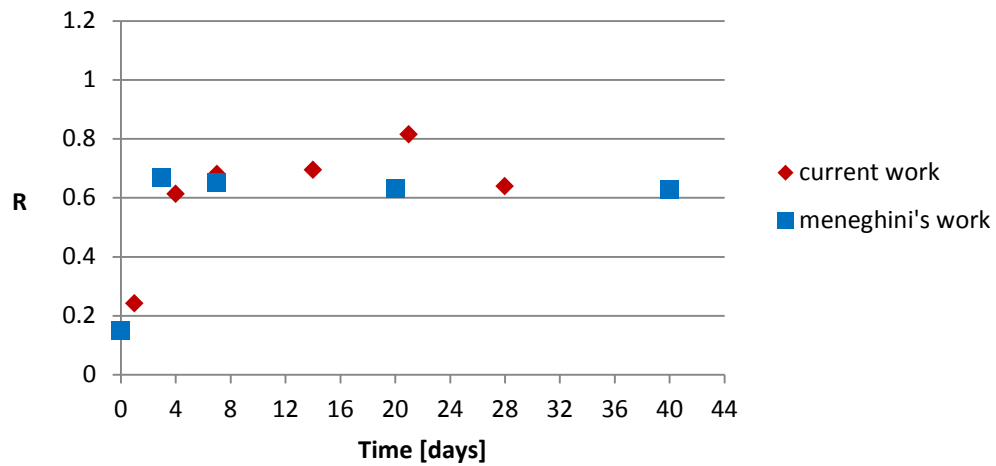
Figure 40: Comparison between R rates of present work and Meneghini's work

Specimens stored at the wet chamber

Figure 41 illustrates the evolution of percentage of each compound for samples collected from specimens stored at high relative humidity conditions (20ºC, 90%RH and CO_2 concentration of 500ppm).
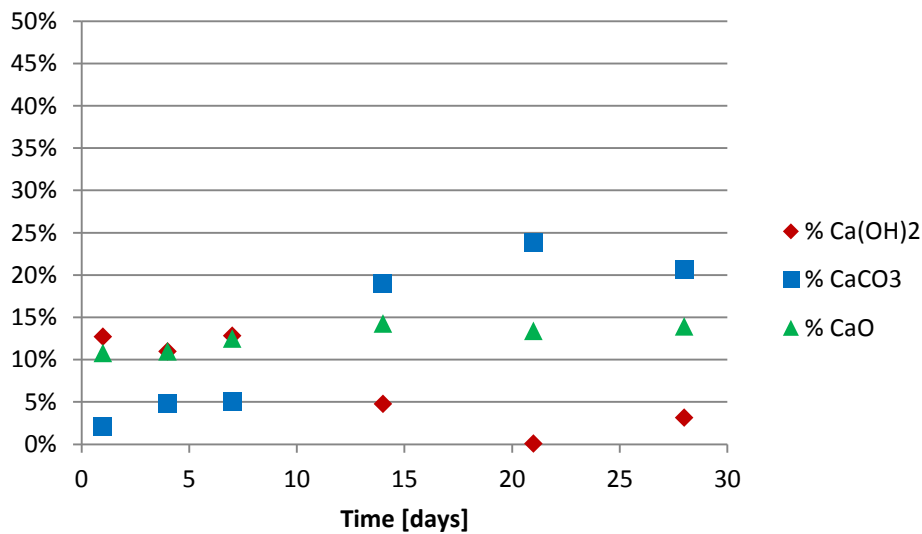

Figure 41: Evolution of compounds of samples taken from disc specimens stored at the wet chamber

Although a slight increase of carbonate content is verified at early ages, with an apparent stagnation from 4 to 7 days, the graphic shows a global tendency of increase of carbonate content. Concurrently, the hydroxide content shows a global decreasing tendency, reporting a modest initial slope, which is compatible with the initial small variation of carbonate.

The variation of relative concentration of carbonate – R given by Figure 42 confirms the carbonation behaviour, followed by a later stabilization tendency.
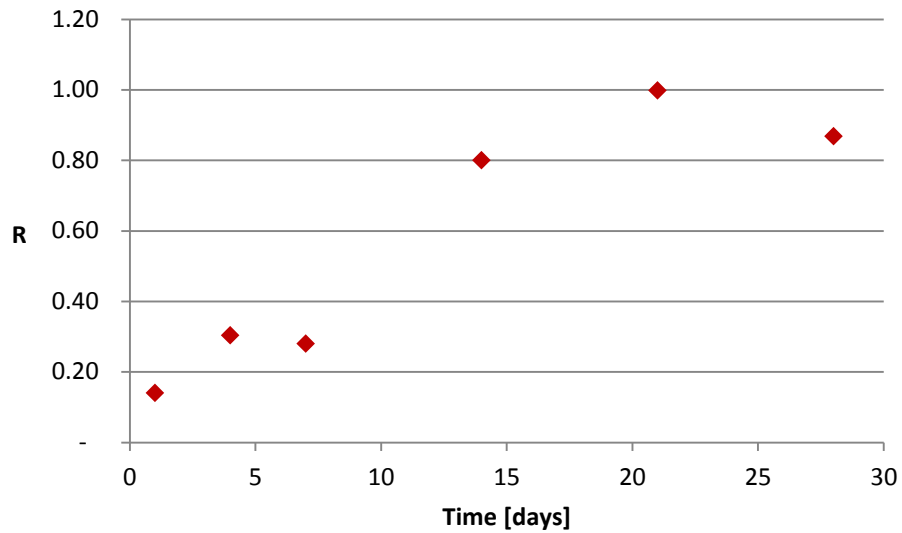
Figure 42: R of samples taken from specimens stored at the wet chamber

Even though the tendency to carbonate is less intense in the wet chamber environment (90%RH) in comparison with that observed in the standard chamber (Figure 38), the carbonate content shows a global increasing tendency anyway. In this way, the result given for the 7th day for the wet chamber (Figure 41) may be considered as an outlier. In fact, these results indicate a significant occurrence of carbonation, even though the specimen is maintained in contact with high humidity for a prolonged period of time.

The humidity of the chamber does not seem to infer hindrance effects on the diffusion of carbon dioxide through mortar.

Specimens stored at the high CO_2 concentration chamber

Figure 43 illustrates the evolution of compounds for samples collected from specimens stored at high carbon dioxide concentration conditions (20ºC, 55%RH and CO_2 concentration of about 4%, or 40000 ppm).
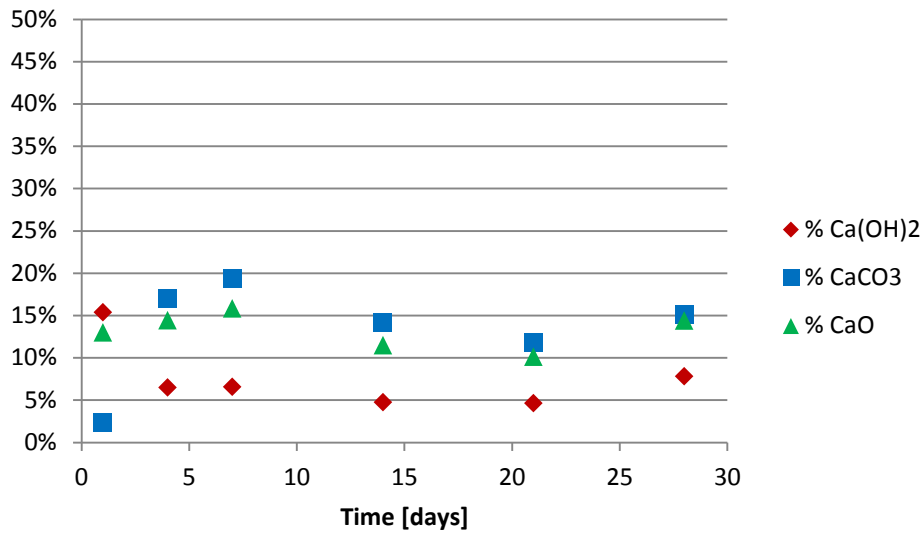
Thermo gravimetric analyses

Figure 43: Evolution of compounds of samples taken from disc specimens stored at the high CO2 concentration chamber

As it is would be expected, in view of the high availability of carbon dioxide in the environment's atmosphere, the graphic shows a steep ascending slope for the carbonate content, accompanied by a compatible decline in the hydroxide content. The content of carbonate reaches a peak of ~20% at 7 days, instant from which the increasing carbonate content appears to exhibit a slight decrease, while the hydroxide seems to stabilize until the end of testing.

Figure 44 illustrates the relative concentration of carbonate. As it can be seen, increasing relative carbonate concentrations can only be seen for the first 4 days; likewise, the concentration reaches its maximum at the referred age. From the first week on, the carbonation may be considered stabilized until the end of testing.
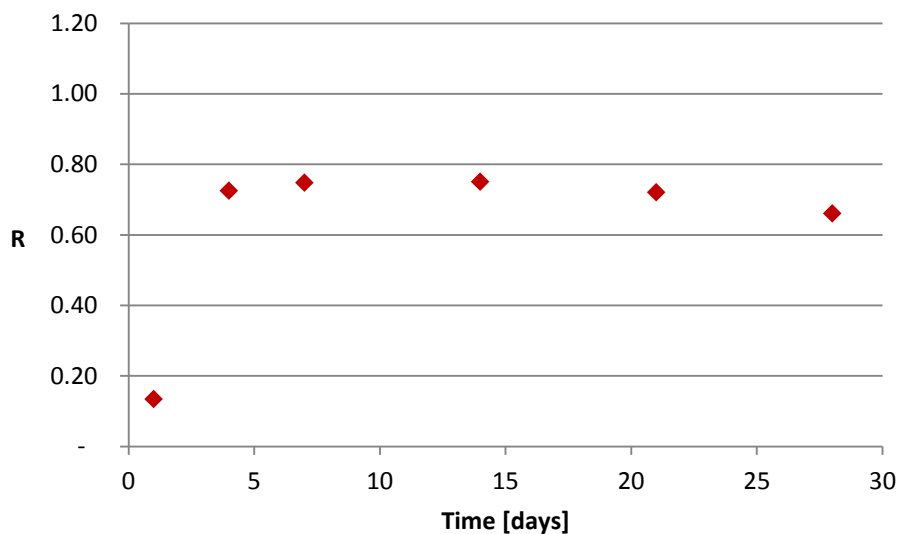

.

Figure 44: R of samples taken from specimens stored at the wet chamber

Although showing initial growth significantly higher in comparison with the standard chamber's specimens results regarding the same period, it is demonstrated a global tendency of stabilization of carbonation after the first 7 days, even though a high amount of carbon dioxide is available to react with the lime. These results are compatible with the statements made by Shin (2009) and Van Balen (2005), that the carbonation is a reaction of zeroth order with respect to CO_2. In fact, in terms of plotted results aspect, the current results have a great similarity with the standard chamber specimen's (Figure 38).

5.1.3   Cylindrical specimens

The quantification of the contents of calcium hydroxide and carbonate according to the sampled depth through the transversal section of the specimen is performed following the same procedure used for the disc specimens. According to section 4.4.1 (Figure 31), material is sampled from different depths at the transversal section: P1 (l=30mm, corresponding to the surface), P2(l=15mm) and P3(l=0mm).

The calcium hydroxide and carbonate contents for each sampling depth are reported from Figure 45. Detailed information on cylindrical specimens sampling data, as well as TGA curves at each testing age are further presented in Annexes VI and VII, respectively.
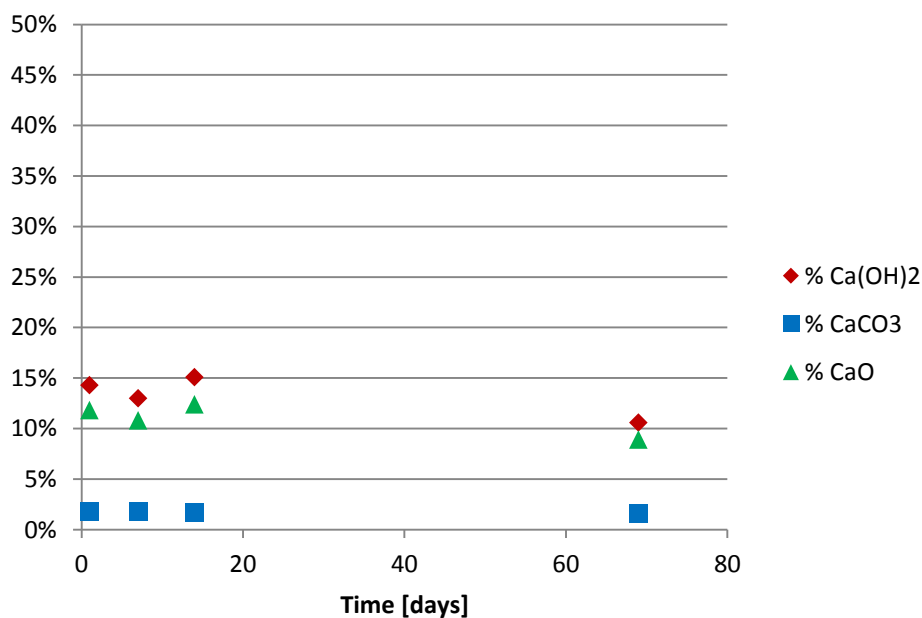

Figure 45: Evolution of compounds for material collected from depht P3 (l=0mm)
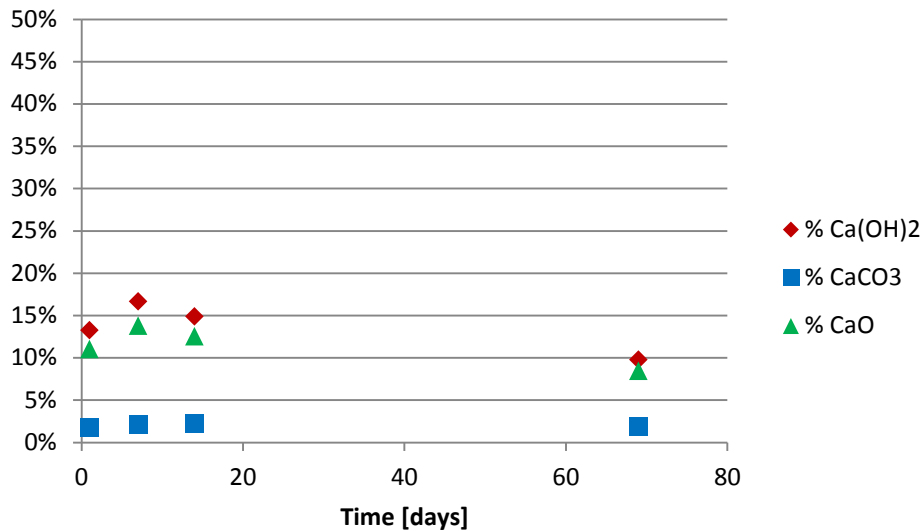
Thermo gravimetric analyses

Figure 46: Evolution of compounds for material collected from depht P2 (l=15mm)

As Figure 45 shows, in central regions of the specimens (P3), the carbonate content remains very low, even for the most advanced ages of sample collection. It can indeed be considered to have a stable value of 2% in weight throughout the entire experiment. Initial hydroxide contents can be considered constant, although a certain degree of scattering is verified. The oldest age of sampling (69 days) shows that this compound content tends to decrease, even though carbonate contents appear to be unaltered. As Figure 46 demonstrates, samples collected from intermediary regions through the radius distance of the section (P2) show a very similar behavior.

It must be noted that the hydroxide and oxide contents of earlier ages reported inFigure 45 and Figure 46 may be potentially higher due influence of the mortar's free water content. The variation of weight measured in TGA during dehydroxilation is assumed to be given due release of water (equation 20), and the hydroxide content is calculated indirectly, according to the supposed water variation. Thereby, higher presence of free water would provide mistakenly higher values.

Figure 47 illustrates the content of free water in the different sampling regions, according to the collection dates. In fact, fresher mortars have higher free water content, mainly in inner regions. Given the fast heating rate adopted in the tests (25ºC/min), it is reasonable to assume that, for initial ages, the free water had not been totally released by the beginning of dehydroxylation. Thereby, the hydroxide contents of earlier ages, given in Figure 45 and Figure 46, may be actually lower. As the mortar ages, the free water content tends to decrease. Thus, results collected at older ages would then be associated with smaller errors. In this way,

the global variation of hydroxide content may be less steep, agreeing with the behaviour demonstrated by the carbonate content.
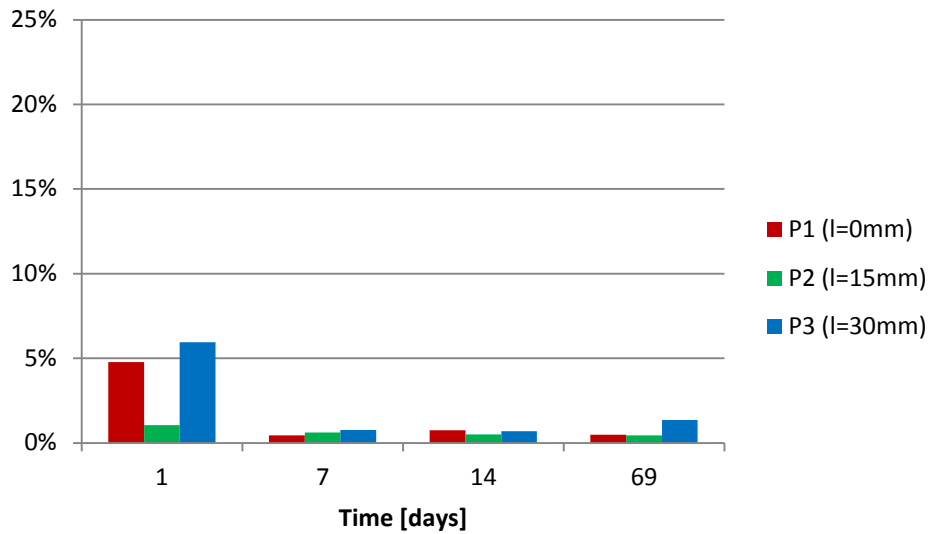

Figure 47: Free water content of cylindrical specimens at different depths according to testing ages

The material collected from the periphery of the section (P1) shows an opposite behavior in comparison with inner samplings. Figure 48 illustrates high initial increase of carbonate content, which tends to stabilize throughout the testing age. This behavior is followed by a concurrent decrease of hydroxide at the related initial intervals and a tendency of stabilization as well, at a lower value.
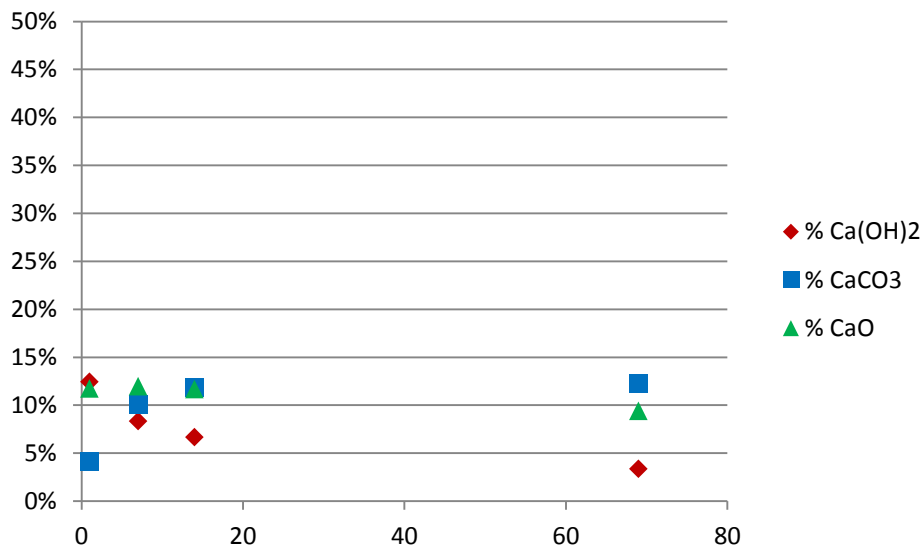

Figure 48: Evolution of compounds for material collected from depth P1 (l=30mm)

In fact, the evolution of the relative concentrations of carbonate complies the referred results. Figure 49 illustrates the similarity between samples collected from the center (P3) and

halfway through the radius (P2), although the first one shows slightly lower rates than the second, and the great difference in relation to the periphery sample's results (P1).
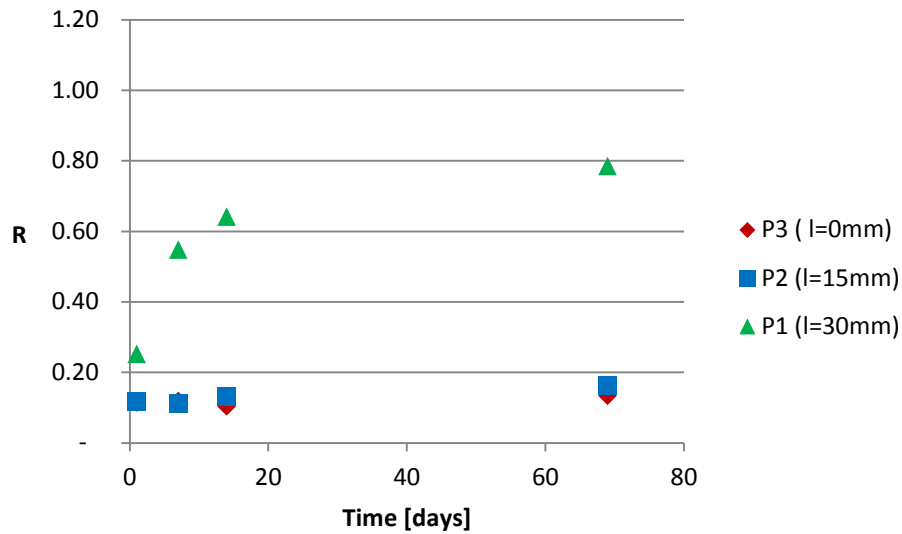

Figure 49: R rate of samples taken from different depths through the transversal section of cylindrical specimens

It is remarkable that samples taken from periphery of cylindrical specimens give carbonate contents comparable with the results given for the disc specimens at same ages. As it can be noted from Figure 38, the carbonate contents are 2,9% at the first day, 11,9% at 7 days and 11,7% at 14 days. From Figure 48, the respective compound contents are respectively 4,1% , 10,0% and 10,7%.
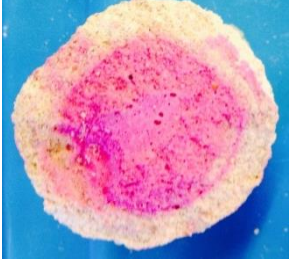
From the analysis of results related above, it can be concluded that inner parts of the mortar show greater difficulty to carbonate in comparison to periphery zones. This could be explained by the fact that inner regions take longer to dry, thus higher moisture within the mortar could be acting as hindrance to the penetration of carbon dioxide through the pores. Also, the progressive carbonation of outer zones is another potential impeditive to the gaseous diffusion through the material due the deposit of carbonate. In fact, the densification of the pore structure may reduce the diffusivity.

5.2 Carbonation front measurement

Phenolphthalein has been sprayed on the fresh-cut interior surfaces of mortar specimens, at different ages. The specimens used in these tests have been reused from TGA and humidity profiles experiments (moulding and curing conditions are reported in 4.3.2). The adopted indicator was phenolphthalein dissolved in ethanol.

Table 13 reports the results of the staining along time. Observations start at the age of 2 days from casting.

Table 13: Results of phenolphthalein staining (specimens stored in the standard chamber)

Specimen	Age of Observation (days)	Spection Diameter (mm)	Uncarbonated Diameter (mm)	Carbonated border thcikness (mm)	% of Carbonated Material	Aspect
3D_T20H60_1	2	54	54	~ 0	~ 0.0%	
3D_T20H60_2	7	56	52	2	7.1%	
3D_T20H60_5	14	60	50	5	16.7%	
HP_T20H60_A	62	55	35	10	36.4%	
3D_T20H60_5	69	64	40	12	37.5%	

Carbonation front measurement

Preliminar HP specimen	82	55	25	15	54.5%	

The progress of the carbonation front towards the inner part of the specimen is clearly visible, and Figure 50 illustrates more precisely its evolution. It is interesting to note that although the carbonated border increases progressively, steeper growth is visible until the 14th day.
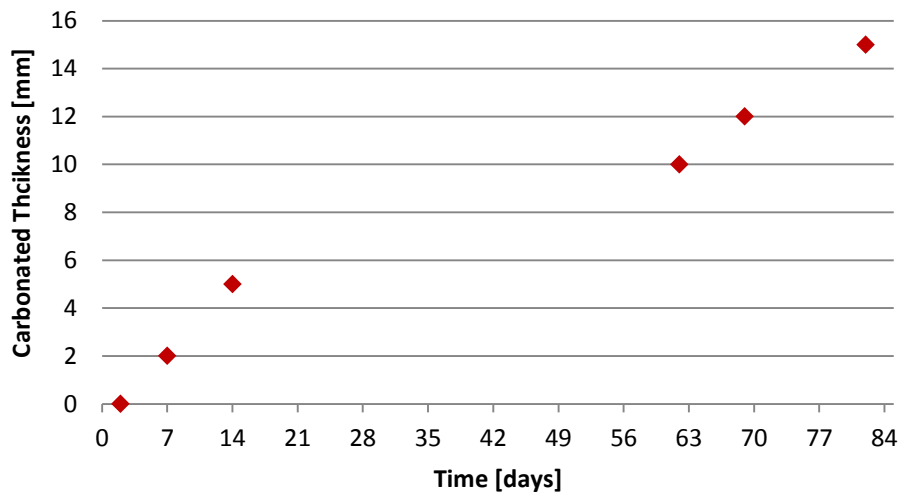

Figure 50: Evolution of carbonation front (% of carbonated material vs time)

The carbonation front tendency agrees with a carbonation depth of 7,3 mm at 36 days, reported by Meneghini (2014).However, results show a deeper carbonation front compared with results obtained from literature for similar ages. Lawrence (2006)reports depths of 9 to 14,5 mm at 90 days. Teutonico (1993) describes even lower thickness: 10 to 17 mm at 120 days.

The phenolphthalein staining can confirm partially the results of the depth investigation, for carbonation deeper than 15 mm only starts to show at about 82 days of exposing. This means that, for the older TGA analysis (69 days), the reaction front had not reached the middle-radius distance yet, thus results of samples collected from the center and the intermediary radius distance do not show significant difference

5.3 Humidity profiles monitoring

Humidity of inner regions of mortar specimens have been monitored through an average period of 20 days. According to section 4.3.2, sensor's probes are inserted in specific sleeves on both central and peripheric regions of five specimens. All specimens have been stored at the standard chamber. The results are displayed in Figure 51 and Figure 52.
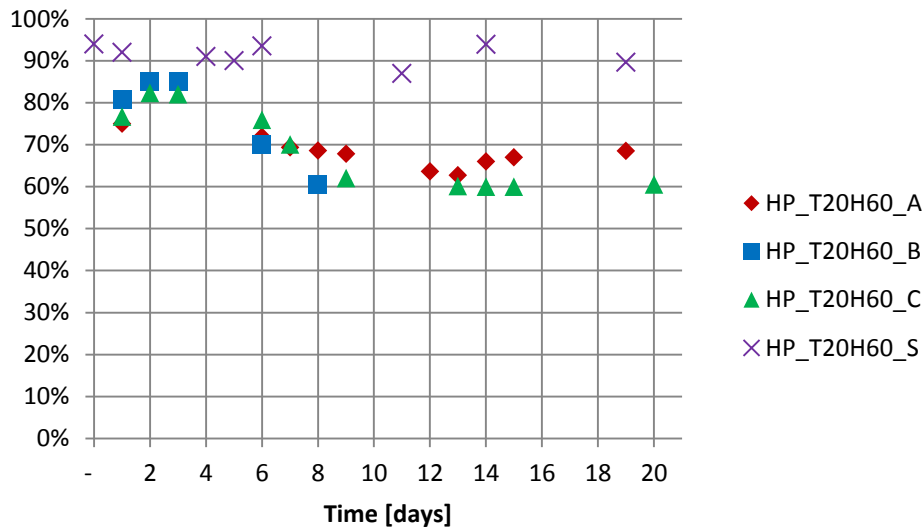
Figure 51: Relative humidity measured in the center of the specimens (depth =3 cm)
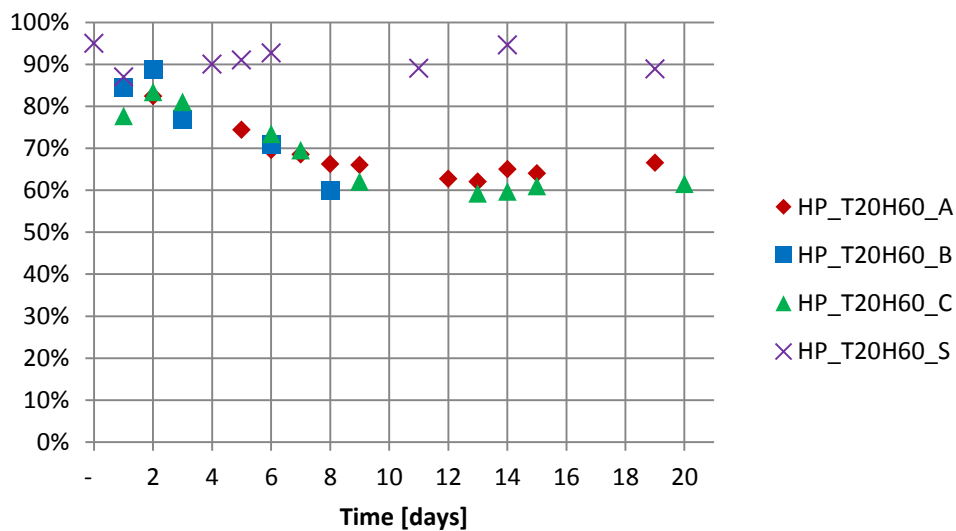
Figure 52: Relative humidity measured close to the periphery of the specimens (depth=1cm)

A first observation can be made regarding a comparison between the center and the peripheric measurements, for the aspect of the moisture variation is very similar in both Figure 51 and Figure 52. In fact, measurements values of center and periphery sleeves are extremely close for the entire testing period, not showing differences wider than the equipment's rage of error, which is ± 5%.

Regarding the sealed specimen, there were no relevant differences in the measured RH at both locations monitored in the sealed specimen (center and periphery), which always remained above ~90%. The deviation in regard to 100% RH suggests a self-consumption of water. However, for water to be consumed by the lime, carbonation would have had to occur. This does not seem as a feasible justification, as the specimen is sealed. Another mechanism is bound to have caused such self-desiccation.

Concerning the exposed specimens, it can be noted that, despite the distinct disposition of sleeves, the measured humidity drops from over 80% within the first 24 hours from casting to a level in the range 60-65% after the first 10 days of exposure. Considering that the chamber's relative humidity is of $60 \pm 5\%$ RH, it can be perceived that the specimens are reaching hygral equilibrium with the environmental humidity at the referred age of 10 days.

At 20 days of age, Meneghini (2014) reports moistures from 75% to 85% for depths of 1 to 4 cm through the mortars, respectively. In fact, in the mentioned work it is assumed that the specimen reaches the moisture equilibrium with the external environment at the age of 40 days. However, it has to be reminded that the specimens used by Meneghini only had one side of exposure with the environment's conditions, while the current work specimens are totally exposed from the first hours.

In order to understand the influence of the de-moulding procedures and curing strategy in the humidity variation, a deeper investigation was conducted during the interval comprehended between the removal of the plastic tube and the net (used to maintain the fresh specimen's shape). The results measured at center and periphery sleeves and a comparison with the variation of the environmental humidity are illustrated in Figure 53.
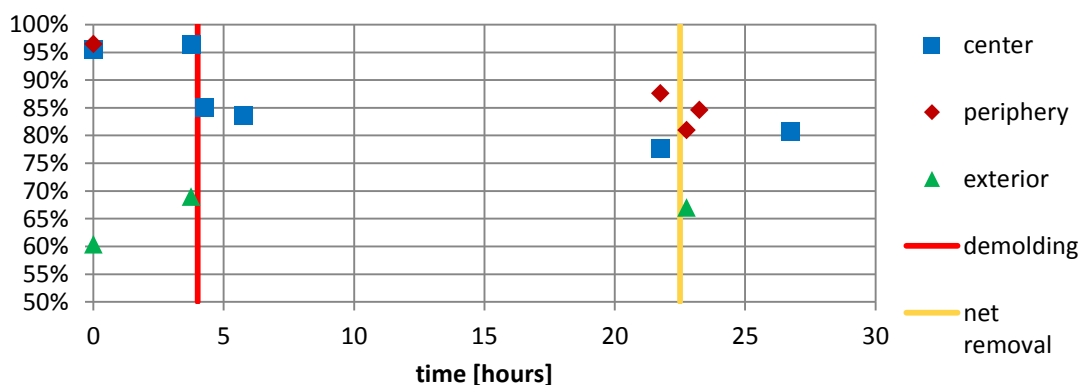

Figure 53: Humidity variation in the first hours

For the first $4 - 5$ hours, while the specimen is still sealed, high moistures are observed in both center and periphery measurement, with values comparable with the sealed specimen's results. After demolding, however, a remarkable drop of humidity is observed on both

measurement points. The following hours are marked by a progressive decrease of humidity that is not significantly altered by the net removal, thus a global tendency of moisture decline starts to take form.

The difference of internal humidity before and immediately after the removal of the mould confirms the influence of the exposure conditions in the development of humidity profiles.

The results lead to the withdrawal of the hypothesis that the delay of carbonation in inner parts of the cylindrical specimen could be associated with higher water contents. In fact, the performed measurements demonstrate a fast decrease of moistures even for central regions, reaching equilibrium with the environment's moisture (60±5%RH) at relatively early ages (about 10 days). The mortar reached a humidity that could not act as hindrance for the diffusion of carbon dioxide through the material, assuming that only moistures close to saturation would assume such characteristic (Van Balen & Van Gemert, 1994).

It is interesting to note that the water transport mechanism does not act in the same proportion as the carbon dioxide penetration inwards the mortar. Thus, the delay in the diffusion of carbon dioxide may rely mainly in the alteration of the porous structure, since this phenomenon is not reportedly related to the drying process in aerial lime mortars.

5.4   Modulus of elasticity

Modulus of elasticity tests were performed in specimens stored in the standard (EM_T20H60_6, EM_T20H60_7 specimens) and wet chambers (EM_T20H90_2, EM_T20H90_3 specimens) at the ages of 7, 15 and 22 days.

At each date, the specimens were weighted and measured, so that the evolution of the density is related to the testing results. Figure 54 and Figure 55 report respectively the evolution of density and the testing results.

From Figure 54 it can be noted a decreasing of density along time, which would demonstrate the evaporation of free water retained by the aggregates. It is visible the acting of the drying process even for the specimens stored at the wet chamber. This observation agrees with the conclusions acknowledged from the TGA results of the disc specimens exposed to high humidity, where despite of the chamber's conditions, the specimens appear to be submitted to a drying process.

During the casting procedure, the fresh density of all specimens respected the adopted value of 2000±100 Kg/m^3. Thus, higher initial densities demonstrated by the specimens kept at

higher moisture suggest the presence of higher water contents. Moreover, the referred specimens demonstrate steeper decrease of density.

As Figure 54 demonstrates, the specimens stored at lower relative humidity conditions are also submitted to drying. Contrary to the verified tendency, more significant carbonation rates would result in higher densities. Disregarding a volumetric variation, the consumption of hydroxide and consequent increase of carbonate would contribute to increase the density, as the second compound has higher molar mass than the first one. However, the weight loss given by drying appears to have higher influence than the increase provided by carbonation. Thereby, the density of the mortar shows a global decreasing tendency. In fact, TGA results for cylindrical specimens showed that significant carbonation only at superficial material, while inner regions show conversions of ~2% in weight (Figure 45 and Figure 46)
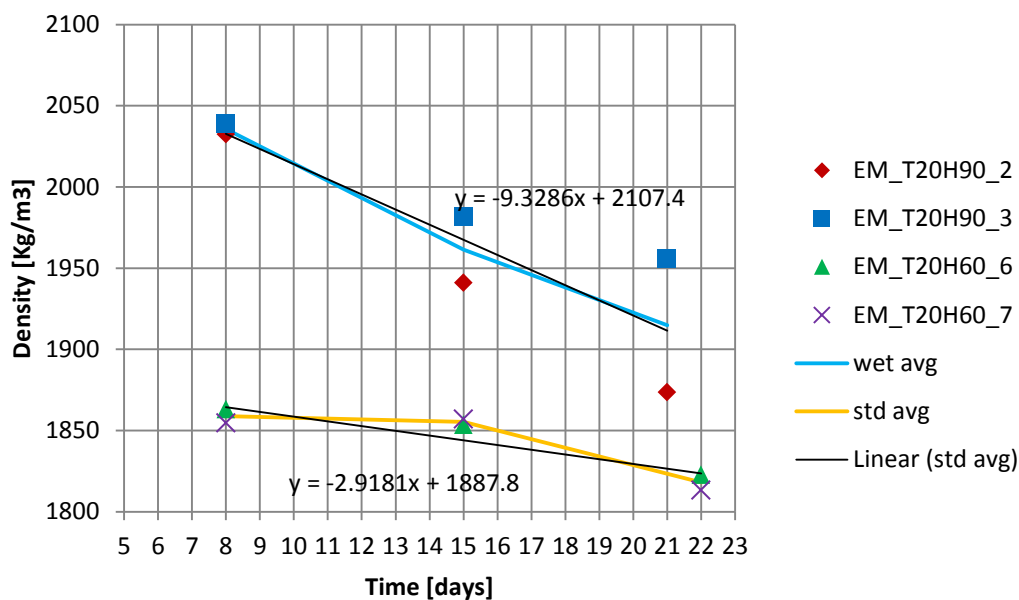

Figure 54: Evolution of density along time

From Figure 55 it can be noted a general increase of the modulus of elasticity, for specimens submitted to both environments. That the average E modulus for specimens stored at 60%RH reaches 3,5 GPa at 22 days, a value that is comparable with Meneghini's results for similar a related age: average of about between 3 GPa between 21 to 25 days (Meneghini, 2014). This result is also comparable with Margalha's, who reported a modulus of 2,97 GPa at 28 days, using a ratio of 1:5 lime:aggregate (Margalha, 2011). For the specimens stored at 90%RH the parameter drops about 75% in relation to the 60%RH specimens, reaching 2 GPa at 22 days.

For both cases, these results suggest that carbonation is responsible for the hardening of the mortar, even though TGA results report more significant effects at periphery regions (Figure 45, Figure 46 and Figure 48). The modulus of elasticity increases, even for the specimens

80

stored at the wet chamber. This demonstrates that carbonation occurs in both environments, in agreement with the results obtained from TGA analysis for wet and standard chambers' discs (where similar carbonation taxes are shown).

However, Figure 55 evidences lower carbonation rates for the wetter specimens, as they show significantly lower E values. The displayed results suggest that lower stiffness of specimens stored in the wet chamber would be directly related to the high presence of water. On the other hand, from TGA results in disc specimens (Figure 41), it would not be reasonable to assume lacks of carbonation due higher water contents.
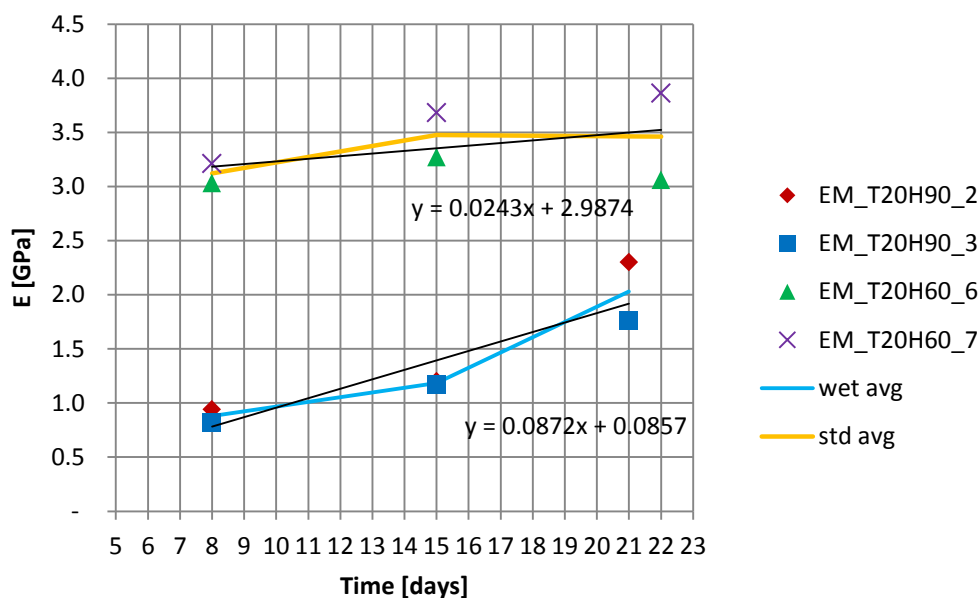

Figure 55: Evolution of E along time

The excess of water affects the interaction between grains, influencing the cohesion of the material (Bastos, n.d.; da Silva & de Carvalho, 2007). In non-saturated granular materials, such as soils, capillary tensions provide attraction force between particles (matrix suction). Attraction forces tend to be reduced with the increase of water content in the voids of the soil, disappearing when saturation is reached (Bastos, n.d.).

In fact, according to Hillel (1980), when a soil has low water contents, its matrix is more resistant, which propitiates greater stiffness. On the other way, when the water content increases, particle's interaction is weakened, as well as the friction between them. Thus, the excessive presence of water in the mortar would be responsible for the decrease of cohesion between particles. In this matter, the interaction between the grains would be lowered, resulting in lower capacity to resist the loads applied in the test, and, thereby, lower stiffness results.

5.5   Compressive strength

Compressive strength testing was conducted on specimens exposed to standard (CP_T20H60_1, CP_T20H60_2 and CP_T20H60_3 specimens) and wet chambers (CP_T20H90_1, CP_T20H90_2 and CP_T20H90_3) at 28 days from casting, following EN 1015-11 (1999) specifications.

Table 14 and Table 15 shows the results obtained for the standard and wet chambers specimens, respectively. Detailed plotted stress vs. strain curves are shown in Annexes VIII and IX.

Table 14: Compressive strength results for standard chamber's specimens at 28 days

Specimen	Failure load (KN)	Density (kg/m3)	Failure stress (MPa)
CP_T20H60_1	2.03	1824.8	0.81
CP_T20H60_2	1.45	1816	0.58
CP_T20H60_3	1.97	1825.6	0.79

Table 15: Compressive strength results for wet chamber's specimens at 28 days

Specimen	Failure load (KN)	Density (kg/m3)	Failure stress (MPa)
CP_T20H90_1	1.21	1804.0	0.48
CP_T20H90_2	1.04	1860.8	0.42
CP_T20H90_3	0.72	1841.6	0.29

Considering the fresh density of 2000 ± 100 Kg/m^3, it can be noted a decreasing tendency of the parameter in both environments. In particular, wetter specimens appear to present higher density decrease. This observation agrees with the behavior reported by the modulus of elasticity test specimens.

The average compressive strength at 28 days for the standard chamber's specimens can be estimated as 0,73 MPa, and the wet chamber's as 0,40 MPa, demonstrating that specimens maintained at higher moistures are about 82,5% weaker than the ones kept in the standard conditions.

These results are compatible with the E modulus results for specimens exposed to the same conditions and confirms that, in terms of mechanical behaviour, wetter mortar tend to be weaker. The related weakness, as previously mentioned, is related to prolonged contact with higher humidity, as the excess of water would lower the interaction between the grains (Bastos, n.d.; Hillel, 1980). The consequence of prolonged explosion to high humidity is thereby reflected in reduced capacity of the material to resist loads (Hillel, 1980). The

lowering of load resistance capacity of soils according to increasing humidity values is reported by several authors in the field of soil sciences (Carpenedo, 1994; Kondo & Dias Junior, 1999; Silva & Cabeda, 2006; Oliveira, 2008).

The compressive strength of the standard chamber's specimens is comparable with Margalha's results, that pointed a 0,81 MPa strength at 28 days (Margalha, 2011). However, this results is not comparable to Meneghini's, as the author report an average of 0,5 MPa at 28 days for the same conditions (Meneghini, 2014). This difference of values could be given due variations in the density of the specimens, for the author does not reports the density at the testing age. It is possible that the current work's specimens are in average denser than the author's, and for that reason generally stronger.

5.6 Lime paste testing

A sample of quicklime and water paste was submitted to an hermetic environment of constant conditions (30ºC, 60%RH), settled inside a thermo gravimetric device (SDT 2960 DSC TGA).

The paste preparation followed the proportion adopted in the mixing process (see section 4.2). The sample was collected using a proper tool (see Figure 30) and showed an initial weight of 105 mg. Before the experimental setting could be started, it was verified a fast weight decrease of the sample. Given the exothermic character of hydration of lime, the weight variation is related exclusively to evaporation of water. It is estimated that the material has lost ~40 mg in about 90 minutes. After this period, the weight did not vary significantly, allowing the starting of the test. The test consisted of a continuous monitoring of the sample weight, during a period of about 25 days. Figure 56 shows the relative variation of weight (with respect to the stabilized weight) by the elapsed time.
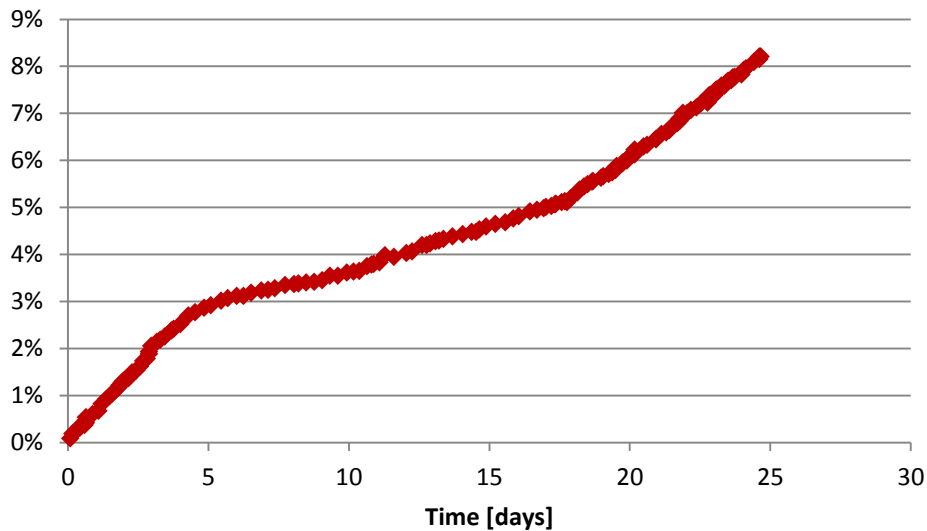
Lime paste testing

The graphic shows a global progressive weight increase. An initial steeper variation is seen until ~5 days, followed by a more modest rate of variation. This decrease in weight loss rate is maintained until ~17 days, when faster rates seem to be retaken.

The lower weight increase could be given by the hydration of lime and later production of carbonate, which would prevent deeper penetration of outside carbon dioxide, as Van Balen (2005) states. In fact, the densities of calcium hydroxide and carbonate are remarkably lower than the oxide's, which would provide the formation of outer hydroxide and carbonate deposits around lime grains (Figure 57). Moreover, the solubility of the calcium carbonate is known to be lower than that of hydroxide. Thereby, the late acting of carbonation, by a gradual deposit of $CaCO_3$, would propitiate the formation of a less permeable outer layer.
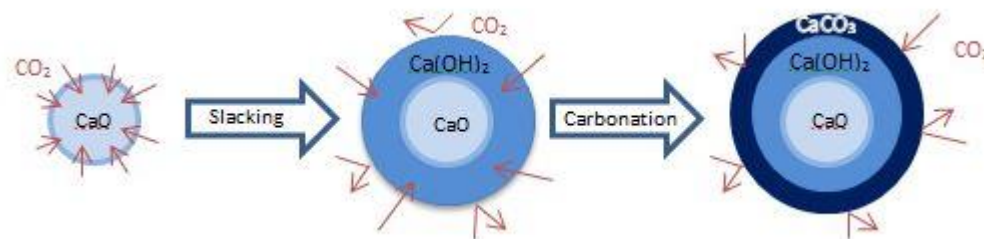

Figure 57: Schematic illustration of hydroxide and carbonate deposits around lime grains

However, the deposition of composites around the lime grains appears to increase up to a maximum limit (at ~17 days), from which it is visible higher conversion rates. This behavior would be explained by a possible disruption of the outer layer. Such disruption would be explained by a possible local retraction due gradual water loss. The alteration of the

impermeable layer propitiates a resumption of the carbon dioxide penetration, thus retaking conversion of uncarbonated material at higher rates.

The isolated behavior of lime corroborates the results of phenolphthalein staining, which indicate a slow and segmented behavior of carbonation (Figure 50). The current results also agree with the apparent stagnation of carbonate conversion verified in the TGA analysis on disc specimens exposed to varied conditions (Figure 38 to Figure 44). Furthermore, it agrees with the hypothesis that the delay of the CO_2 diffusion through the mortar is mainly affected by the alteration of the porous matrix, rather than the water content. This infers a conclusion of a self-limiting conduct of the reaction.

6. CONCLUSIONS

6.1 Main conclusions

As explained in the introduction, the current work had the main objective of continuing and extending a previously developed study on the behaviour of aerial lime mortars, in view of the necessary models and parameters for multi-physics modelling of this material. The following main conclusions can be withdrawn from the present research work:

- High values of environmental relative humidity may slow the process of drying of the mortar but do not eliminate it at all. Consequently, carbonation still has the opportunity to occur, even if the environmental humidity lies above 90%. It is however remarked that this observation is not consistent with Van Balen (2005), who stated a threshold of 53,4 kg/m^3 as a critical water content, above which the carbon dioxide diffusion through mortar would be prevented;

- A greater concentration of carbon dioxide in the surrounding environment does not imply higher carbonation rates. This conclusion is coherent with Shin (2009) and Van Balen (2005) conclusions of carbonation being a zeroth-order reaction in respect to CO2. Actually, the kinetics of the reaction appears to rely mainly on how the gas is diffused throughout the material;

- Inner parts of mortar show greater difficulty to carbonate. This observation can be related to restricted access of CO_2 to such areas. The monitoring of humidity profiles on exposed specimens showed a fast decrease of RH (moistures varied from saturation to 60±5%RH in ~10days), suggesting that the delay on carbon dioxide diffusion is not related to higher water contents;

- The carbonation front progresses gradually towards inner parts of the mortar. However, carbonation is a reaction of a very slow nature and, although progressive, demonstrates a segmented behavior along time. It is presented as a self-limiting process. This characteristic is suggestively influenced by alteration of the porous matrix by sedimentation of carbonation's product itself;

- Drying was observed to have greater influence than carbonation on the evolution of mortar density, leading the decrease of such parameter along time. Although low rates are suggested, carbonation is responsible for the hardening of the mortar, even under high humidity. High water contents tend to have negative influence on the material's

mechanical properties. Wetter mortars are significantly weaker in comparison with specimens stored at dryer conditions, showing lower stiffness and strength parameters.

6.2   Further work

The current study experienced some limitations regarding a more profound investigation of carbonation behaviour facing different conditions of exposure. In this matter, from the mentioned conclusions and also in the matter of adapting of a multi-physics model for carbonation field, the following issues are suggested on the development of further works:

- Direct measuring of carbon dioxide content through inner regions of the mortar specimens could allow a more accurate quantification of the diffusion of this gas within the material;

- The subjection of specimens to environments of humidity lower than the standardized 60%RH could provide further information on the material's behaviour face dryer conditions, and would be an interesting form of comparison with the results from wetter environment specimens. Likewise, the submission to a zero carbon dioxide concentration environment could attest the behaviour with respect to this reactant ;

- An alternative test regarding the evaluation of porosity of mortar is possible to be made by mercury intrusion. When performed in specimens submitted to different exposing conditions and storage environments, this analysis could provide deeper information on the alteration of the porous structure through the evolution of the carbonation front;

- An attempt to repeat humidity profiles measurements in specimen subjected to exposure environments of relative humidity different than 60%RH could be an interesting test to confront the results obtained from the standard condition, and would provide a deeper understanding of the drying process and the water transport mechanism.

REFERENCES

Adams, J., & Dollimore, D. (1993). Thermal Analytical Investigation of Ancient Mortars from Gothic Churches. *Journal of Thermal Analysis, 40*, 275-284.

Arandigoyen, M. (2005). Lime pastes with different kneading water: pore structure and capillary porosity. *Applied surface science 252*, pp. 1449-1459.

ASTM C51 -11. (n.d.). *Standard terminology relating to lime and lime stone (as used by industry).*

Baronio, G., Binda, L., & Saisi, A. (2000). mechanical and physical behaviour of lime mortars reproduced after the characterisation of historic mortar. *international RILEM workshop*, (pp. 307-321).

Bastos, C. A. (n.d.). *Reisistencia ao cisalhamento dos solos*. Retrieved from http://www.scielo.br/scielo.php?pid=S0100-06832007000500003&script=sci_arttext

Boynton, R. (1984). Lime and lime stone. In *Encyclopedia of chemical technology 3rd* (pp. 343-382). New York.

BS EN 1015-11. (1999). *Methods of test for mortar for masonry. Determination of flexural and compressive strength of hardened mortar.*

BS EN 12390-3. (2002). *Testing hardened concrete. Compressive strength of test specimens.*

BS EN 13139. (2002). *British and European Standard.*

BS EN 459-1. (2010). *BSI Standards Publication Building lime Part 1: Definitions, specifications and conformity criteria.*

BS EN 459-2. (2010). *BSI Standards publications buildings lime part 2: test methods.*

Callebaut, K. (2000). *Characterisation of Historic Lime Mortars in Belgium: implications for Restoration Mortars.* Leuven: Katholieke Universiteit.

Callister Jr, W. (2007). *materials science and egineering 7th ed.* new york: John Wiley and sons inc.

Carpenedo, V. (1994). *Soil compressibility in management systems.* Brasil: Federal University of Rio grande do sul.

Cazalla, O. e. (2000). Aging of lime-putty : effects on traditional lime mortar carbonation. *J.Am. Ceram. Soc. 83*, 1070-1076.

Cizler, Ö., Van Balen, K., & Gemert, D. (n.d.). *Carbonation Reactionin lime mortars.* Retrieved from http://web.abo.fi/fak/tkf/vt/aceme10/6-3 %C3%96zlem Cizer_ACEME10.pdf.

Coppola, L. (n.d.). *Dalle calci idrauliche al cemento Portland.* Retrieved from http://www.unibg.it/dati/corsi/20057/33179-L5_calceIdraulica_Cemento.pdf.

Coutinho, M. (2002). *Melhoria Materiais de Construção 2 - 1ª parte.* Porto, Portugal: Universidade do Porto.

Cultrone, G., Sebastián, E., & Ortegas Huertas, M. (2005). Forced and natural carbonation of lime-based mortars with and without additives: Mineralogical and textural changes. *Cement and Concrete Research*, pp. 2278–2289.

da Silva, A. J., & de Carvalho, F. G. (2007). Cohesion and shear strength as related to physical and chemical properties of a Yellow Latosol of coastal plain. *Rev. Bras. Ciênc. Solo vol.31 no.5* .

de Magalhães, n. J. (2013). *Influencia dos parametros da formulação na rigidez de solos estabilizados: estudo experimental.* Portugal: Universidade do Minho.

de Vasconcelos, R. F., Cantalice, J. R., Moura, G. B., Rolim, M. M., & Montenegro, C. E. (2012). Compressibility of a yellow latosol under different management systems with sugarcane. *Rev. Bras. Ciênc. Solo vol.36 no.2* .

Dheilly, R., Tudo, J., & Sebábi, Y. (2002). Influence of storage conditions on the carbonation of powdered Ca(OH)2. *Cosntruction and building materials 16*, 155-161.

Elert, K. (2002). Lime Mortars for the Conservation of Historic Buildings. *Studies in Conservation, 47(1)*, 62–75.

Farkas, E., & Kliege, P. (1986). uniformity of cement strength. *A symposium sponsored by ASTM commitee C-1 on cement, 1.* Louisville, United States.

Ferretti, D., & Bazant, Z. (2006). Stability of ancient masonry towers: Moisture diffusion, carbonation and size effect. *Cement and Concrete Research 36(7),*, pp. 1379–1388.

Gimbert, S. (2008). A combined empirical and computacional approach to creep in replicas of historic mortar. Pennsylvania, United States: Pennsylvania State University.

Grandet, J. (1975). Contribution a l'etude de la prise et de la carbonatation des mortiers au contact des materiaux poreux. Univ. Paul Sabatier, Toulouse, França.

Granja, J., Azenha, M., de Sousa, C., Faria, R., & Barros, J. (2014). Hygrometric Assessment of Internal Relative Humidity in Concrete: Practical Application Issues. *Journal of Advanced Concrete Technology , vol 12 (8)*, 250-265.

Hassibi, M. (2009). An overview of lime slacking and factors that affect the process. Chemco Systems.

References

Heck, N. (n.d.). *Introdution to metalurgic engineering.* Retrieved september 2014, from Introdution to metalurgic engineering- UFRGS – DEMET: http://www.ct.ufrgs.br/ntcm/graduacao/ENG06638/IEM-Texto-4.pdf

Hillel, D. (1980). *Fundamentals of soil physics.* New York: Academic Press.

Holmes, S., & Wingate, M. (1997). Building with lime. London: Intermediate Technology Publications.

Introduction to the Stone Cycle and the Conservation of Historic Buildings. (2013, Novembro). *Quarterly Journal of Engineering Geology and Hydrogeology.*

Judice, F., & Perlingeiro, M. (2005). *Resistencia dos Materiais IX.* Retrieved 2014, from http://www.uff.br/resmatcivil/Downloads/ResMatIX/apostila_resmatIX.pdf

Kondo, M., & Dias Junior, M. (1999). Compressibilidade de latossolos em função da umidade e uso. *R. Bras. Ci. Solo, 23* , pp. 211-218.

Lanas, J., & Alvarez, J. (2003). Masonry repair lime-based mortars: factors affecting the mechanical behavior. *Cement and Concrete Research*, pp. 1867–1876.

Lawrence, R. (2006). A study of carbonation in non-hydraulic lime mortars. University of Bath.

Lawrence, R. (2007). Effects of carbonation on the pore structure of non-hydraulic lime mortars. *Cement and Concrete Research 37(7)*, pp. 1059–1069.

Lime Stuff Ltd. (n.d.). *Hydraulic or non hydraulic lime.* Retrieved 2014, from Lime Stuff. Traditional Breathable building and decorating products: http://www.limestuff.co.uk/pages/user-guides/hydraulic-or-non-hydraulic-lime.html

Lourenço, P. (2004). Local and global models for seismic safety assessment. Guimarães, Portugal: University of MInho.

Margalha, G. e. (2011). Traditional methods of mortar preparation: the hot lime mix method. *Cement and concrete composites 33 (8)*, 796-804.

Meneghini, A. (2014). EXPERIMENTAL CHARACTERIZATION OF AERIAL LIME MORTARS IN VIEW OF MULTIPHYSICS MODELLING. Universidade do Minho, Guimarães, Portugal.

Moffat, W., & Wimsley, M. (2006). Understanding lime calcination kinectics for energy cost reduction. *59th Appita Conference.* Auckland, New Zealand.

Moorehead, D. (1986). Cementation by the carbonation of hydrated lime. *Cement and concrete research, 16*, pp. 700-708.

Moropoulou, A. (2005). strength development and lime reaction in mortars for repairing historic masonries. *cement and concrete composites 27 (2)*, pp. 289-294.

Ngoma, A. (2009). *Characterisation and Cosolidation of historical Lime mortars in cultural heritage buildings and associated structures in east Africa.* Stocholm: Royal Institute of Technology.

Oates, J. (1998). Lime and Limestone. WILEY-VCH.

Oliveira, V. (2008). *Compaction on cohesive soils of Alagoas coast trays .* Alagoas, Brasil: Rural Fedral University of Pernambuco.

Ostwald, W. (1897). A-linien von R.E.Liesegang. *Z.Phys.Chem 23*, 365.

Shin, H. (2009). Effect of Reactivity of Quicklime on the porperties of hydrated lime sobent for SO2 removal. *Jornal of material science and technology, 25(3)*, 329-332.

Silva, A., & Cabeda, M. (2006). Compation and compressibilty of soils under manegement systems and humidity layers . *R. Bras. Ci. Solo, 30*, pp. 921-930.

Società Impianti calce. (n.d.). Retrieved from Storia della calce: http://www.sic-lime.it/it/default.asp?Subs=423&Liv1=414.

Stewart, J. e. (2001). field and laboratory assessment of lime-based mortars. *JOrnal of architectural conservation 7 (1)*, 7-41.

Teutonico, J. e. (1993). The Smeaton Project. *APT Bulletin 25 (3)*, 32-49.

Thomson, M. (2002). Plasticity, water retention, soundness and sand carrying capacity: what a mortar needs. *Proceedings of the International RILEM Workshop on Historic Mortars: Characterisation and Tests* (pp. 163–172). RILEM Publication S.A.R.L.

UNI EN 1936:2007. (2007). *Natural stone test methods - Determination of real density and apparent porosity and of total and open*.

Válek, J., & Matas, T. (2010). Experimental study of hot mixed mortars in comparison with lime putty and hydrate mortars. *2nd historic mortars conference HMC20120 and RILEM TC 203-RHM final workshop*, (pp. 1229-1240). Prague, Czech Republic.

Van Balen, K. (2005). Carbonation reaction of lime, kinetics at ambient temperature. *Cement and concrete research 35(4)*, 647-657.

Van Balen, K., & Van Gemert, D. (1994). Modelling lime mortar carbonation. *Materials and Structures, 27(7)*, pp. 393–398.

Veiga, M. d., Fragata, A., Velosa, A. L., & Magalhães, A. C. (2010). lime-based mortars: viability for use as substitution renders in historical buildings. *international journal of architectural heritage 4 (2)*, 177-195.

Vestrynge, E., Schueremans, L., & Germert, D. (2010). Time-dependent mechanical behaviour of lime-mortar masonry. *Materials and Structures 44(1)*, pp. 29-42.

Viollet-le-Duc, E. (1854). *Disctionnaier raisoneé de l'architecture française du XIe au XVIe siècle, tome IV*.

ANNEX I – SUMMARY OF LITERATURE RESULTS

Author	Type of Binder used	Type of Aggregates used	Curing conditions	Ratio lime:aggregates and water:lime (parts by volume)	Open Porosity results	Elasticity Modulus results	Compressive strength results
Teutonico (1993)	Lime putty	Not specified	Not specified	• 1:2,5 and 1:3 (l:a)	Not measured	Not measured	Not measured
Baronio (2000)	• Lime putty • Dry hydrated	Silicate sand	• 90% RH – 1st day • 75% RH- 1st to 3rd day • 60%RH from 3rd day	• 1:5 and 1:3 (l:a)	• 29-32% (lime putty) • 26-29% (dry hydrated lime)	0,11-0,59 GPa (28 days)	Not measured
Cazalla (2000)	• Dry hydrated lime	Not specified	Not specified	Not specified	• 19,1% (fresh, lime putty)	Not measured	Not measured

	Lime putty				• 29% (fresh, dry hydrated lime) • 23,5 % (14 days, lime putty) • 28% (1 year, lime putty)		
Lanas & Alvarez (2003)	Dry hydrated lime	• Calcitic fillers • Silicate sand	60% RH	• 1:1,1:2,1:3, 1:4 (l:a) • 1:2 to 6:5 (w:l)	19-25% (365 days)	Not measured	• 0,45-0,60 MPa (14 days) • 0,5-0,9 MPa (28 days)
Moropoulou	Dry hydrated	Not specified	Not specified	• 1:1,5 and	Not measured	Not measured	• 0,69-

(2005)	lime			1:1,8 (l:a) • 0,7:1 to 1,2:1 (w:l)			0,90 MPa (1 month, dry hydrate lime) • 1,56-2,90 (15 months, lime putty)
Van Balen (2005)	• Dry hydrated lime Lime putty – extra watered	Not specified	Not specified	Not specified	Not measured	Not measured	Not measured
Lawrence (2006)	• Dry hydrated lime	• bioclastic and oolitic lime	• 90%RH – first 7 days	• 1:1, 1:2, 1:3 (l:a) • 0,57:1 to	• 29% (bioclastic and oolitic	Not measured	Not measured

	• kibbled high purity quick lime • other lime putties	stones • silicate sand	• 60% RH	1,08:1 (w:l)	lime stones) • 19% (silicate sand)		
Válek and Matas (2010)	• Dry hydrated lime • Quick lime	silicate river sand	• 65% RH • dry-wet cycles	• 1:3 and 1:0,9 (l:a)	Not measured	Not measured	Not measured
Rosário Veiga (2010)	• Dry hydrated lime	Not specified	Not specified	Not specified	1:3	2 – 4 Gpa (90 days)	Not measured
Margalha (2011)	Lime putty	fine and coarse silicate sands	Not specified	• 1:2 and 1:3 (l:a)	Not measured	• 2,97 GPa (28 days) • 4,6	Not measured

						GPa (90 days)	

ANNEX II – CHARACTERIZATION OF QUICKLIME – CL90 Q

A) Properties (Meneghini, 2014)

Classification according to BS EN 459-1: 2010	Supplier	Reactivity [s]	Chemical composition	Granulometry
CL 90 Q	Lusical	t60° ≤ 120 tu ≈ 3 min	more than 80% wt CaO	more than 80% retained

B) Chemical Composition (Meneghini, 2014)

Compound	Content in weight
CaO_{disp}	≥ 80 %
CO_2	≤ 4,0 %
MgO	≤ 1,0 %
SO_3	≤ 2,0 %
SiO_2	≤ 0,3 %
Al_2O_3	≤ 0,2 %
Fe_2O_3	≤ 0,2 %
CaO+MgO	≥ 90 %

C) Granulometry (Meneghini, 2014)

Retained at 200µ m	< 30 % max
Retained at 90µm	≤ 50 % max
Retained at 2mm	≤ 5 % max
Retained at 5mm	0

D) Hydroxide and carbonate contents (Meneghini, 2014)

Compound	Amount [wt%]
$Ca(OH)_2$	7,5
$CaCO_3$	11,8

ANNEX III – CHARACTERIZATION OF AGGREGATES

A) Chemical composition - x ray fluorescence analysis results (Meneghini, 2014)

Compound name	Concentration [%]	Absolute Error [%]	Concentration [%]	Absolute Error [%]
	fine sand		coarse sand	
Al_2O_3	3,71	0,06	5,25	0,06
BaO	0,0372	0,001	0,0297	0,001
CaO	0,142	0,01	0,219	0,01
Cr_2O_3	0,0679	0,004	0,099	0,005
CuO	0,0119	0,001	0,0140	0,001
Fe_2O_3	0,681	0,01	1,39	0,02
K_2O	2,40	0,06	2,39	0,06
MgO	0,161	0,005	0,0495	0,003
Na_2O	0,526	0,03	0,921	0,04
P_2O_5	0,0744	0,006	0,148	0,009
Rb_2O	0,0106	0,001	0,0169	0,001
SO_3	-	-	0,0524	0,005
SiO_2	92,0	0,3	88,7	0,3
SrO	0,00567	0,001	0,00571	0,001
TiO_2	0,117	0,01	0,666	0,02
ZnO	0,00769	0,001	0,00823	0,001
ZrO_2	0,00552	0,001	0,0201	0,001

ANNEX IV – DETAILED RESULTS OF TGA ANALYSIS ON DISC SPECIMENS

Standard chamber	Absolute Values				% in respect to sample					conversion %			carbonation
Age	Sample Weight	Ca(OH)2 Weight	CaCO3 weight	CaO weight	Total	Ca(OH)2	CaCO3	CaO	total	Ca(OH)2	CaCO3	CaO	R
1	62.463	5.860	1.872	5.483	13.215	9.382%	2.996%	8.778%	21.156%	44.35%	14.16%	41.49%	0.2421
4	58.655	5.147	8.147	8.457	21.750	8.774%	13.889%	14.418%	37.081%	23.66%	37.46%	38.88%	0.6128
7	73.310	4.509	9.586	8.780	22.874	6.150%	13.075%	11.976%	31.202%	19.71%	41.91%	38.38%	0.6801
14	60.766	4.582	10.398	9.290	24.271	7.540%	17.112%	15.289%	39.941%	18.88%	42.84%	38.28%	0.6941
21	68.568	2.361	10.382	7.601	20.345	3.444%	15.142%	11.086%	29.671%	11.61%	51.03%	37.36%	0.8147
28	71.288	5.162	9.142	9.026	23.330	7.241%	12.824%	12.661%	32.727%	22.13%	39.19%	38.69%	63.91%

Wet chamber	Absolute Values				% in respect to sample					conversion %			carbonation
Age	Sample Weight	Ca(OH)2 Weight	CaCO3 weight	CaO weight	Total	Ca(OH)2	CaCO3	CaO	total	Ca(OH)2	CaCO3	CaO	R
1	55.004	6.998	1.135	5.932	14.065	12.723%	2.064%	10.784%	25.571%	49.76%	8.07%	42.17%	0.1396
4	59.778	6.552	2.849	6.554	15.955	10.960%	4.767%	10.964%	26.690%	41.06%	17.86%	41.08%	0.3031
7	62.774	8.049	3.126	7.842	19.016	12.822%	4.980%	12.492%	30.294%	42.33%	16.44%	41.24%	0.2797
14	59.057	2.812	11.223	8.413	22.44	4.761%	19.00	14.24	38.011	12.53%	50.00	37.48%	0.7996

Annex IV – Detailed results of TGA analysis on disc specimens

					8		4%	5%	%		%		
21	67.736	0.042	16.124	9.062	25.228	0.063%	23.805%	13.378%	37.245%	0.17%	63.91%	35.92%	0.9974
28	56.180	1.766	11.590	7.826	21.182	3.143%	20.630%	13.931%	37.704%	8.34%	54.72%	36.95%	0.8678

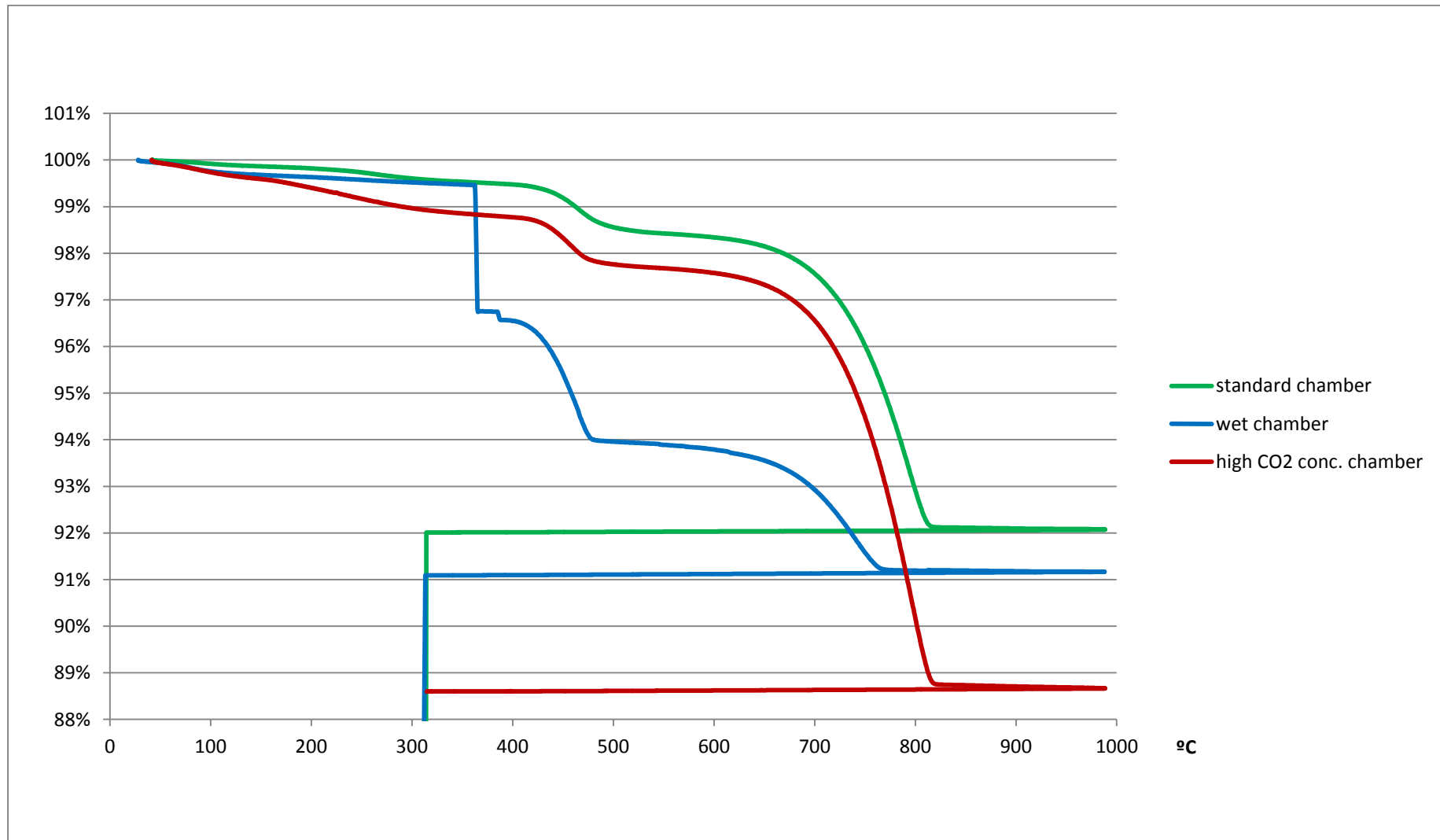| High CO2 concentration chamber	Absolute Values				% in respect to sample					conversion %			Carbonation
Age	Sample Weight	Ca(OH)2 Weight	CaCO3 weight	CaO weight	Total	Ca(OH)2	CaCO3	CaO	total	Ca(OH)2	CaCO3	CaO	R
1	56.391	8.667	1.333	7.306	17.307	15.370%	2.365%	12.956%	30.691%	50.08%	7.70%	42.21%	0.1333
4	57.556	3.724	9.774	8.291	21.789	6.470%	16.981%	14.406%	37.857%	17.09%	44.86%	38.05%	0.7241
7	61.800	4.044	11.966	9.761	25.771	6.544%	19.362%	15.795%	41.701%	15.69%	46.43%	37.88%	0.7474
14	66.566	3.140	9.402	7.641	20.183	4.717%	14.125%	11.479%	30.320%	15.56%	46.58%	37.86%	0.7497
21	76.573	3.521	9.044	7.729	20.294	4.598%	11.810%	10.094%	26.503%	17.35%	44.56%	38.09%	0.7198
28	66.758	5.208	10.105	9.600	24.913	7.802%	15.136%	14.381%	37.319%	20.91%	40.56%	38.53%	0.6599

ANNEX V – TGA CURVES OF DISC SPECIMENS

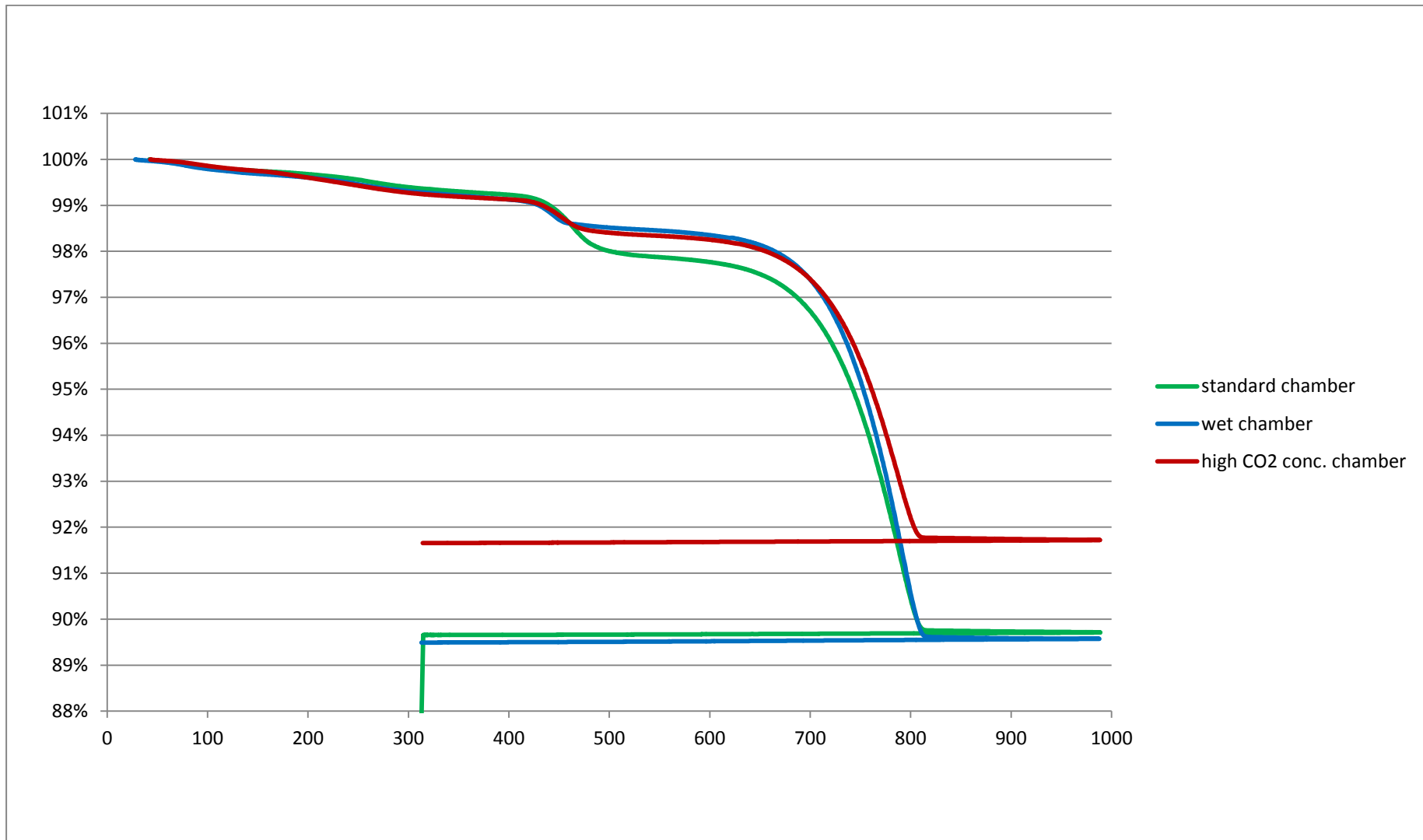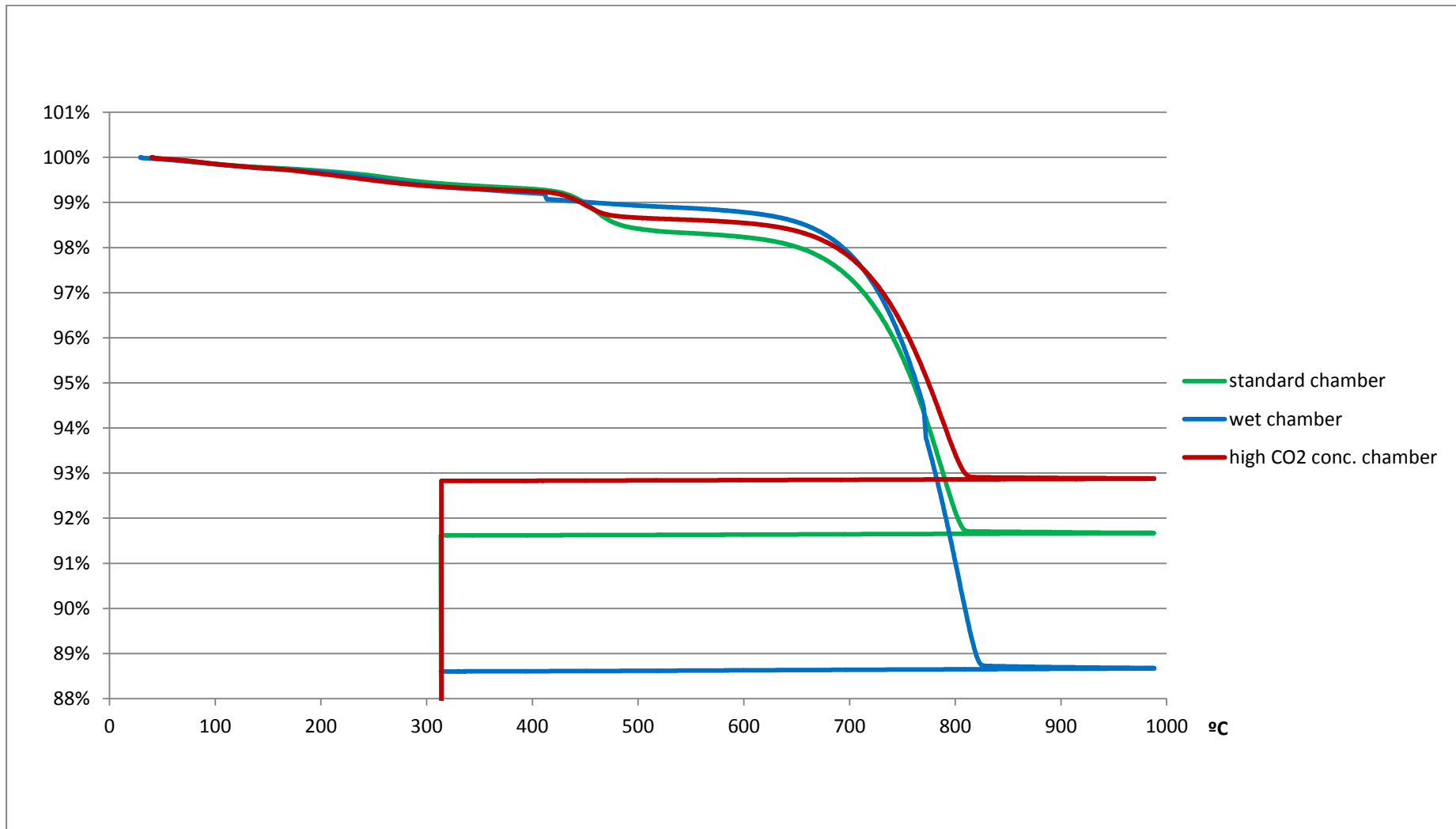1 day from casting
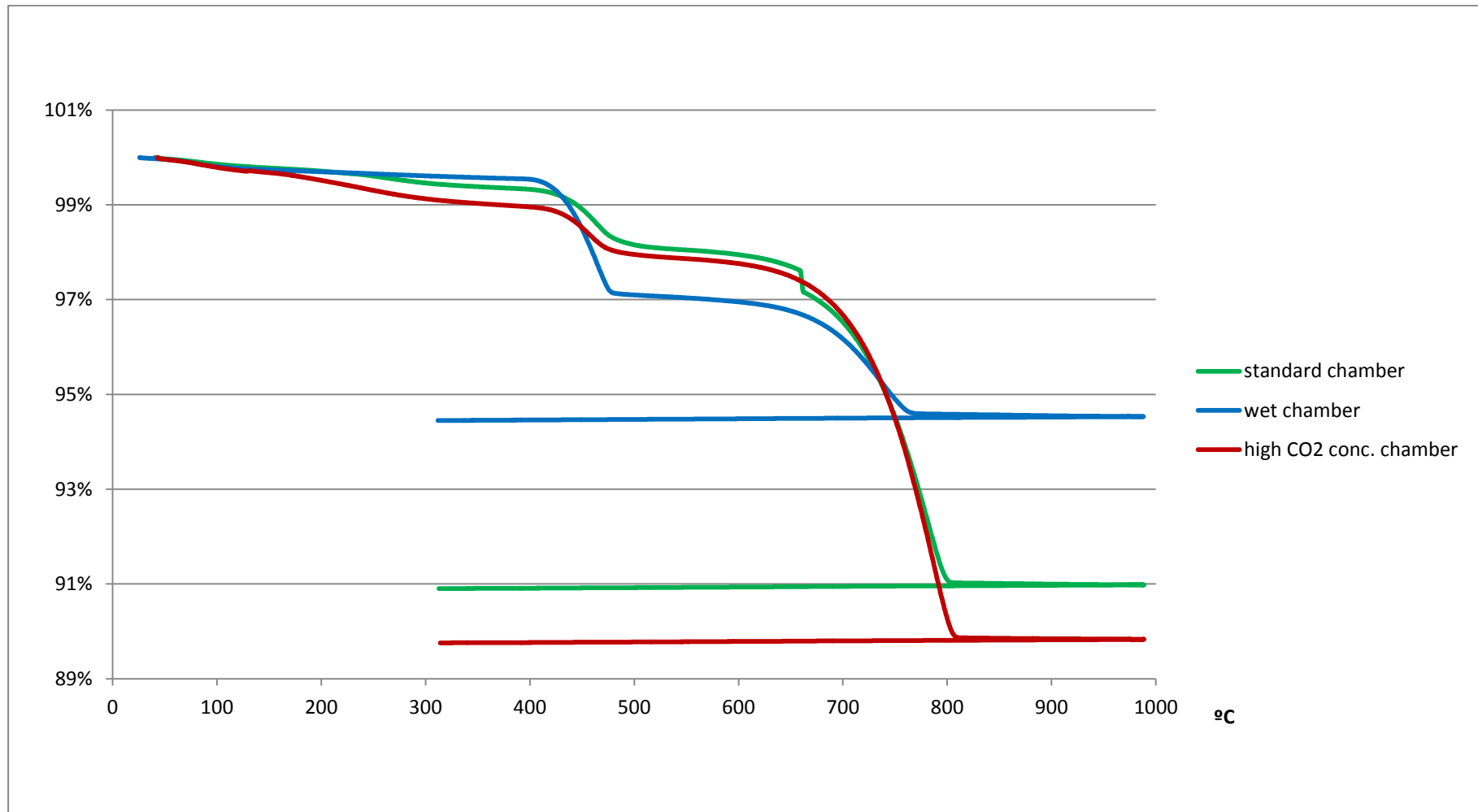
4 days from casting

7 days from casting

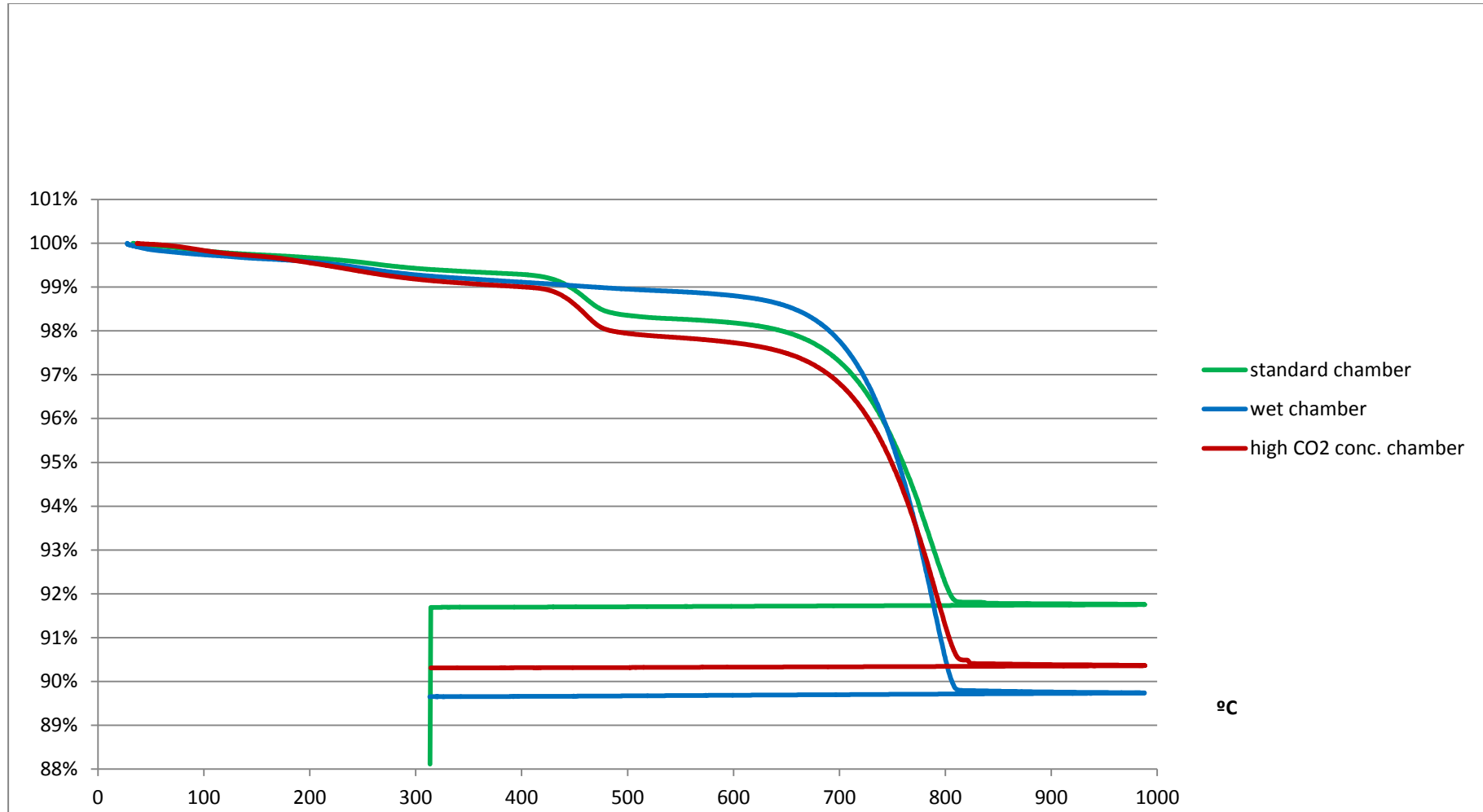14 days from casting

21 days from casting

28 days from casting

ANNEX VI – DETAILED RESULTS OF TGA ANALYSIS ON CYLINDRICAL SPECIMENS

Center (P3)	absolute values					% in respect to the sample				% of conversion			carbonation
Age (days)	sample weight	Ca(OH)2 weight	CaCO3 weight	CaCO3+ Ca(OH)2	Total	Ca(OH)2	CaCO3	CaO	total	Ca(OH)2	CaCO3	CaO	R
1	51.296	7.332	0.935	8.27	14.338	14.293%	1.822%	11.837%	27.951%	51.14%	6.52%	42.35%	0.1131
7	70.103	9.120	1.226	10.35	17.935	13.010%	1.748%	10.825%	25.583%	50.85%	6.83%	42.31%	0.1185
14	79.430	11.990	1.375	13.36	23.208	15.095%	1.731%	12.392%	29.218%	51.66%	5.92%	42.41%	0.1029
69	79.150	8.383	1.282	9.66	16.726	10.591%	1.620%	8.922%	21.133%	50.12%	7.67%	42.22%	0.1327

Middle (P2)	absolute values					% in respect to the sample				% of conversion			carbonation
Age (days)	sample weight	Ca(OH)2 weight	CaCO3 weight	CaCO3+ Ca(OH)2	total	Ca(OH)2	CaCO3	CaO	total	Ca(OH)2	CaCO3	CaO	R
1	54.768	7.244	0.965	8.21	14.231	13.226%	1.762	10.996	25.984	50.90%	6.78%	42.32	0.1176

							%	%	%			%	
7	66.636	11.088	1.399	12.49	21.661	16.639%	2.100%	13.767%	32.506%	51.19%	6.46%	42.35%	0.1120
14	66.482	9.884	1.487	11.37	19.682	14.866%	2.236%	12.503%	29.606%	50.22%	7.55%	42.23%	0.1308
69	76.681	7.496	1.439	8.94	15.414	9.776%	1.876%	8.449%	20.101%	48.63%	9.34%	42.03%	0.1610

Periphery (P1)	absolute values					% in respect to the sample				% of conversion			carbonation
Age (days)	sample weight	Ca(OH)2 weight	CaCO3 weight	CaCO3+ Ca(OH)2	total	Ca(OH)2	CaCO3	CaO	total	Ca(OH)2	CaCO3	CaO	R
1	42.757	5.312	1.780	7.09	12.109	12.424%	4.164%	11.734%	28.322%	43.87%	14.70%	41.43%	0.2510
7	66.327	5.529	6.694	12.22	20.157	8.337%	10.093%	11.961%	30.390%	27.43%	33.21%	39.36%	0.5476
14	66.663	4.437	7.913	12.35	20.138	6.655%	11.870%	11.684%	30.209%	22.03%	39.29%	38.68%	0.6407
69	77.999	2.627	9.530	12.16	19.482	3.369%	12.218%	9.391%	24.977%	13.49%	48.92%	37.60%	0.7839

114

ANNEX VII – TGA CURVES OF CYLINDRICAL SPECIMENS

1 day from casting

7 days from casting

14 days from casting

69 days from casting
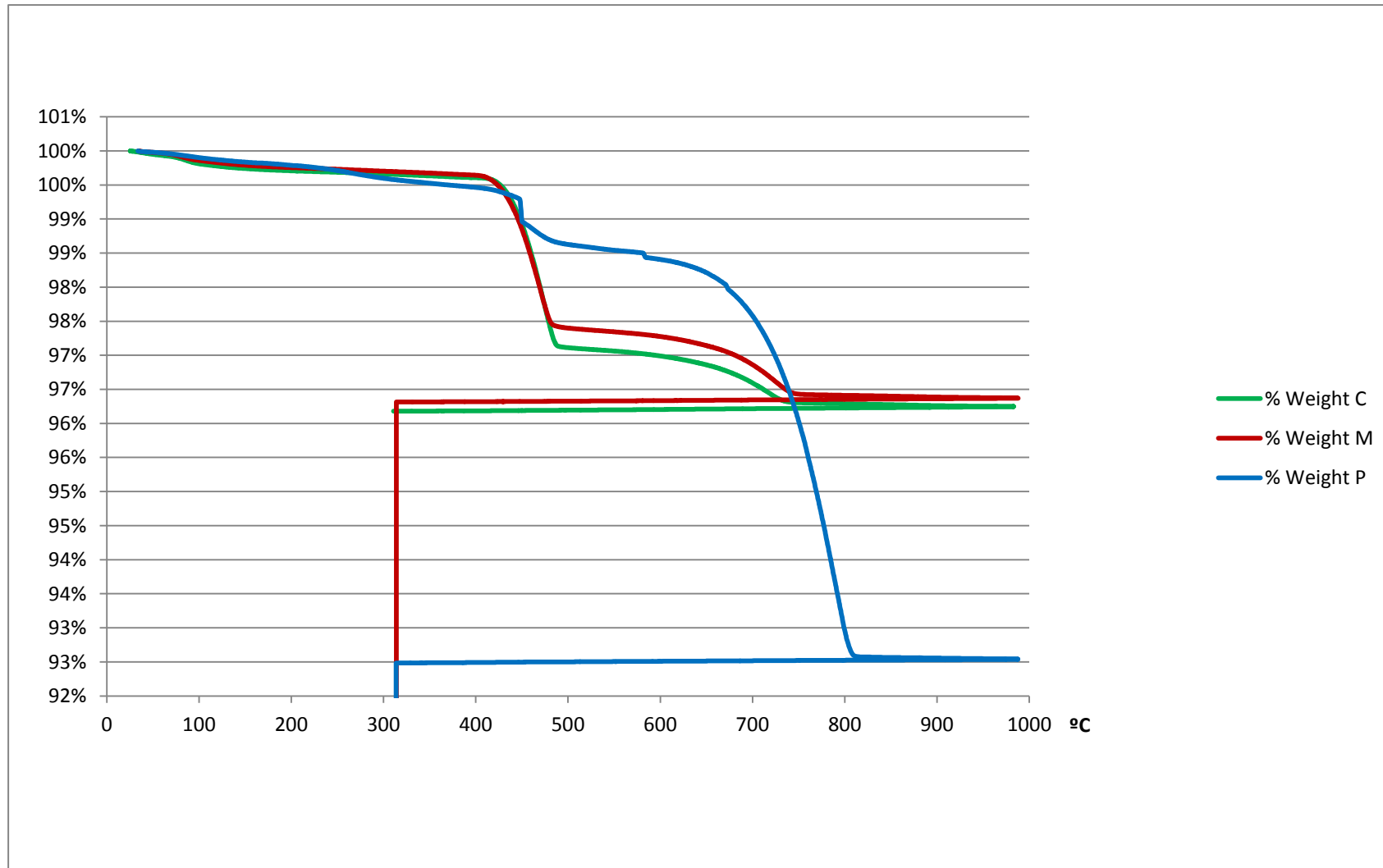
ANNEX VIII – COMPRESSIVE STRENGTH TEST CURVES – STANDARD CHAMBER SPECIMENS
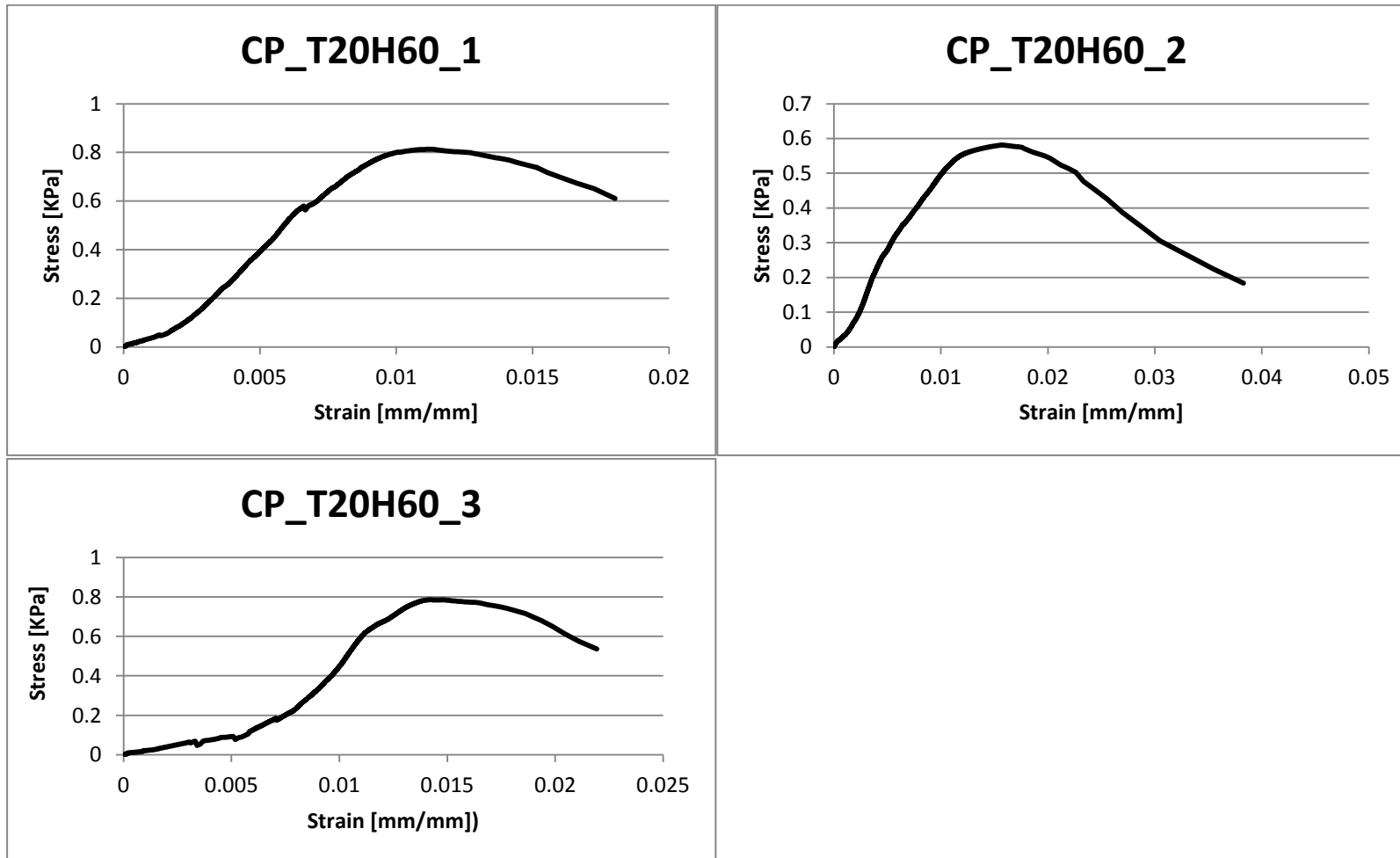
ANNEX IX – COMPRESSIVE STRENGTH TEST CURVES – WET CHAMBER SPECIMENS